Electron-scattering constraints for neutrino interactions and oscillations

A.Papadopoulou (apapadop@mit.edu)

For the e4ν collaboration

New Directions, March 15 2021

Laboratory for Nuclear Science @ MIT

Absolute QE-Like C(e,e'p) Cross Sections

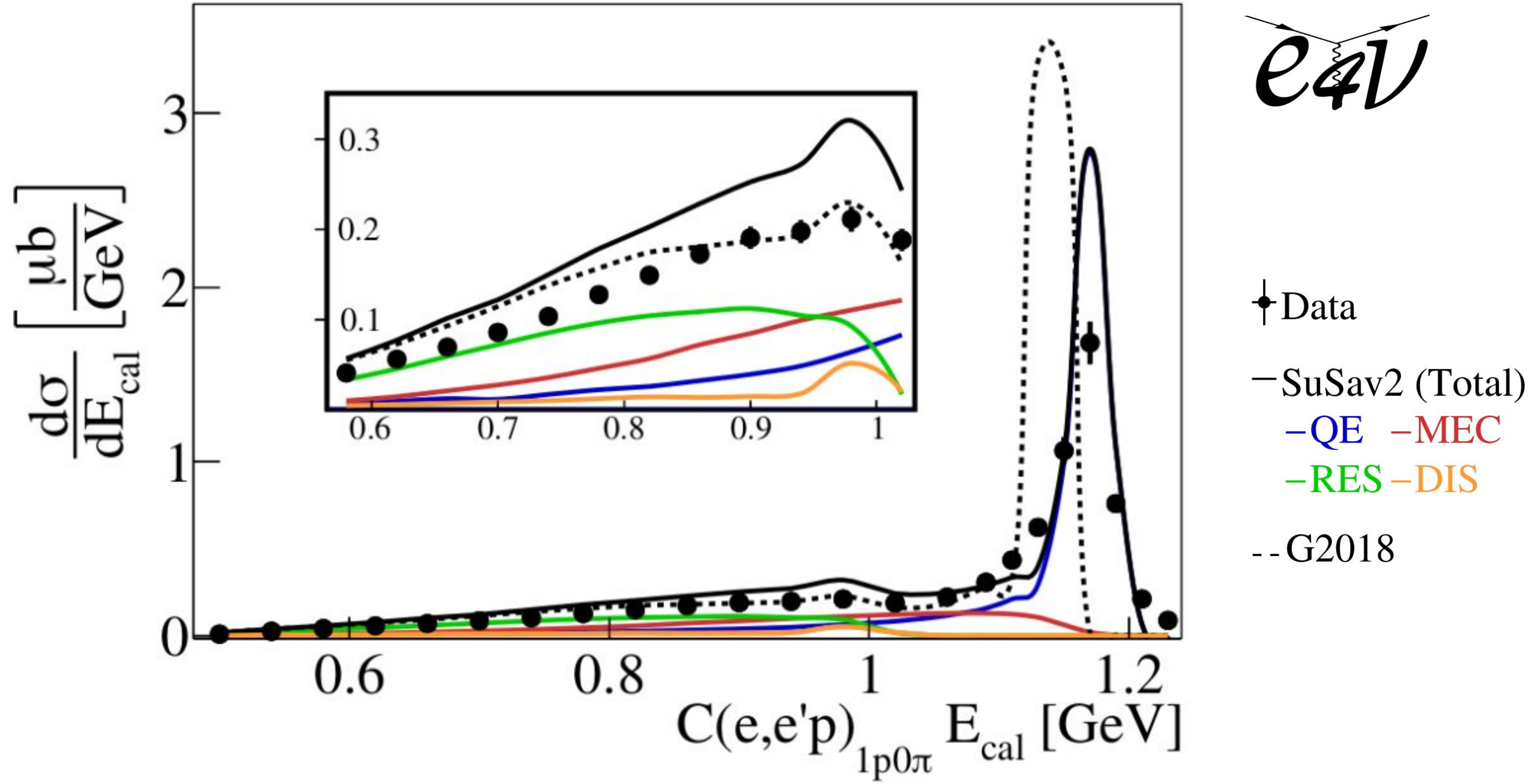

Wealth of New Results…

- Many nuclei & beam energies
- (e,e’) & (e,e’p)
- Energy reconstruction
- Single transverse variables
- Multiplicities

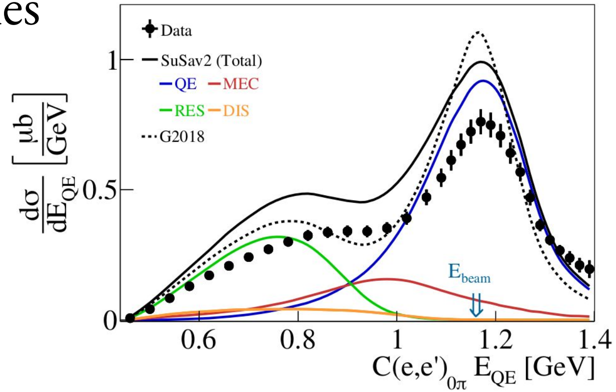

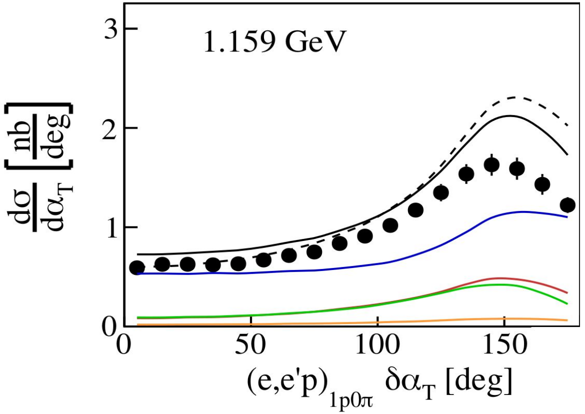

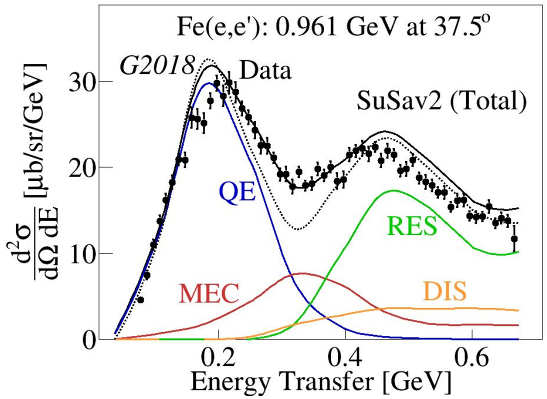

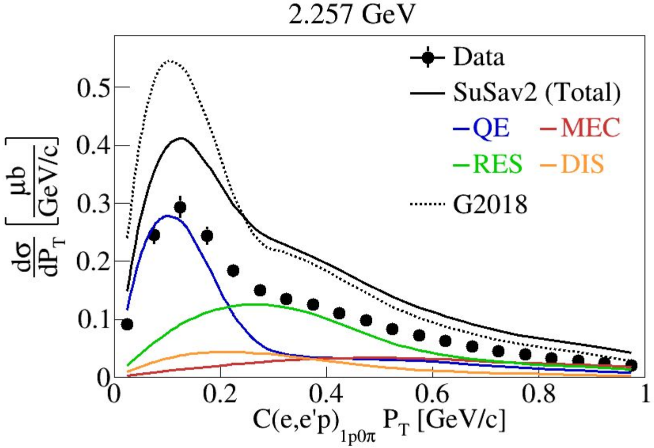

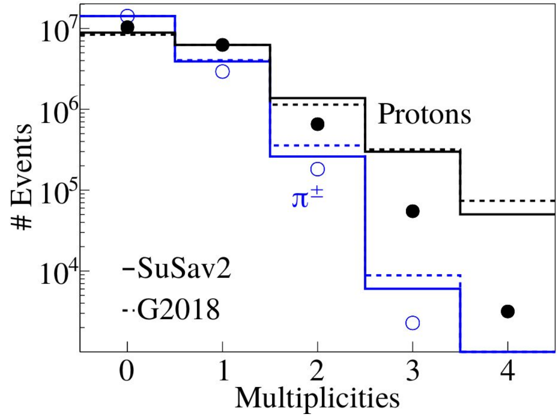

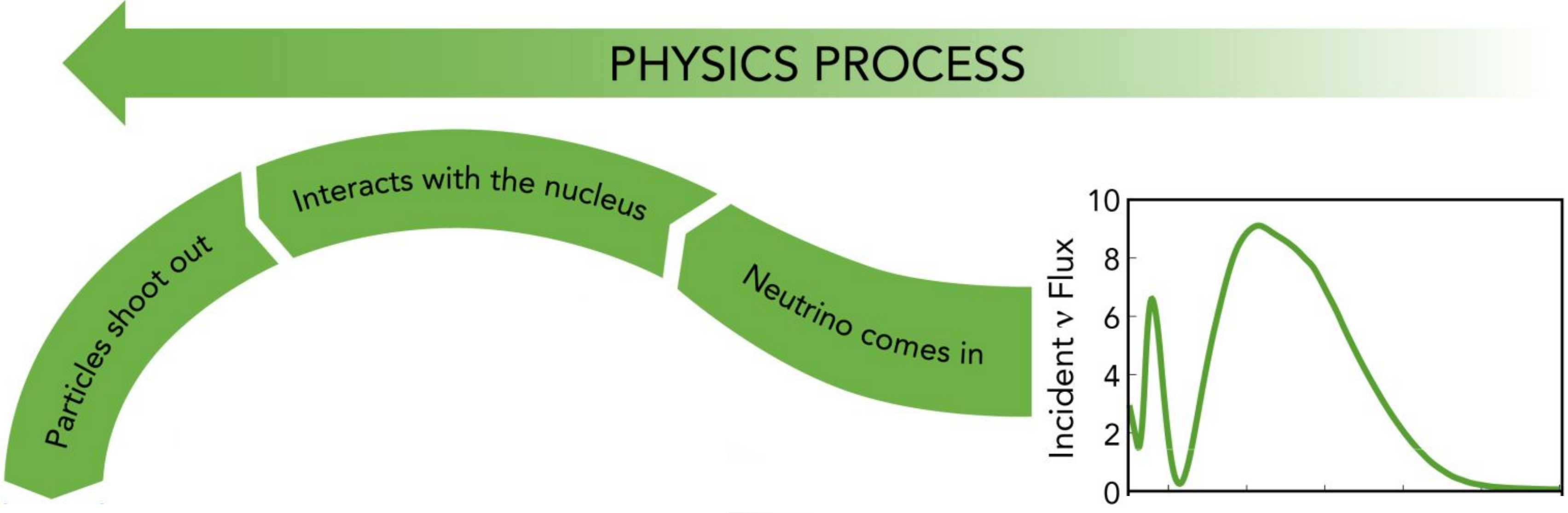
PHYSICS PROCESS
Particles shoot out
Interacts with the nucleus
Neutrino comes in
Incident ν Flux
10
8
6
4
2
0

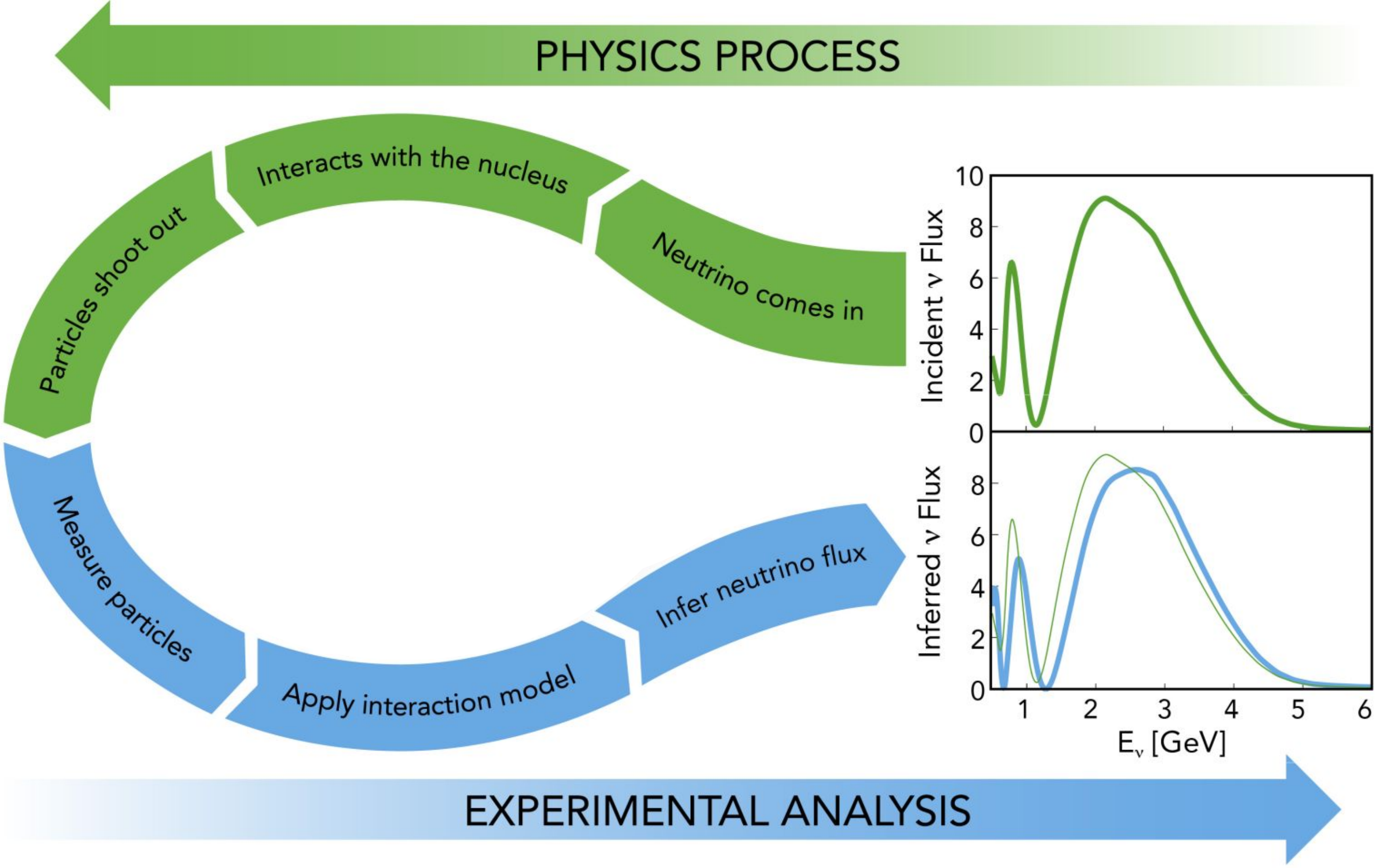
PHYSICS PROCESS
Interacts with the nucleus
Particles shoot out
Neutrino comes in
Measure particles
Apply interaction model
Infer neutrino flux
Incident ν Flux
Inferred ν Flux
E_ν [GeV]
EXPERIMENTAL ANALYSIS

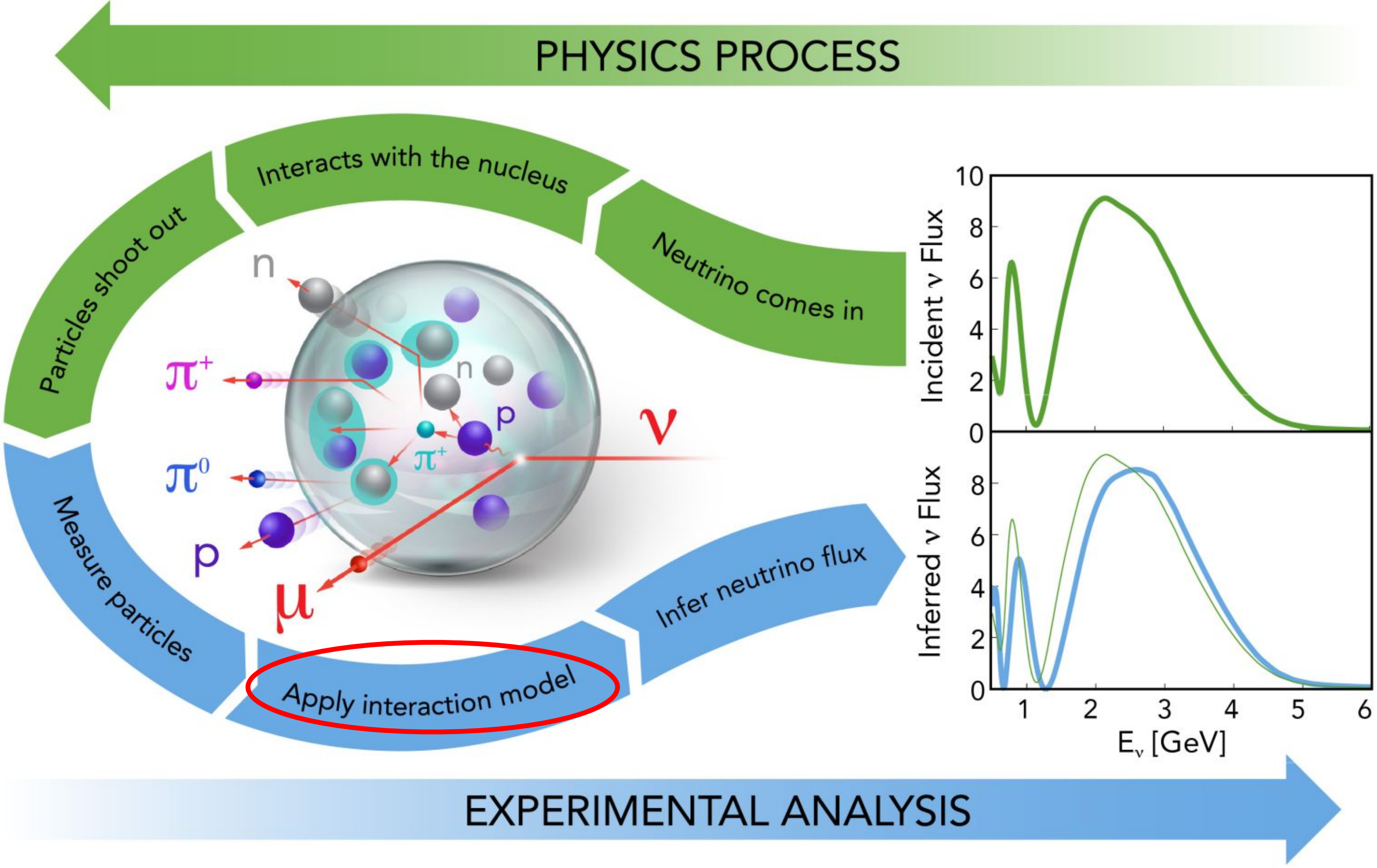
PHYSICS PROCESS
Interacts with the nucleus
Particles shoot out
Neutrino comes in
n
π+
π0
p
μ
ν
Measure particles
Apply interaction model
Infer neutrino flux
Incident ν Flux
Inferred ν Flux
Eν [GeV]
EXPERIMENTAL ANALYSIS

Improving Modeling Input

- ν near detector constraints

PRL 125, 201803 (2020)

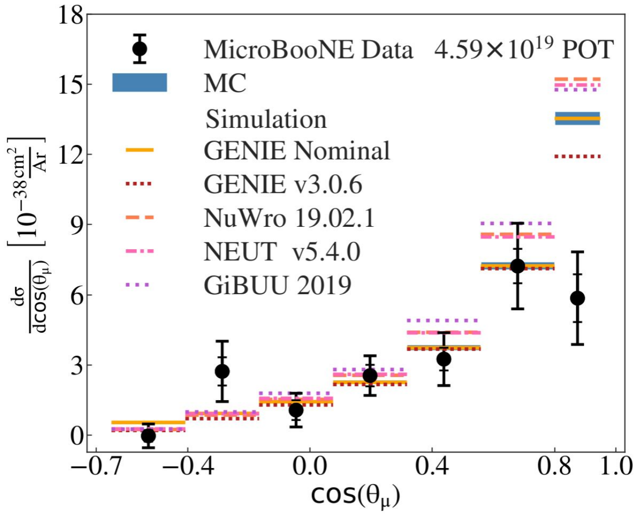

Today

• ν near detector constraints

• **Modelling development**
e & ν consistency

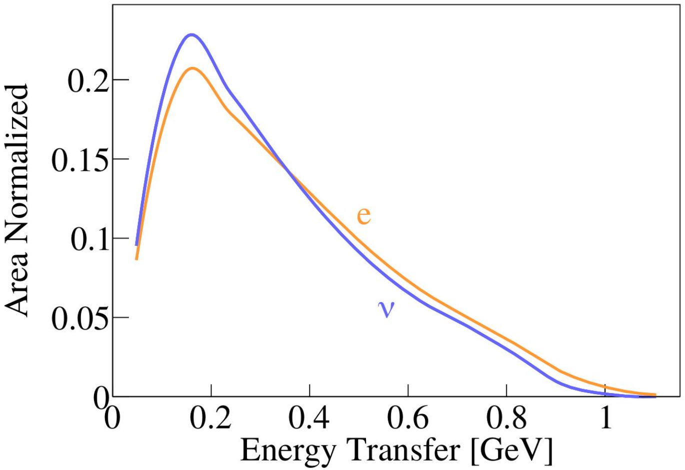

See talks by
Steven Gardiner & Marco Roda

arXiv:2009.07228 [nucl-th]

Today

- ν near detector constraints

- Modelling development

- **External Data**

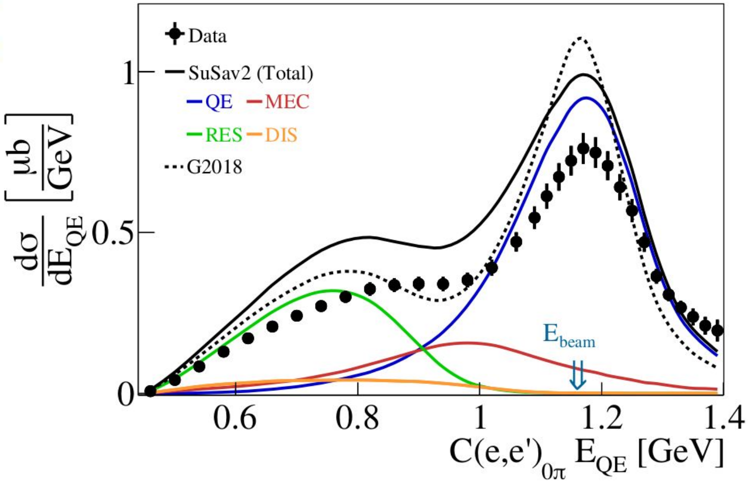

Why electrons?

- Very similar interactions

  Vector vs Vector + Axial-Vector

- Nuclear & FSI effects practically identical
- Monoenergetic electron beams

→ Benchmark ν event generators

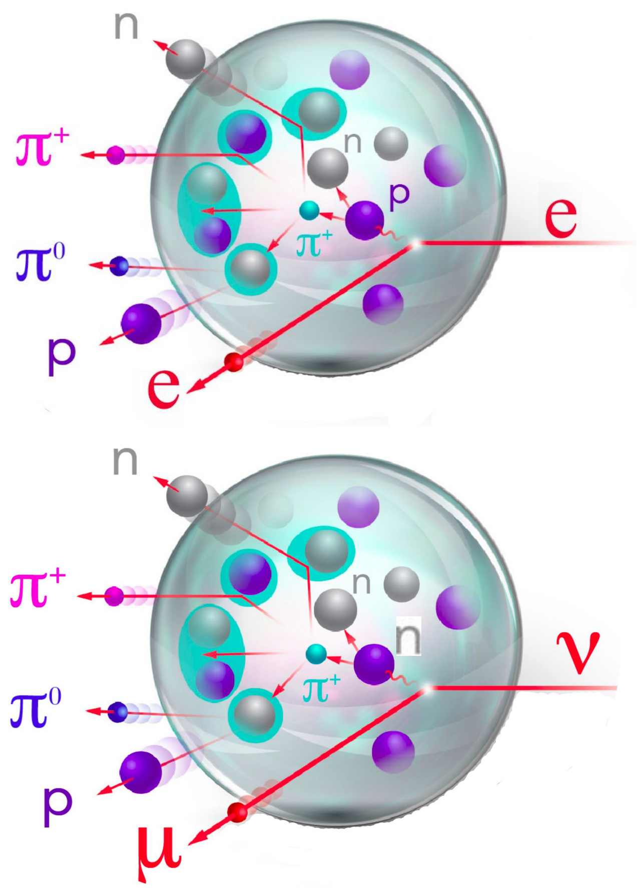

Model Configurations

Using GENIE v3: Fermilab

- **SuSav2**: QE & MEC SuSav2 (GTEST19_10b_00_000)

  PRD 101, 033003 (2020)

- **G2018**: Rosenbluth QE & Empirical MEC (G18_10a_02_11a)

GENIE Reproduces Inclusive e & ν Data

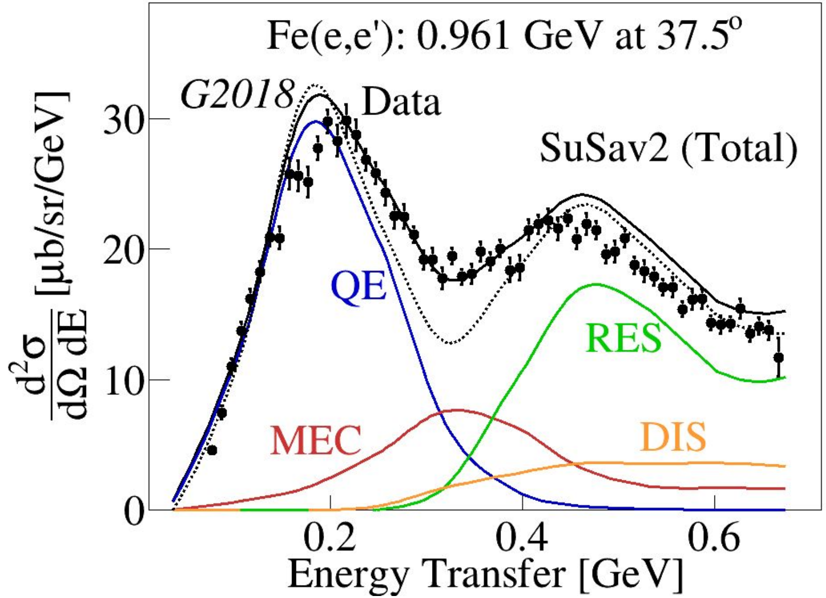

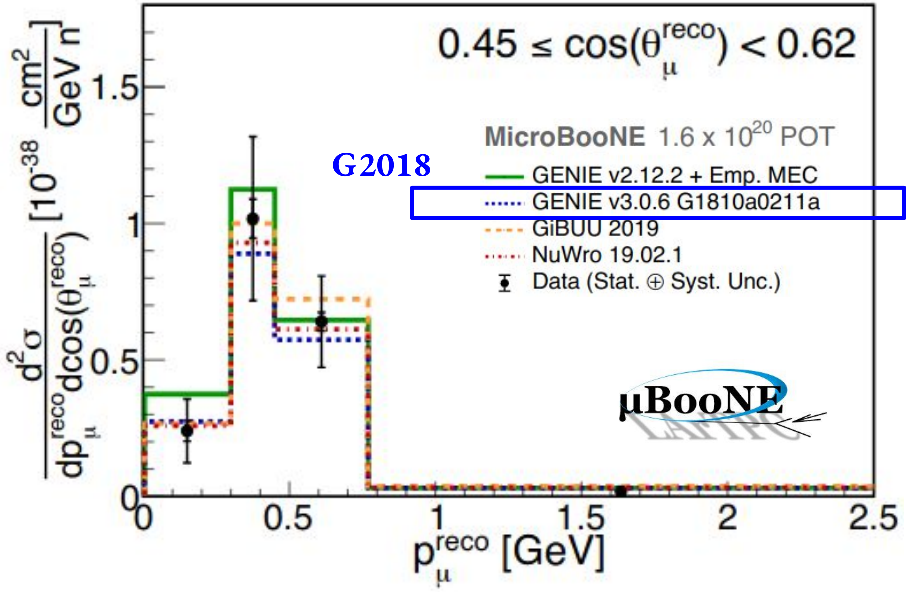

arXiv:2009.07228 [nucl-th]

PRL 123, 131801 (2019)

Issues To Be Further Investigated

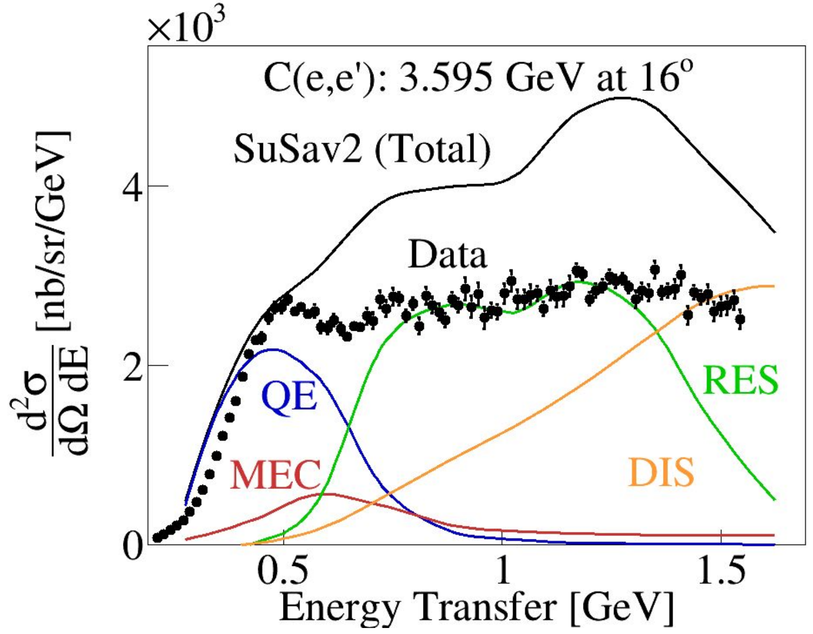

arXiv:2009.07228 [nucl-th]

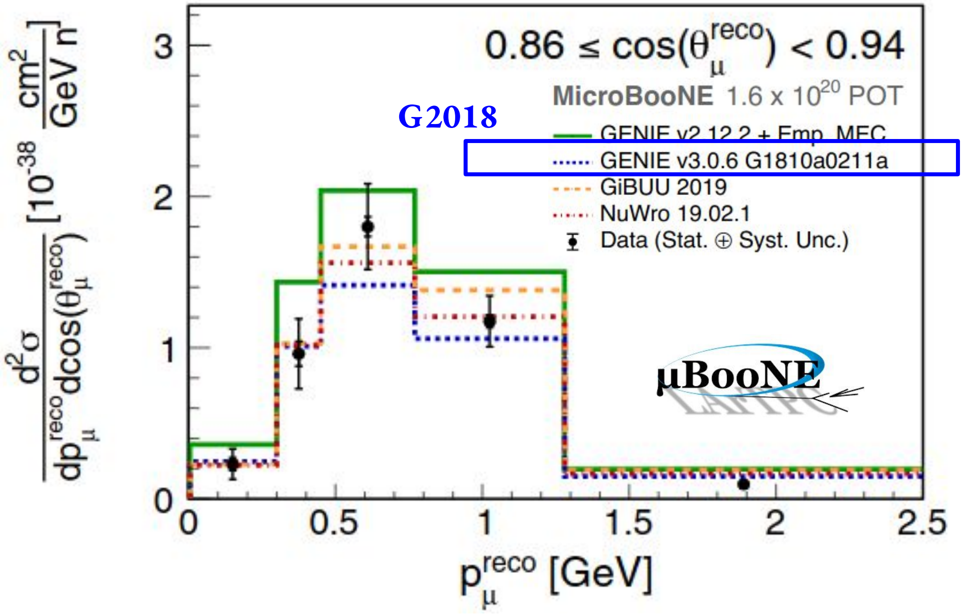

PRL 123, 131801 (2019)

Similar ν & e Distributions in Exclusive Reaction

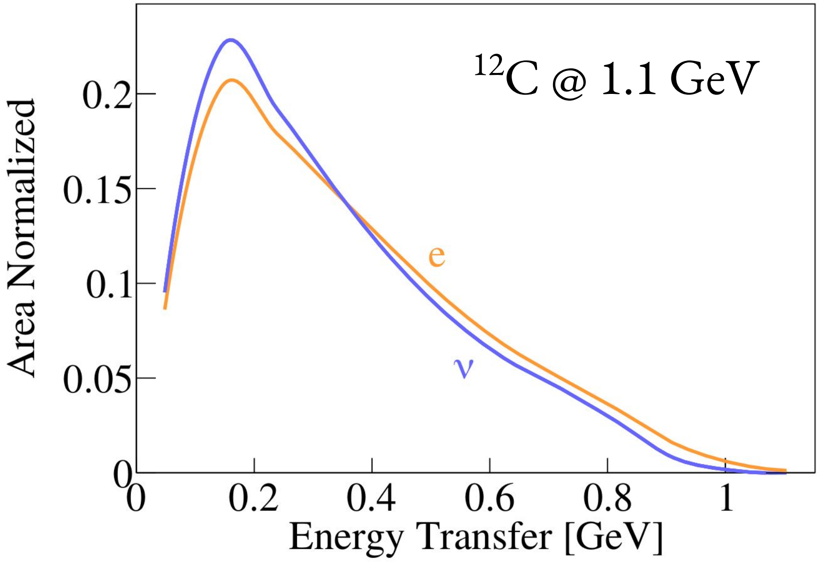

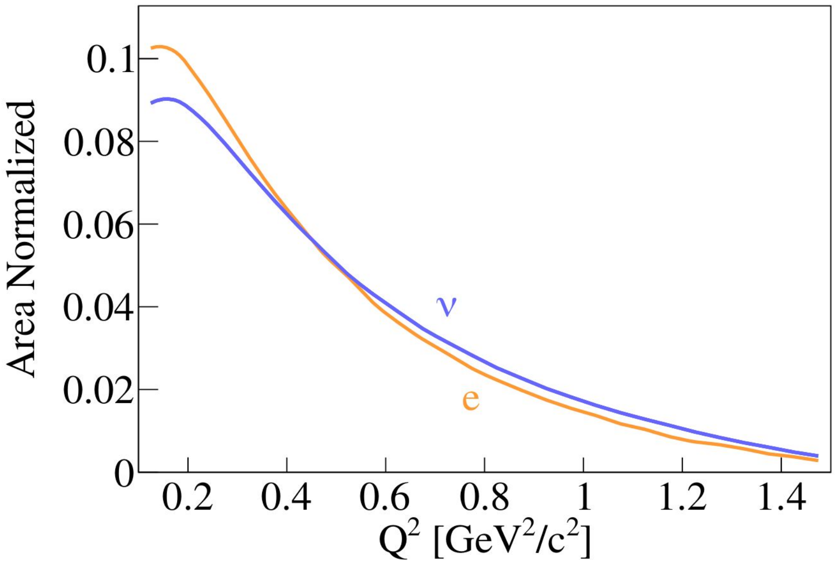

1 proton > 300 MeV/c, no $\pi^{+/-}$ > 70 MeV/c, no γ/π^0; Electron scaled by Q^4

Using SuSav2 / GTEST19_10b_00_000 with $Q^2 > 0.1$

e4ν Data-Mining W/ CLAS6

- Large acceptance @ $\theta_e > 15^o$
- Charged particle threshold similar to ν tracking detectors
- Energies: 1, 2 & 4 GeV
- Targets: ^{4}He, ^{12}C, ^{56}Fe

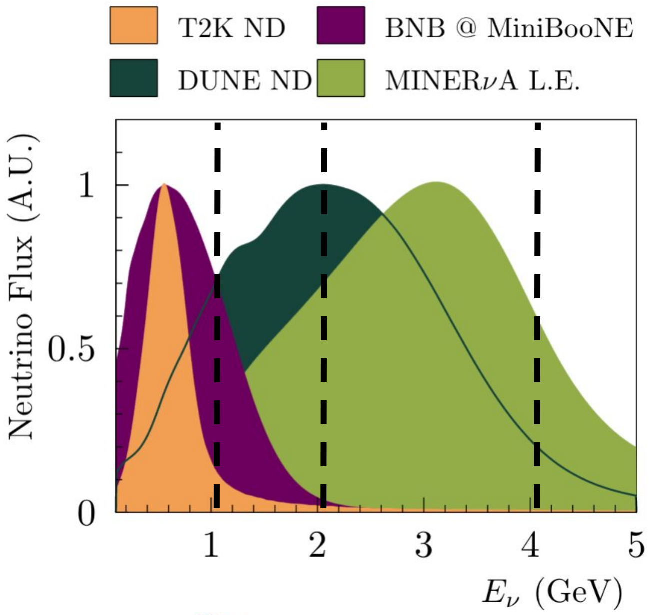

T2K H_2O

NOvA CH

SBN Program DUNE Ar

Playing The QE-like Neutrino Game

Strategy:

Select "clean" (e,e'p) events:
- 1 proton (> 300 MeV/c)
- No $\pi^{\pm}$ (> 150 MeV/c)

Scale by $\sigma_{\nu N} / \sigma_{eN} \propto Q^4$

Objectives

- Study ν energy reconstruction
- Benchmark ν event generators
- Report absolute cross sections

Cross Section Extraction

- Subtract non-(e,e'p) backgrounds
- Scale counts by luminosity
- Correct for (e,e'p) acceptance & radiation

Systematic uncertainties on each correction above & difference between detector sectors

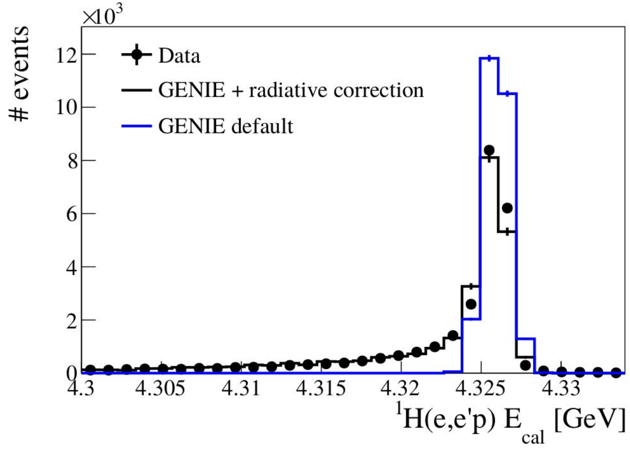

Hall A@ JLab

H(e,e'p) @ 4.32 GeV

Absolute QE-Like C(e,e'p) Cross Sections

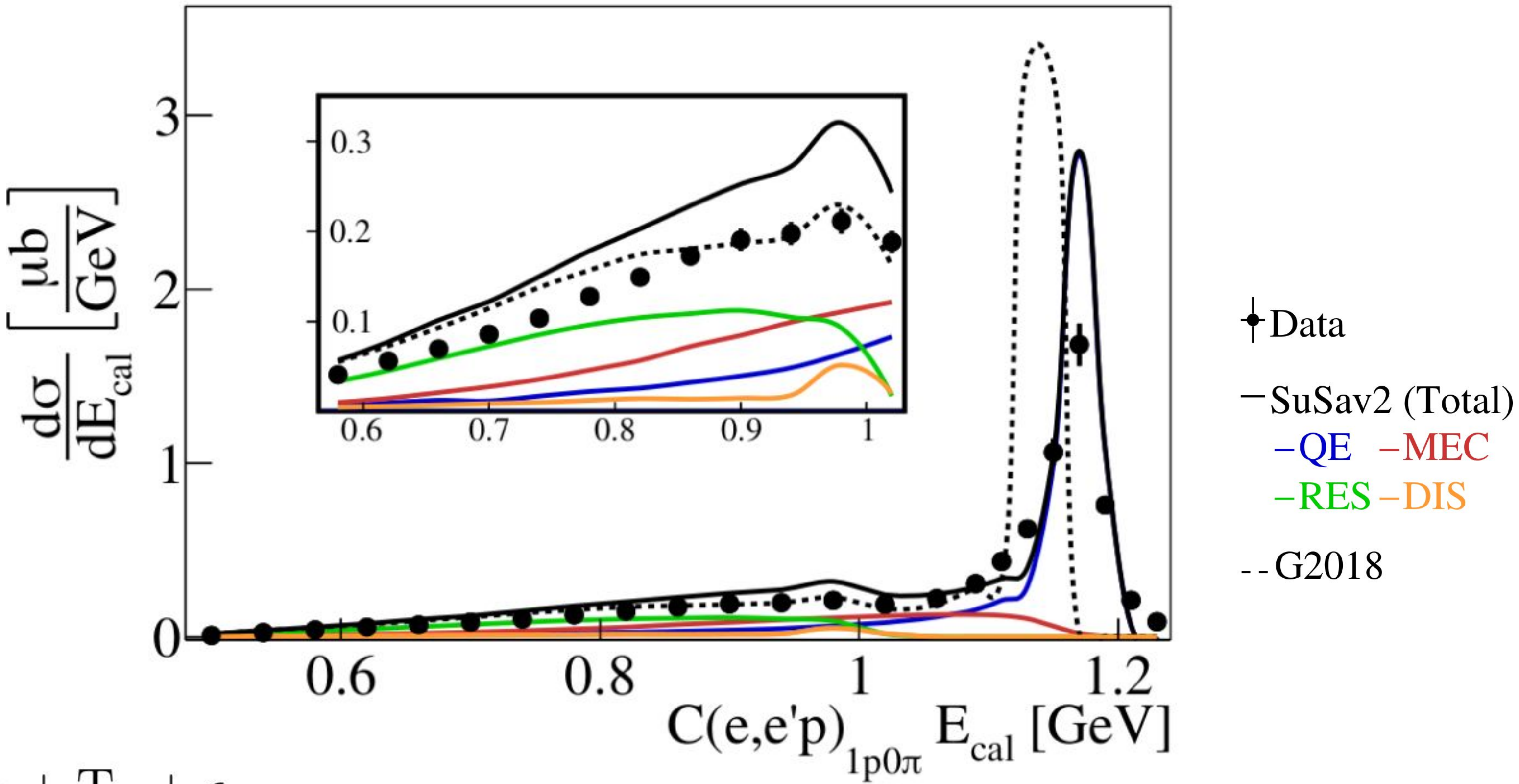

$$E_{cal} = E_l + T_p + \epsilon$$

A & E Dependence

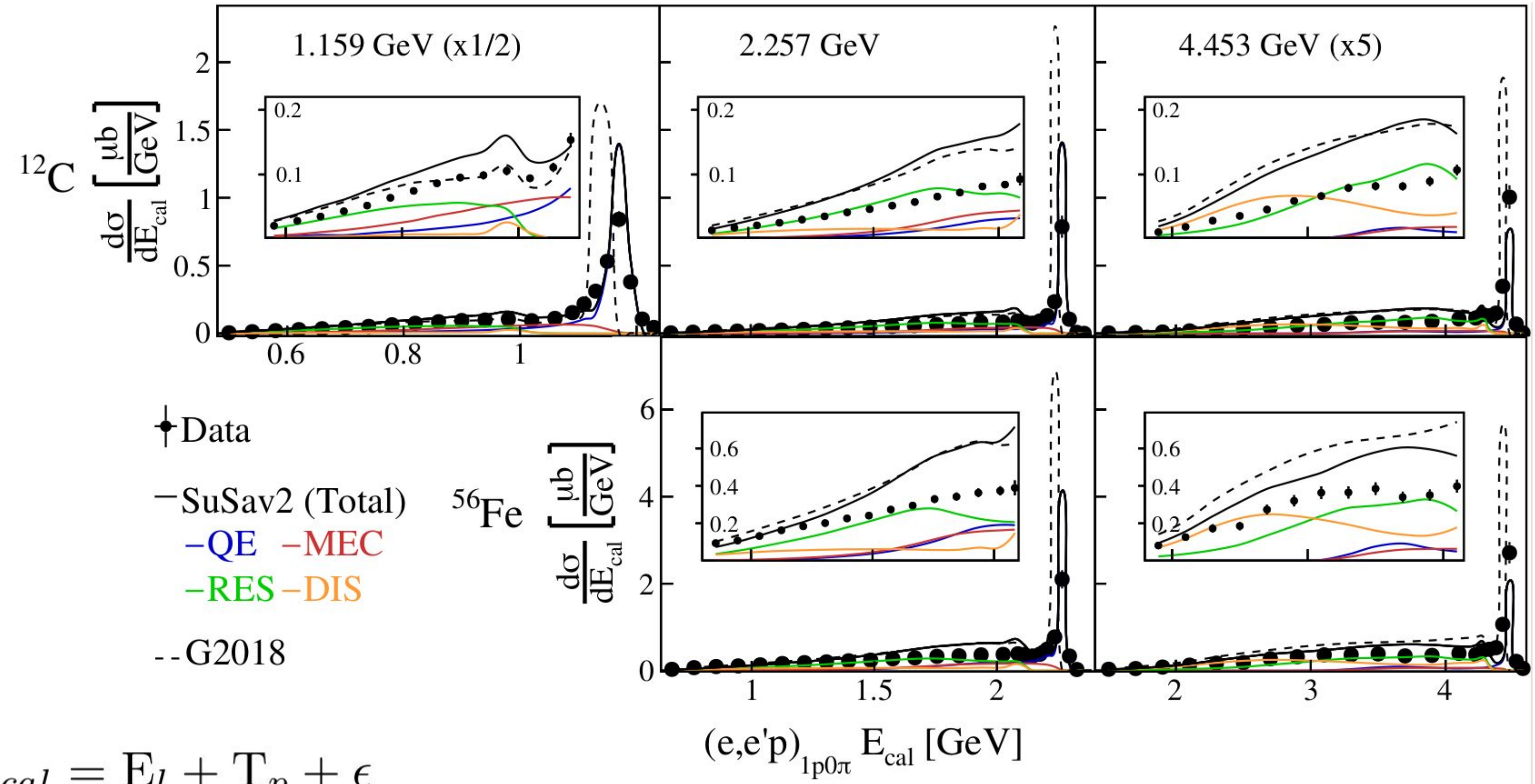

$$E_{cal} = E_l + T_p + \epsilon$$

A & E Dependence

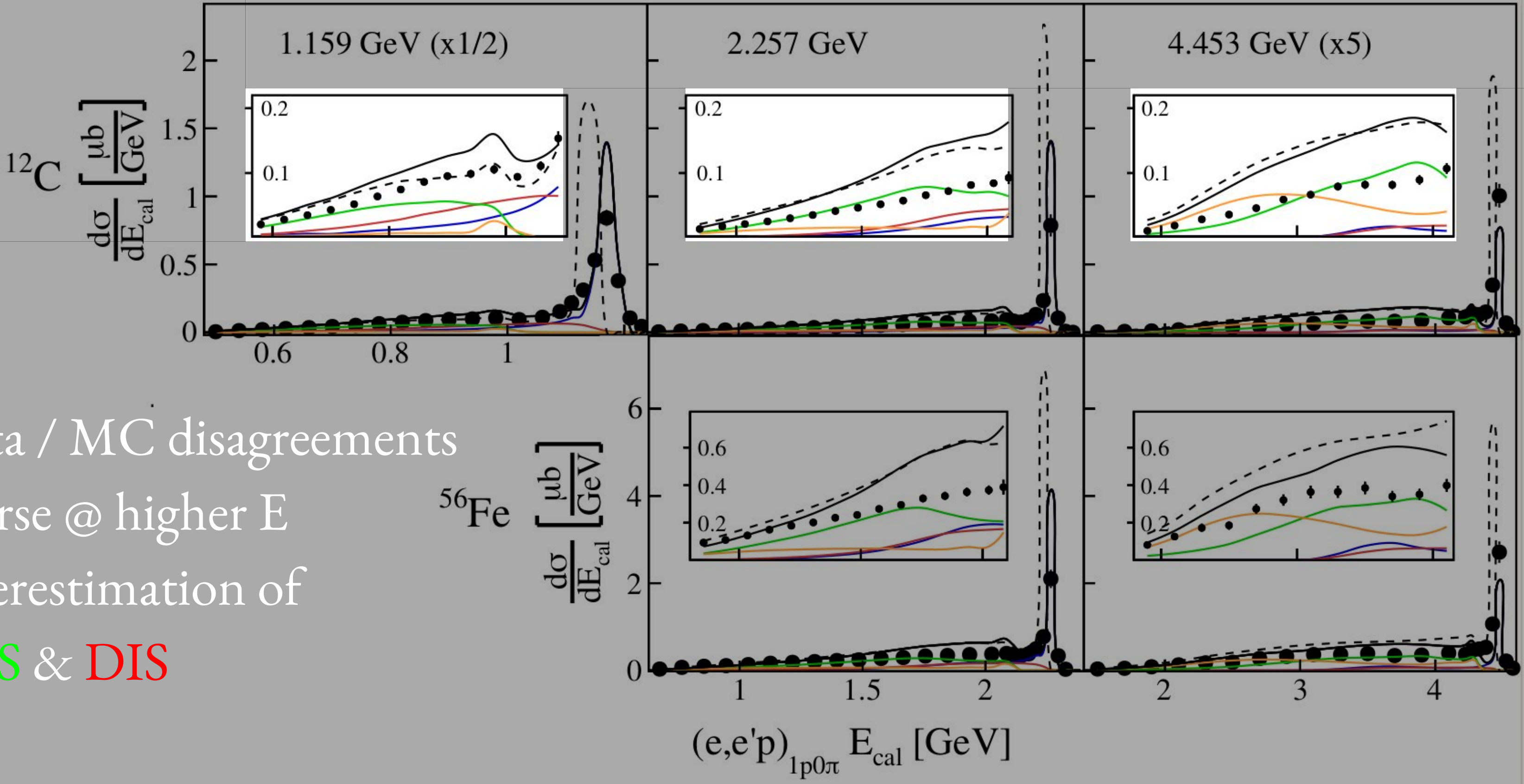

- Data / MC disagreements
- Worse @ higher E
- Overestimation of RES & DIS

A & E Dependence

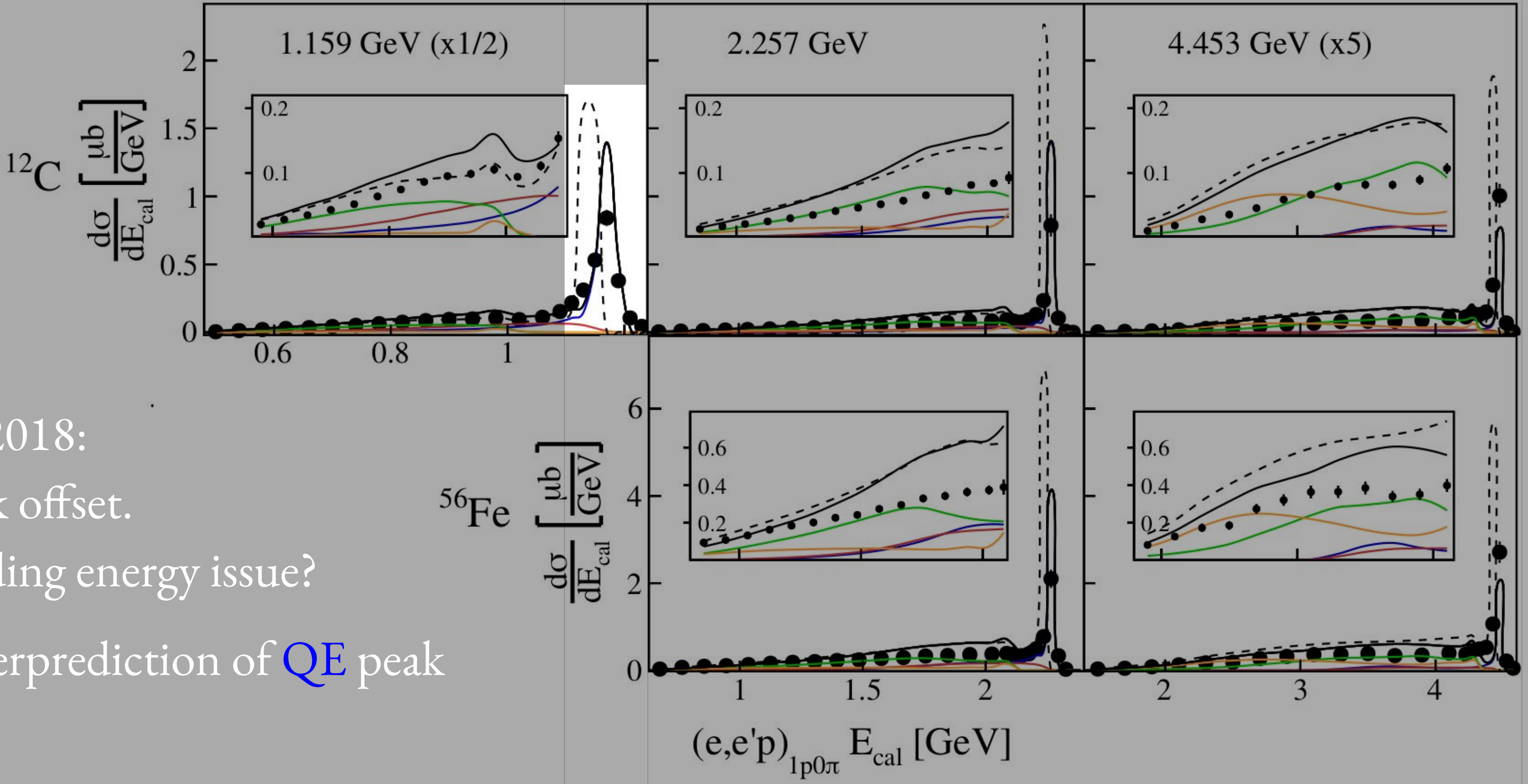

--- G2018:

- Peak offset.
  Binding energy issue?
- Overprediction of QE peak

A & E Dependence

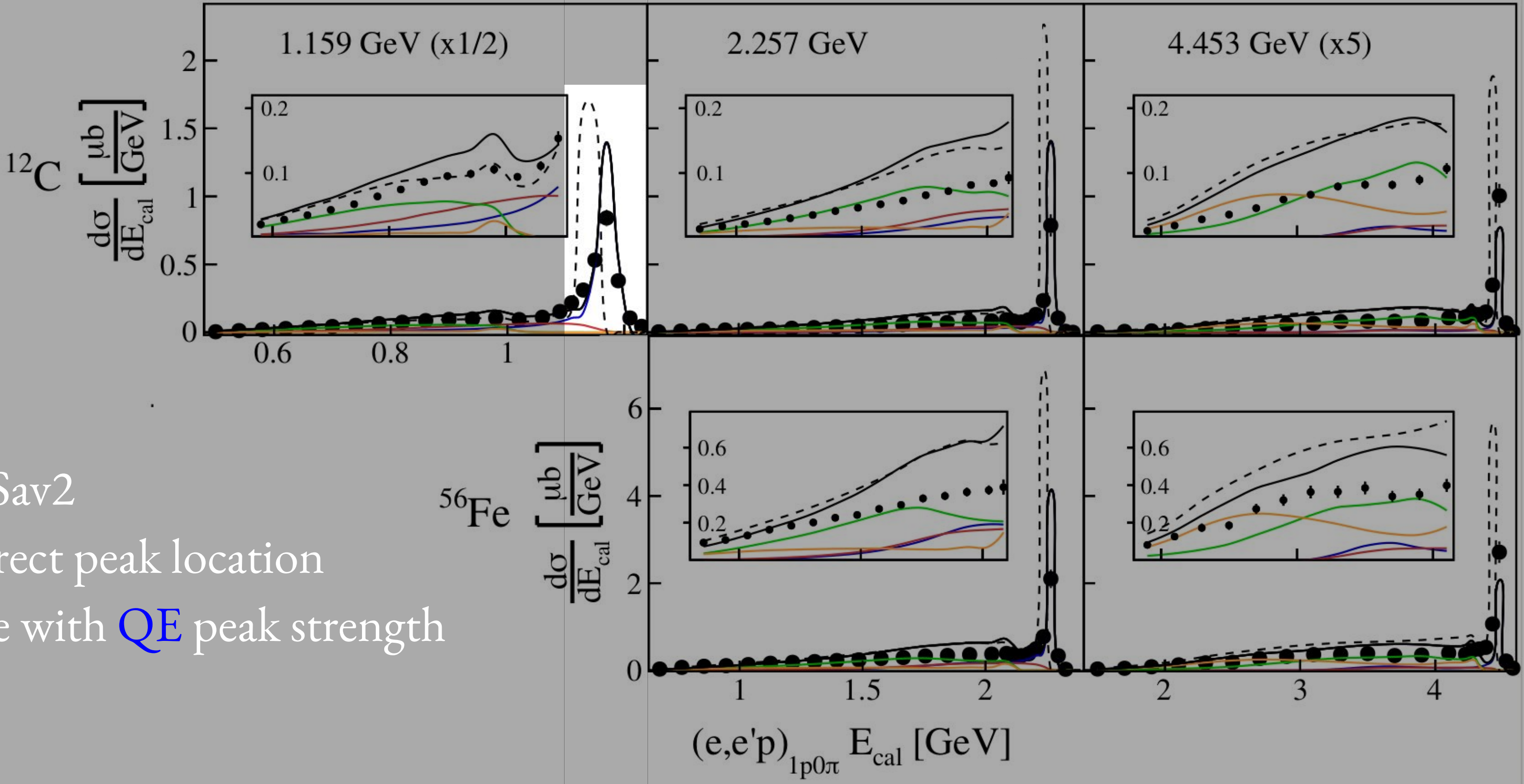

– SuSav2

- Correct peak location
- Issue with QE peak strength

QE Energy Reconstruction

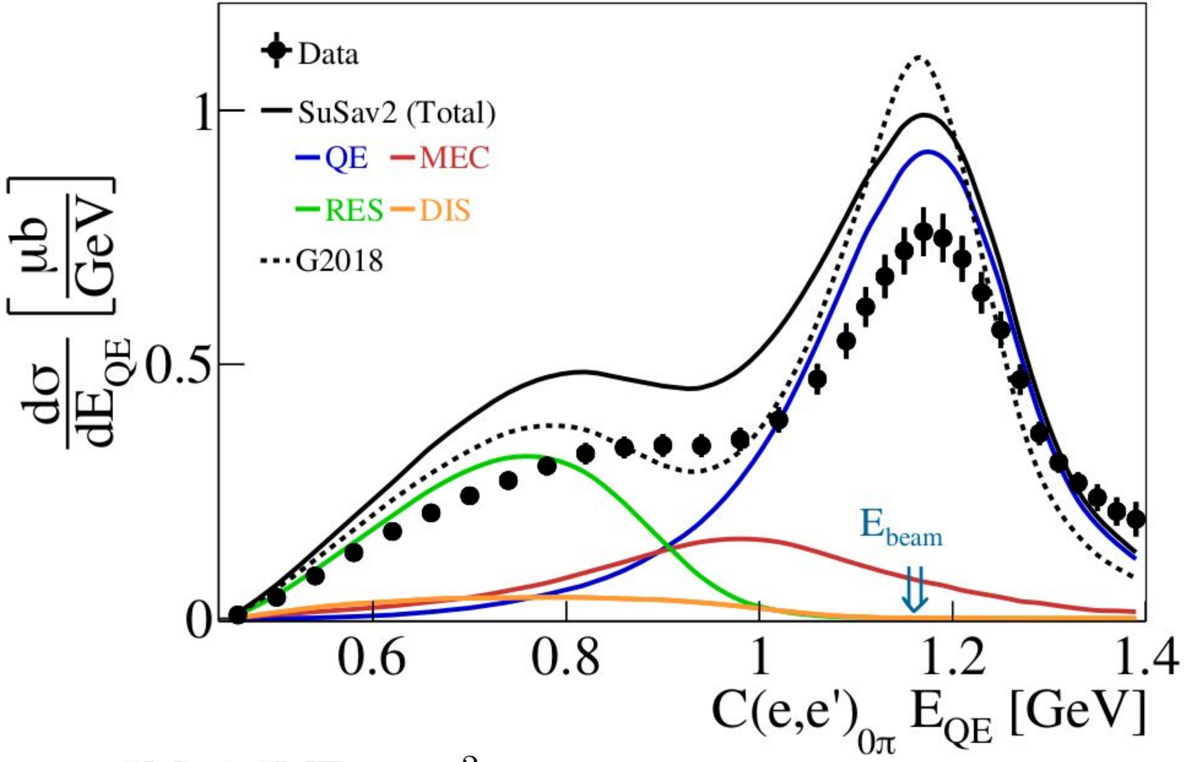

- Relevant for T2K
- Overestimation of QE peak & RES tail

$$E_{QE} = \frac{2M\epsilon + 2ME_l - m_l^2}{2\,(M - E_l + |k_l|\cos\theta_l)}$$

Transverse Missing Momentum

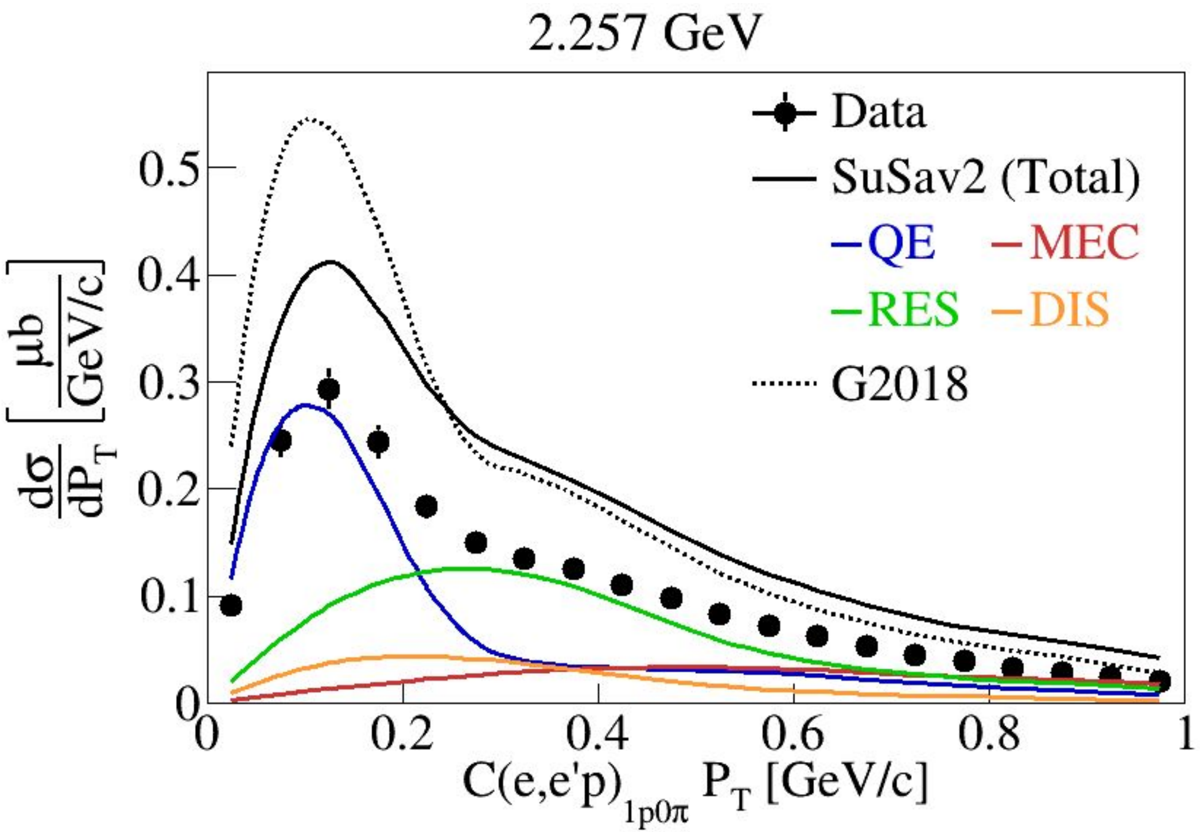

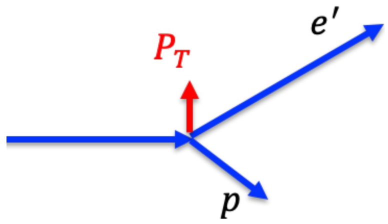

- Overestimation of QE peak & RES tail

A & E Dependence

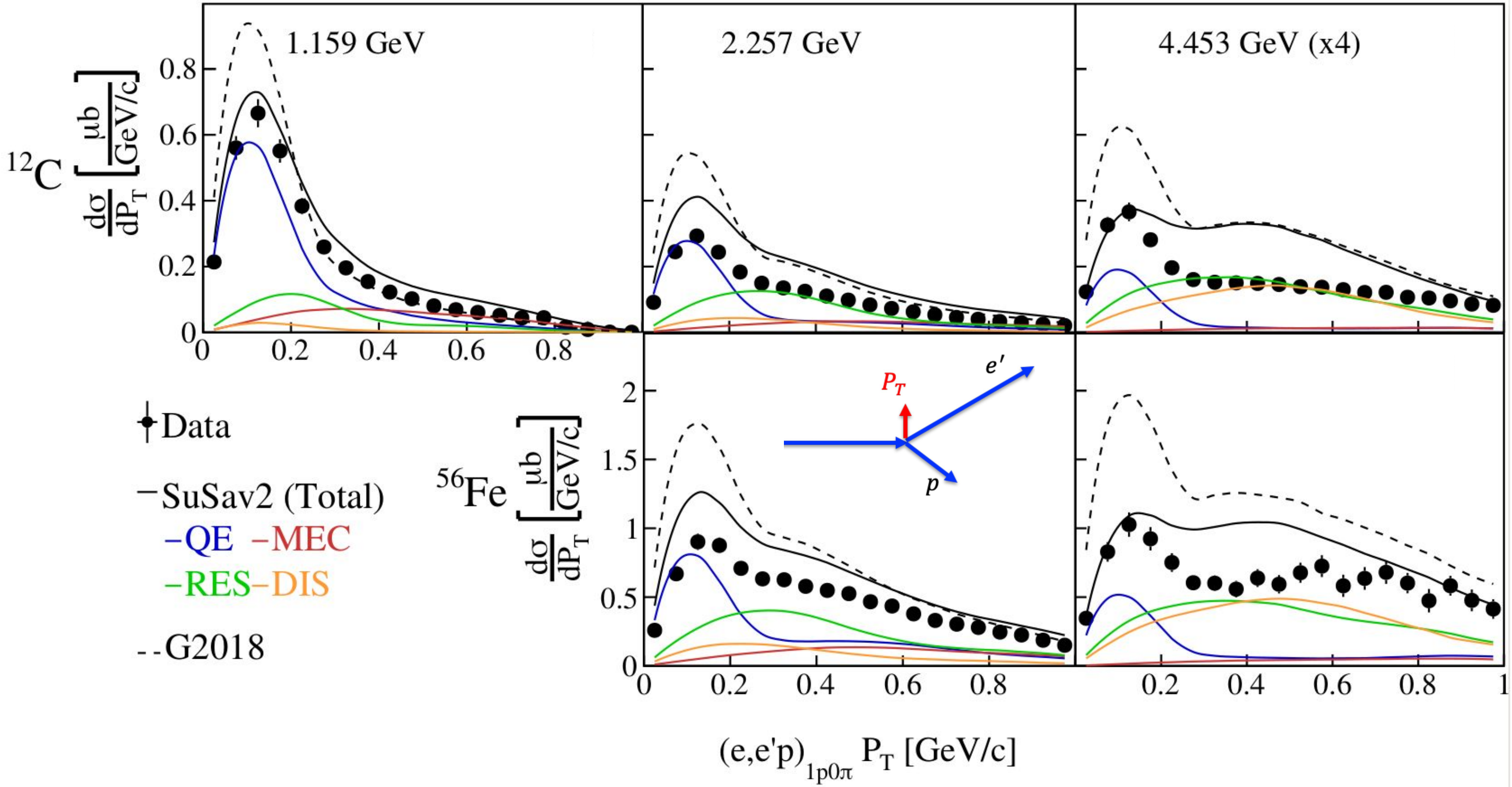

Angular A & E Dependence

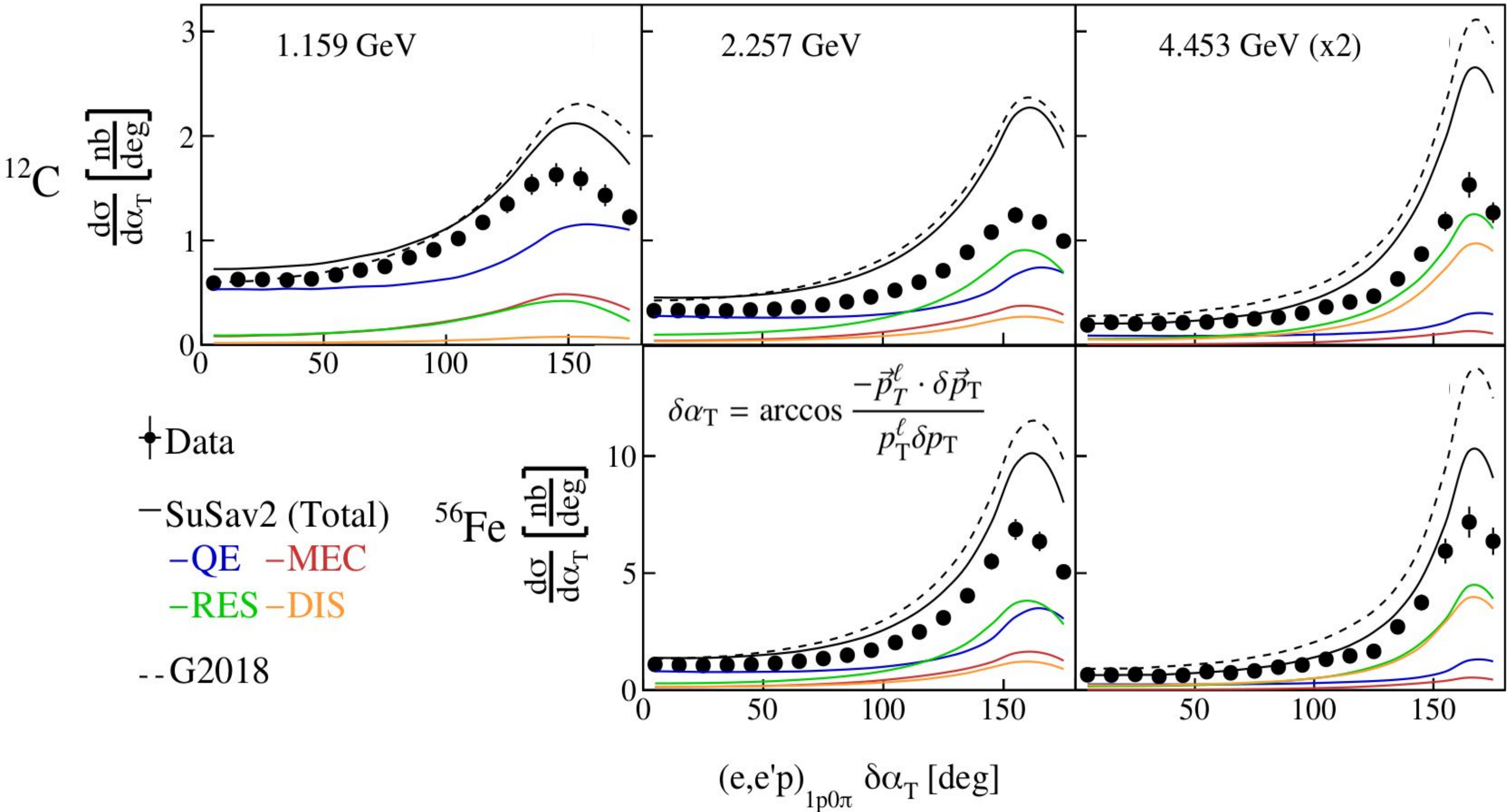

Angular A & E Dependence

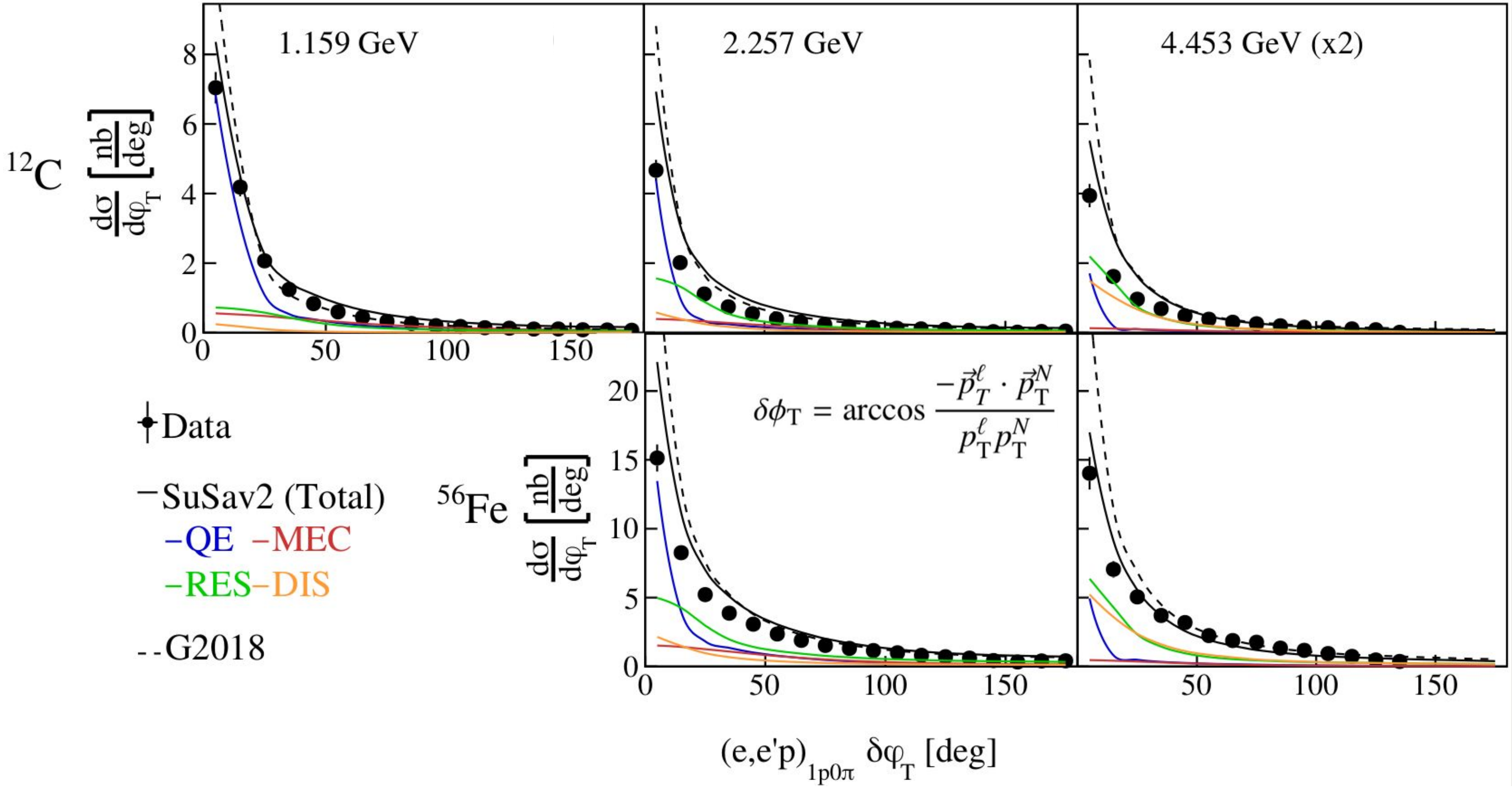

Energy Reconstruction In P_T Slices

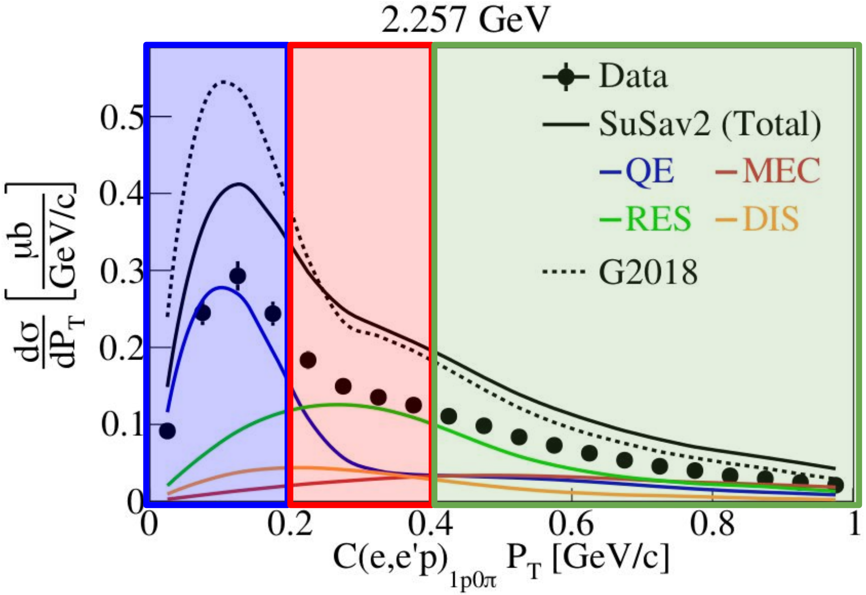

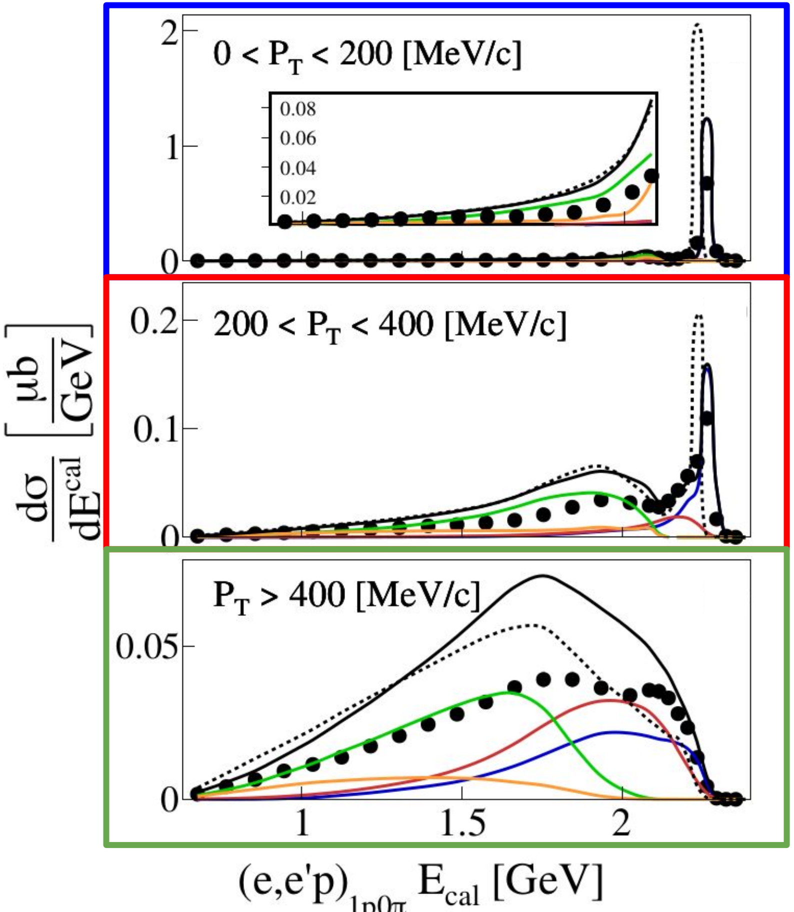

Multi-dimensional study

Detected Hadron Multiplicities

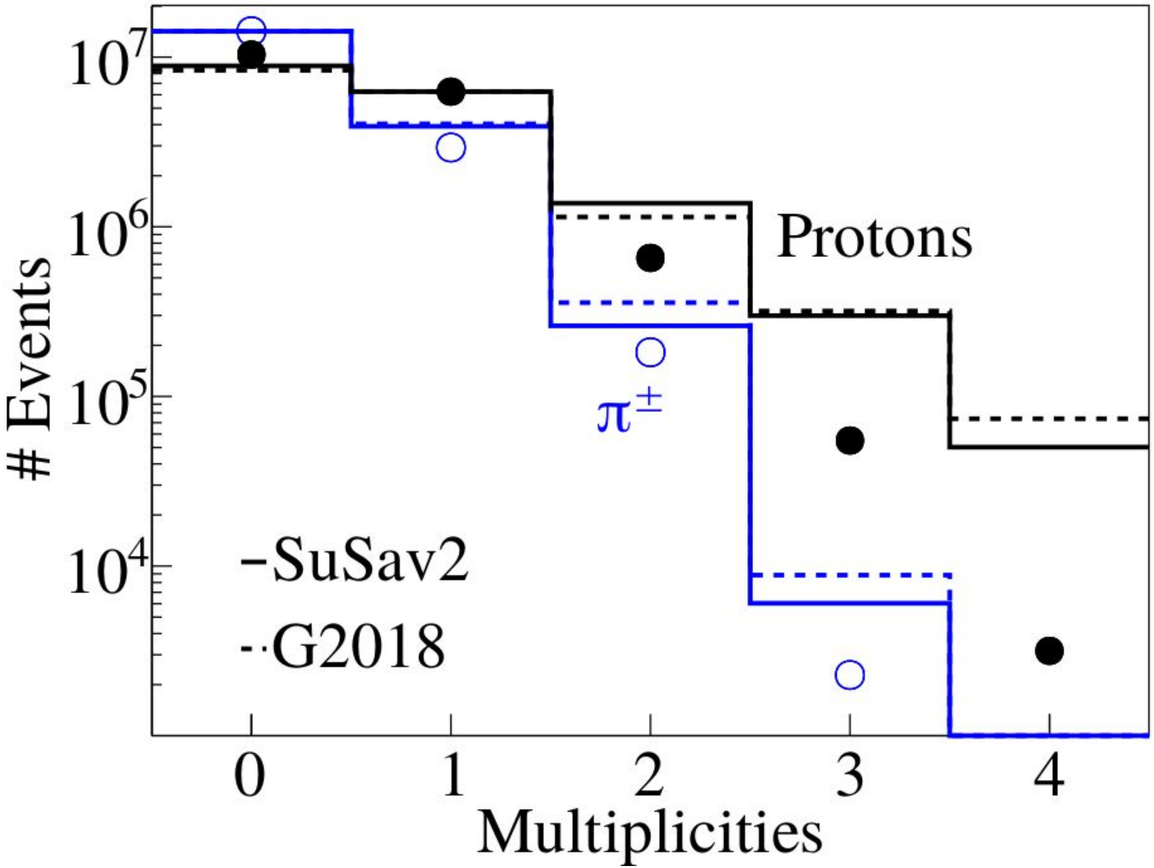

^{12}C @ 2.2 GeV

P_p > 300 MeV/c
P_π > 150 MeV/c

GENIE overpredicts hadron multiplicities

e4ν Wrap Up

- Benchmarking ν models against wide phase-space electron data

- Data/MC disagreements even for QE-like topologies

- Need for more electron scattering datasets in relevant phase-space to constrain ν models

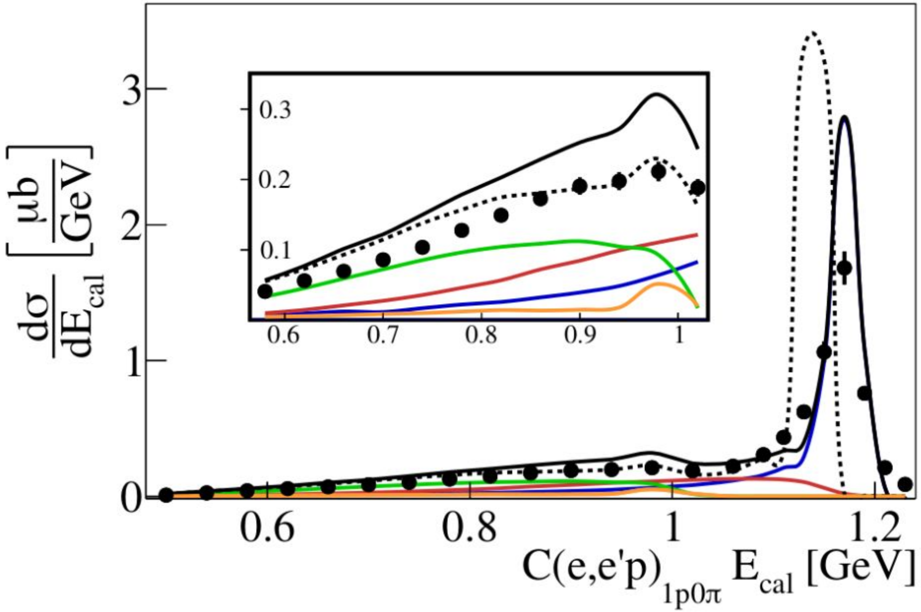

Potential impact on DUNE

Coming Fall '21: New Data W/ CLAS12

- Acceptance down to 5°
- x10 luminosity [10^{35} cm^{-2} s^{-1}]
- Targets
  ^{2}D, ^{4}He, ^{12}C, ^{16}O, **^{40}Ar**, ^{120}Sn
- 1 - 7 GeV beam energies
- Better neutron & gamma detection

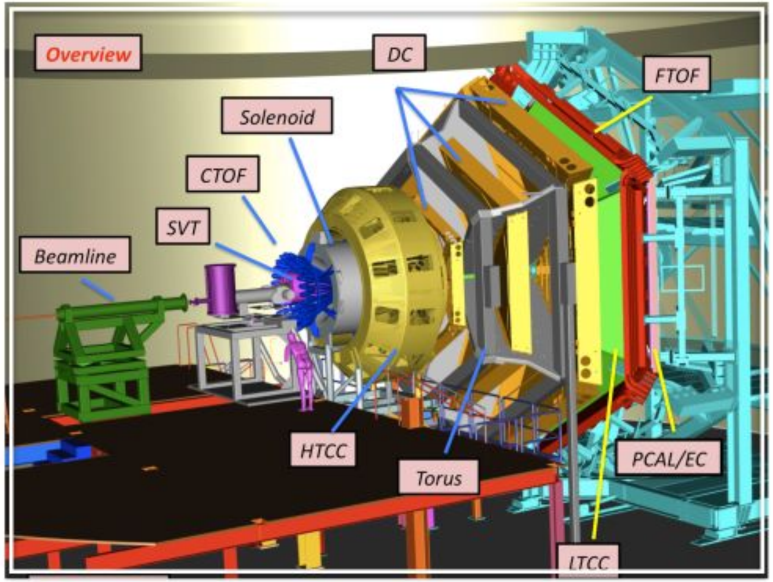

Support Letters

DUNE · IceCube South Pole Neutrino Observatory · Hyper-Kamiokande · T2K · NOvA · MINERvA · Fermilab · GiBUU The Giessen Boltzmann-Uehling-Uhlenbeck Project · Genie · µBooNE

Thank you !

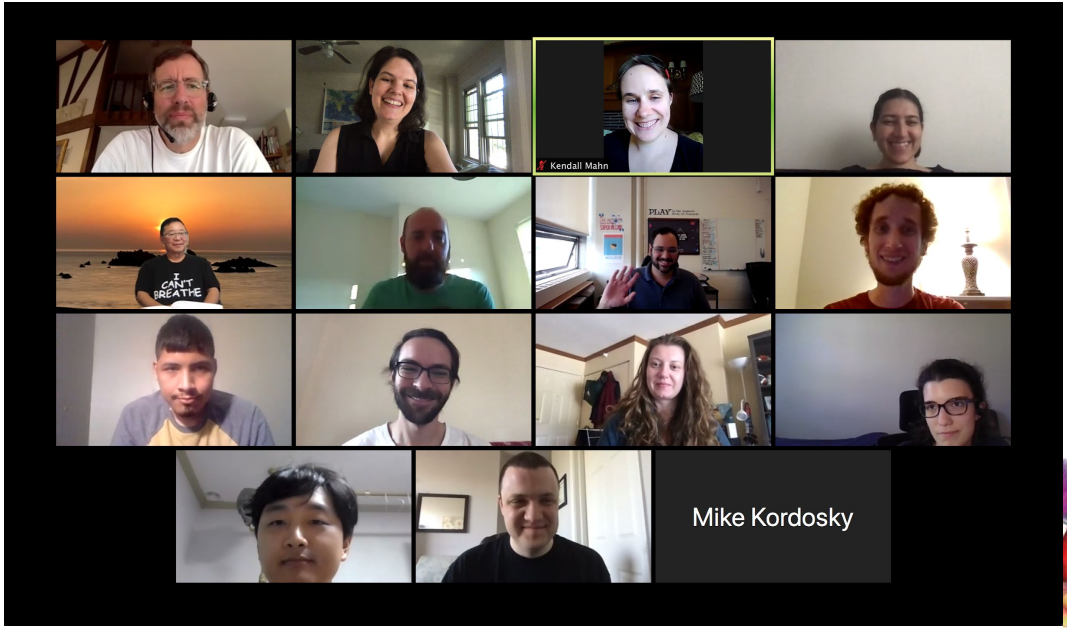

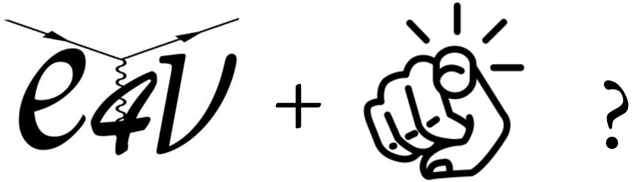

[come join us! :]

Thank you !

Joint theory & experimental effort

- New data with CLAS12 / …
- More interaction channels (1p1π, 1π, NN, …)
- Tuning efforts
- Implications on ν oscillation studies

e4ν +  ?

[come join us! :]

Parallel Efforts

e4V @ Jefferson Lab
Thomas Jefferson National Accelerator Facility

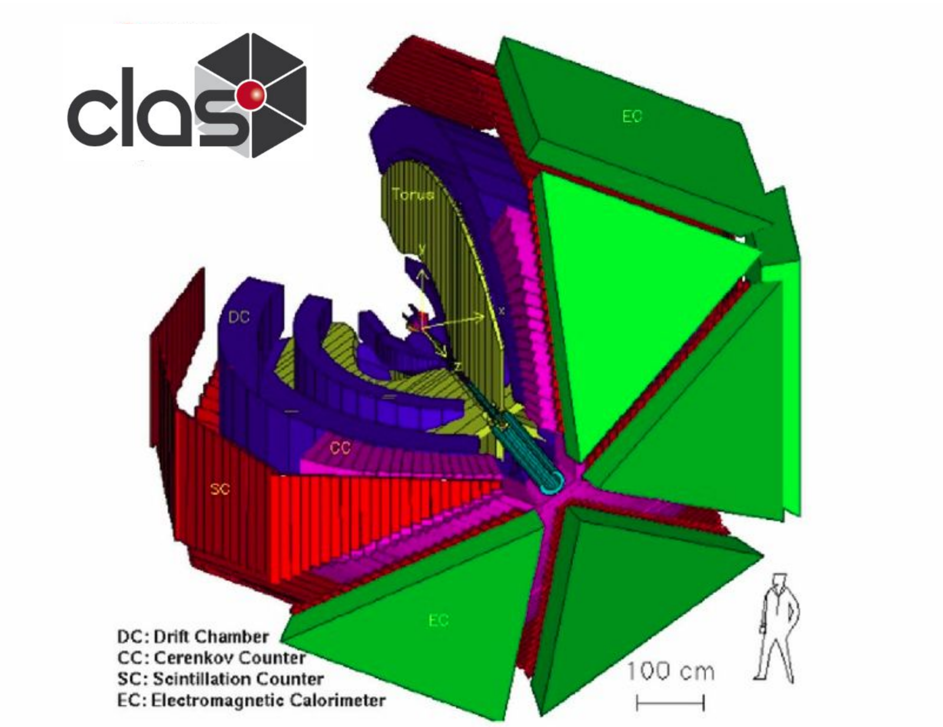

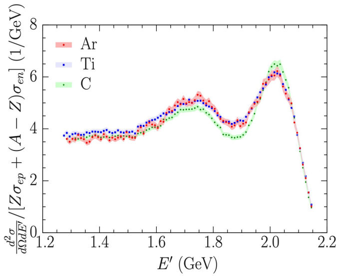

<u>ArTi (e,e’) & (e,e’p)</u>
See talk
by L. Jiang

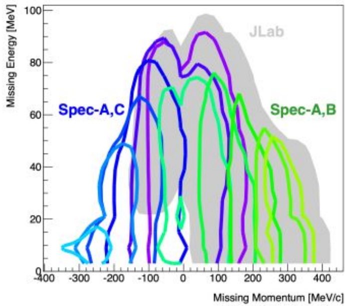

See talk
by L. Doria

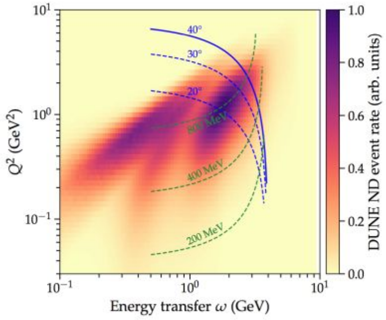

SLAC

See talk
by A. Ankowski

Thank you !

Backup Slides

Energy Reconstruction

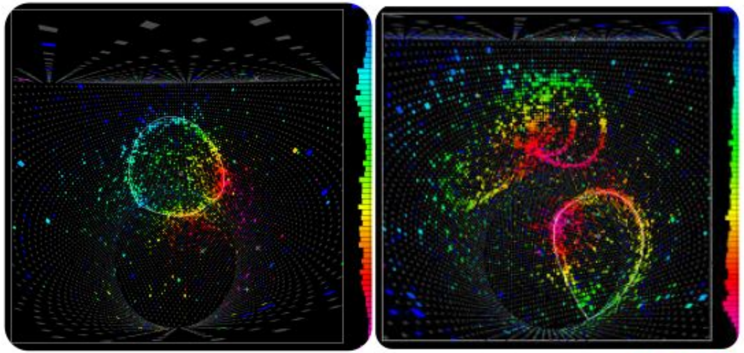

Cherenkov detectors

Assuming QE interaction

Using lepton kinematics

$$E_{QE} = \frac{2M\epsilon + 2ME_l - m_l^2}{2\left(M - E_l + |k_l|\cos\theta_l\right)}$$

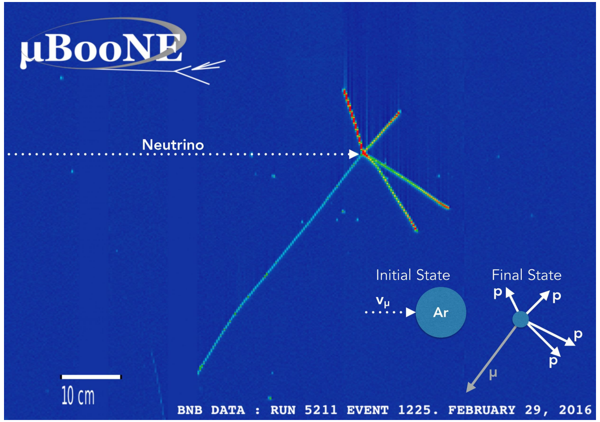

Tracking detectors

Calorimetric sum

Using all detected particles

$$E_{cal} = E_l + T_p + \epsilon$$

nucleon separation energy ϵ ~ 20 MeV

Inclusive Electron Scattering C

arXiv:2009.07228 [nucl-th]

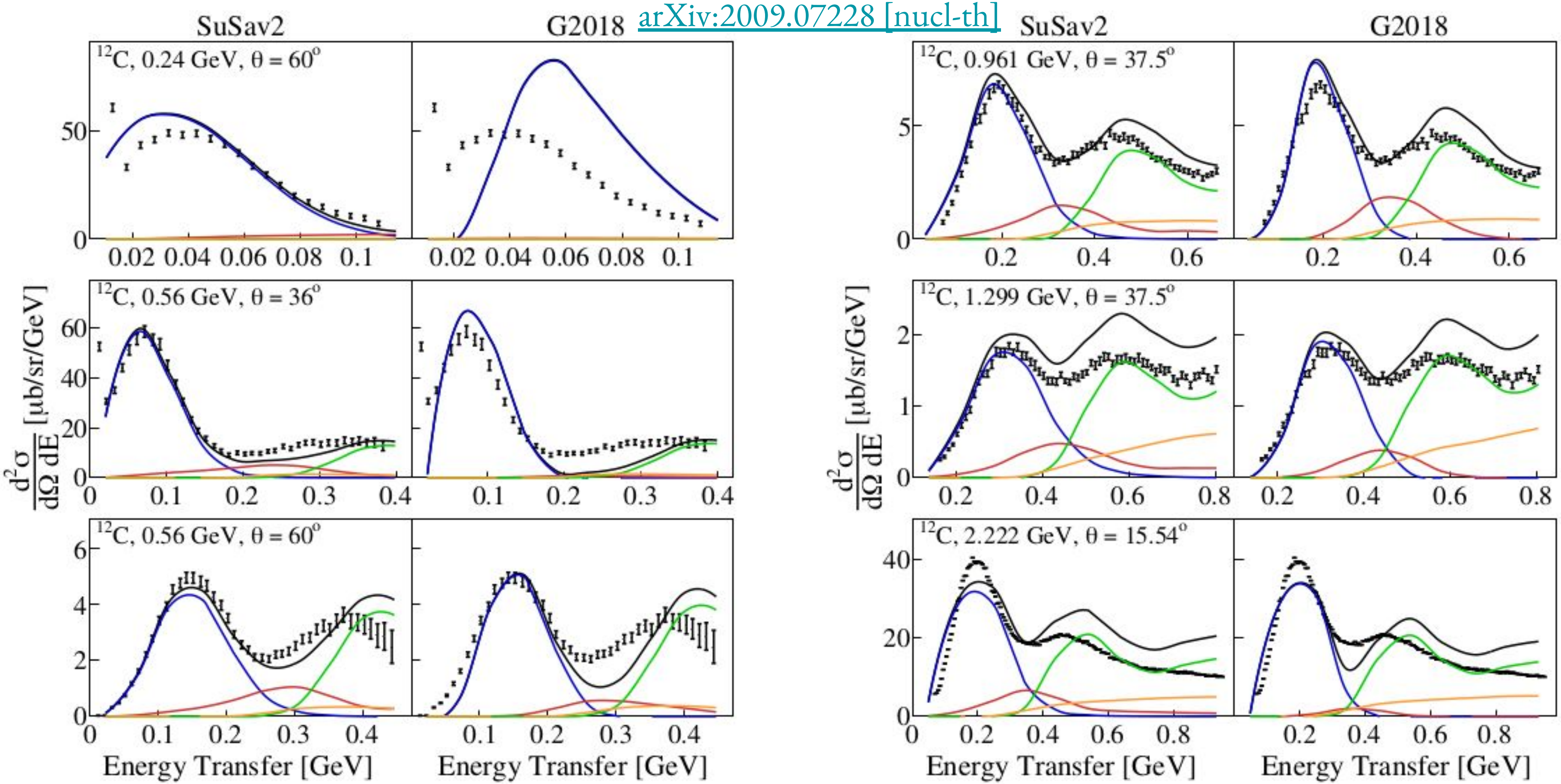

Inclusive Electron Scattering C & Fe

arXiv:2009.07228 [nucl-th]

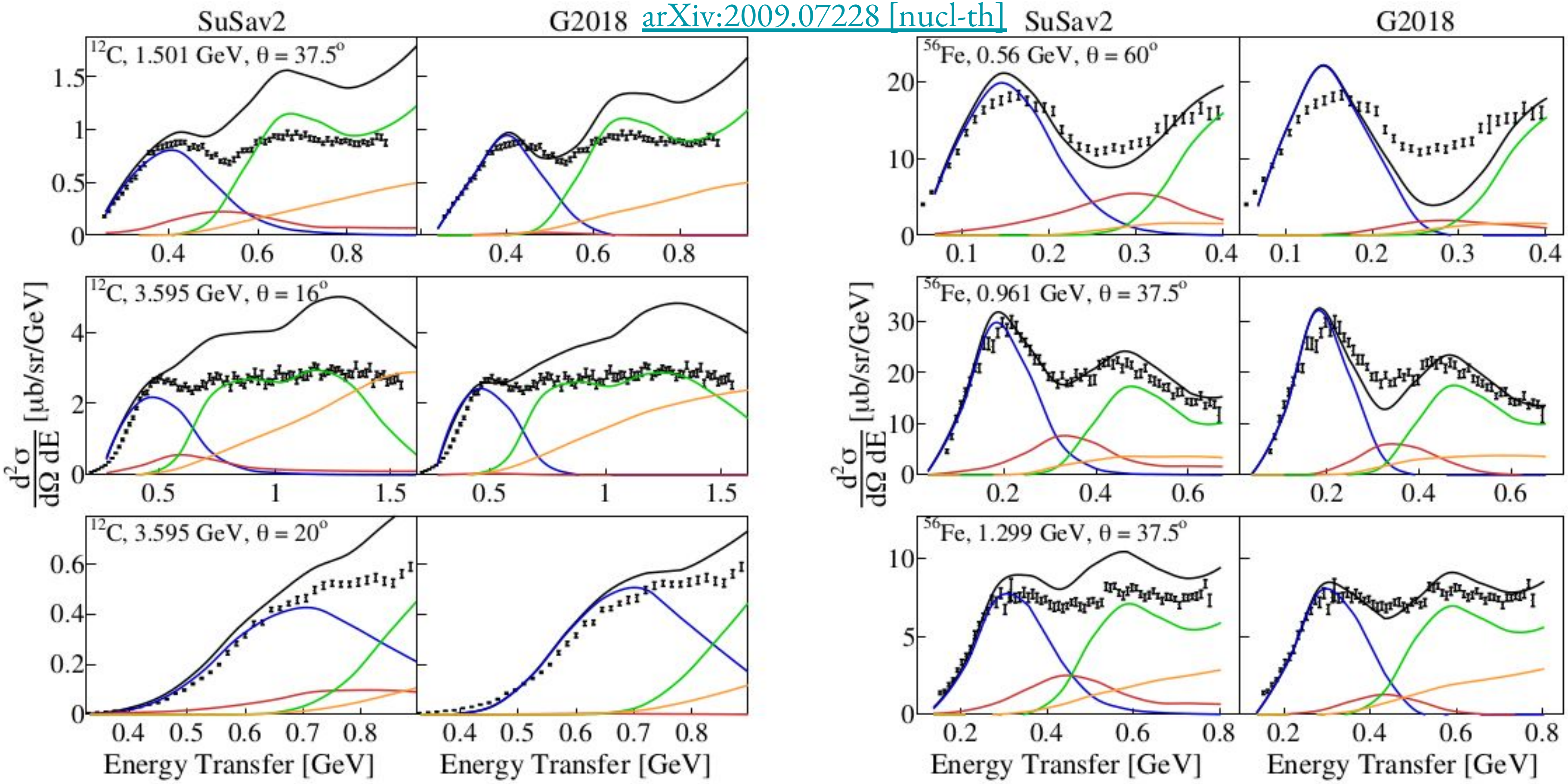

Inclusive Electron Scattering Ar

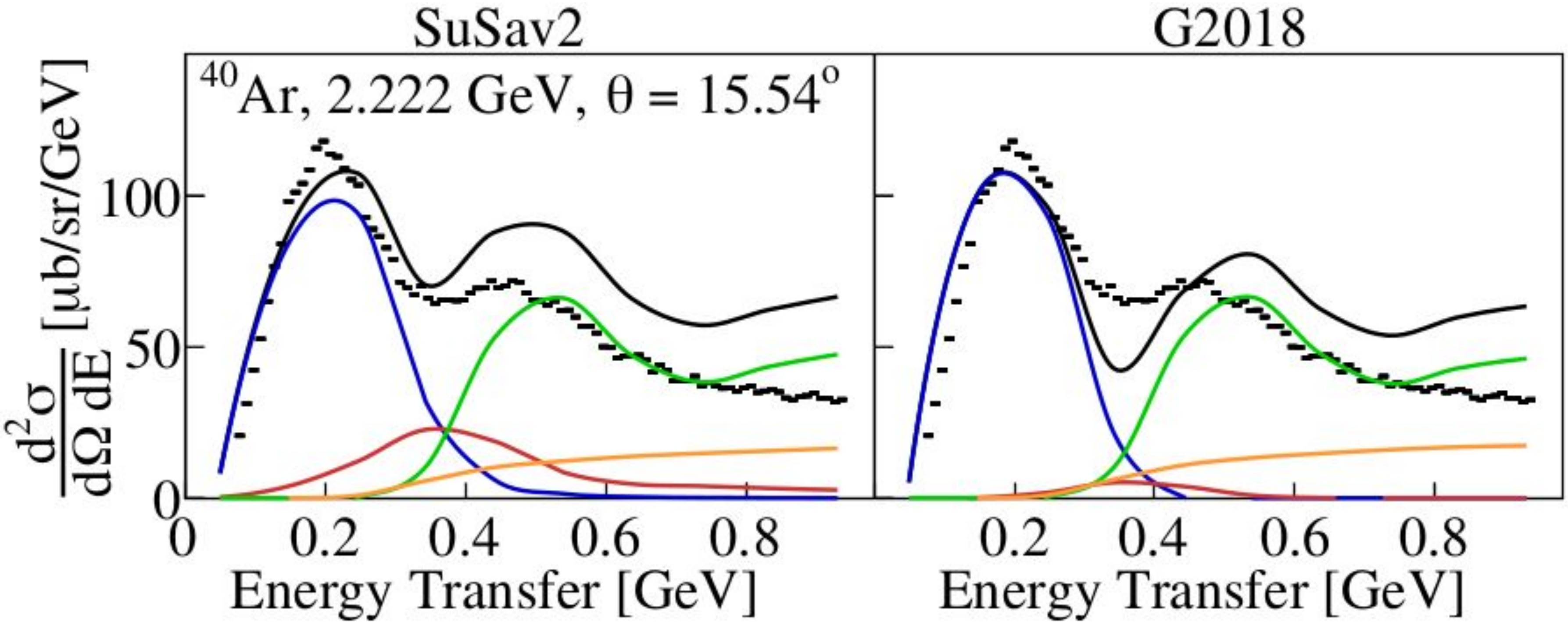

arXiv:2009.07228 [nucl-th]

GENIE v2 vs v3

v2

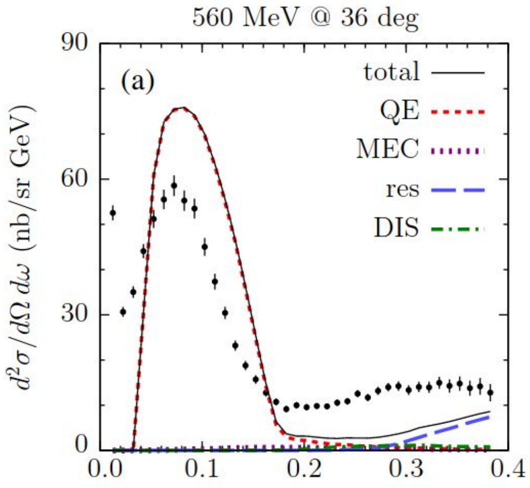

[PRD 102, 053001 (2020)]

v3

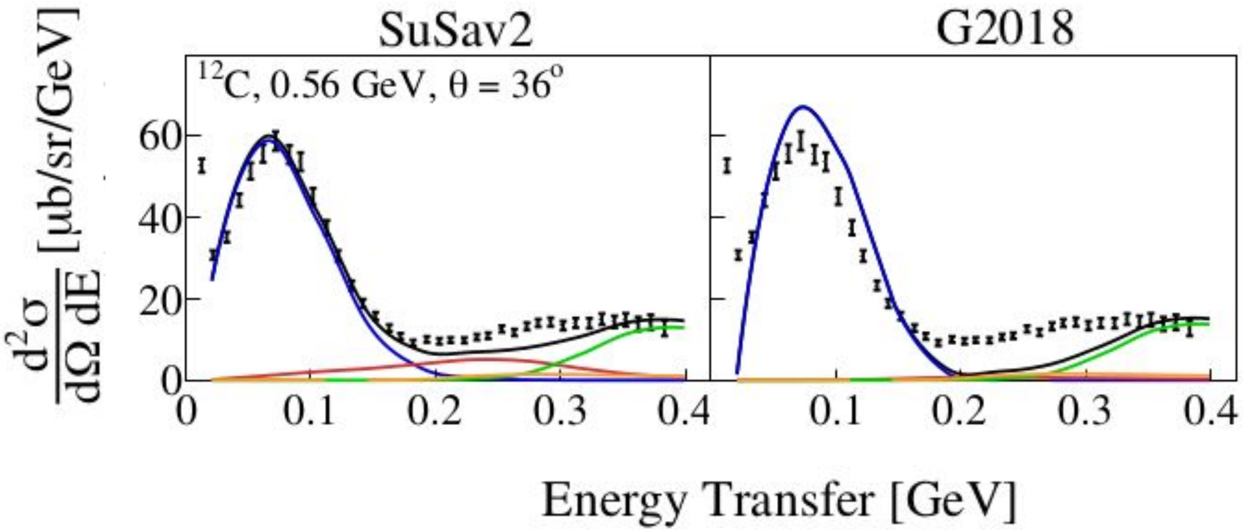

[arXiv:2009.07228 [nucl-th]]

GENIE v2 vs v3

v2

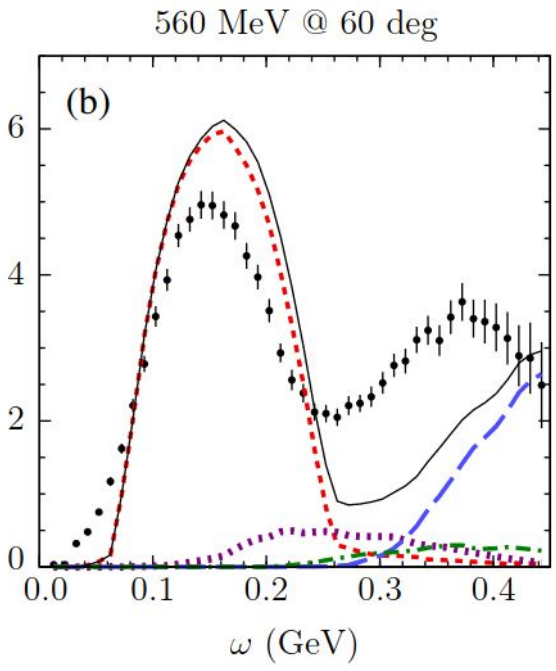

v3

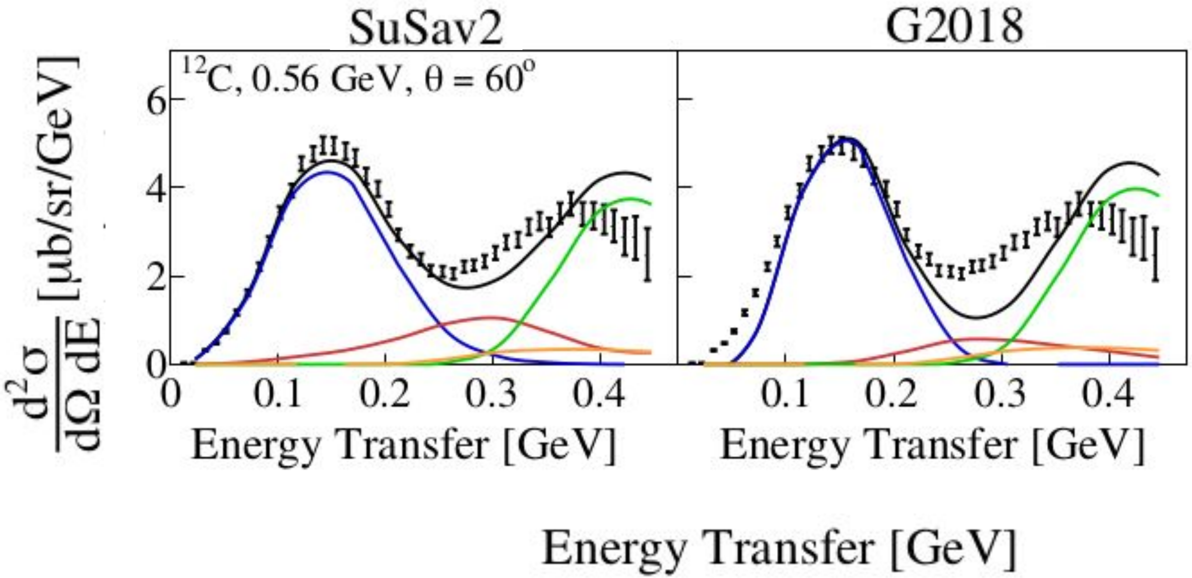

arXiv:2009.07228 [nucl-th]

PRD 102, 053001 (2020)

GENIE v2 vs v3

v2

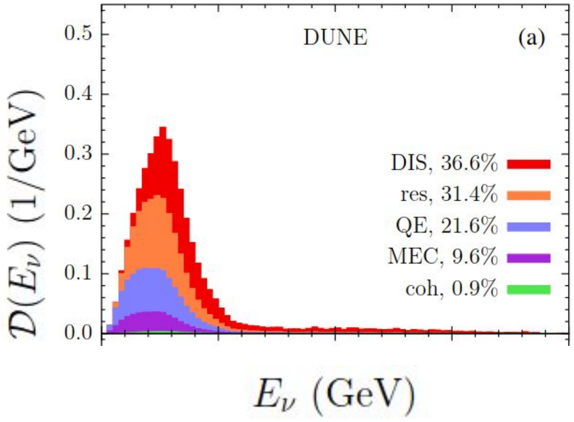

[PRD 102, 053001 (2020)]

v3

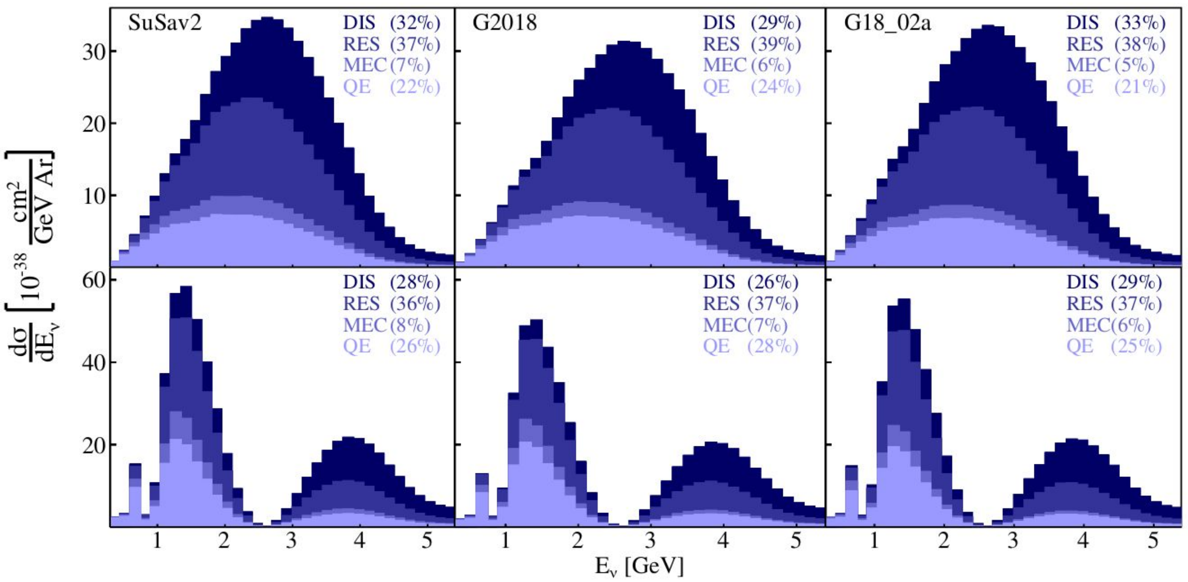

[arXiv:2009.07228 [nucl-th]]

GENIE v2 vs v3

v2

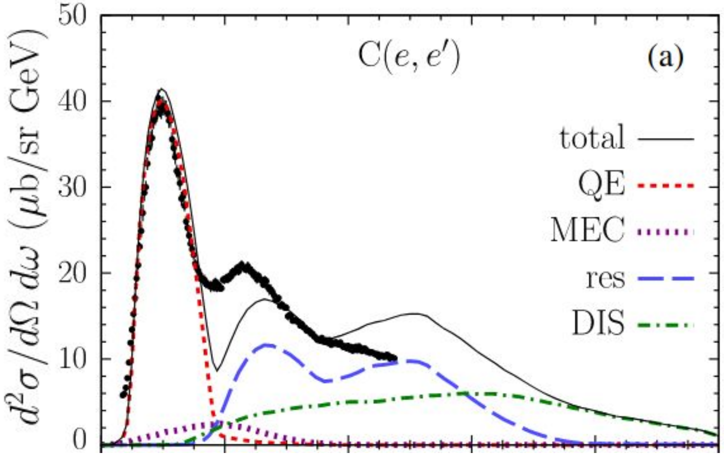

v3

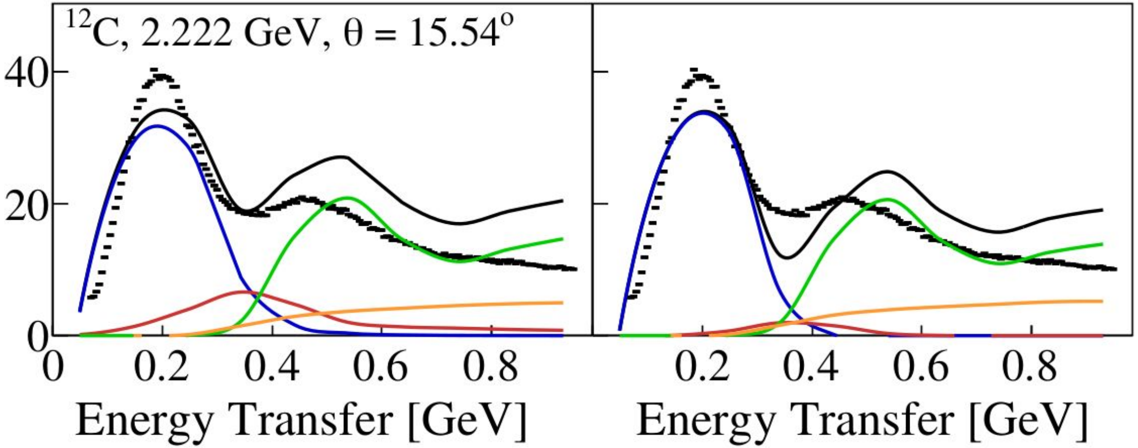

PRD 102, 053001 (2020)

arXiv:2009.07228 [nucl-th]

GENIE v2 vs v3

v2

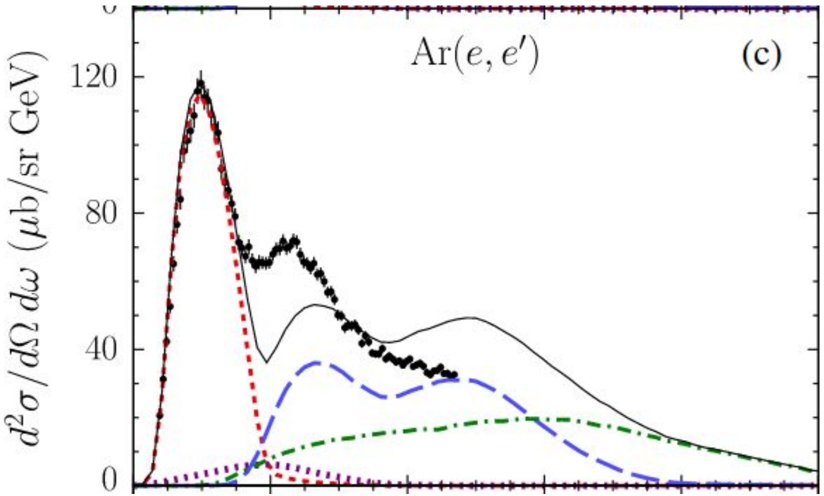

v3

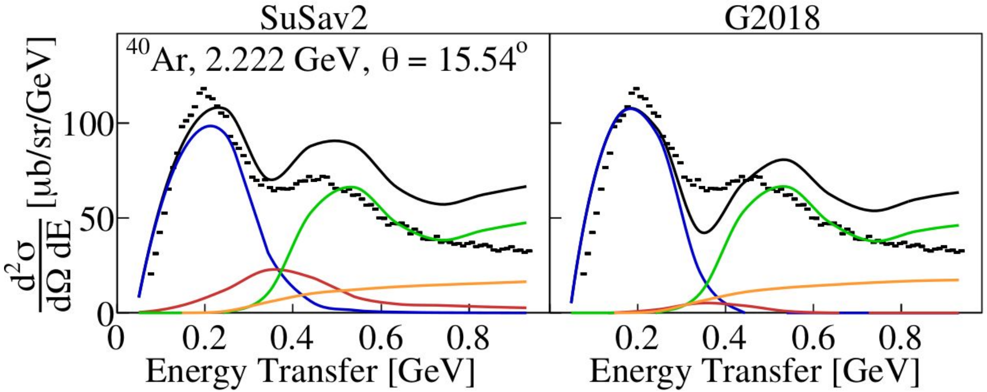

PRD 102, 053001 (2020)

arXiv:2009.07228 [nucl-th]

GENIE v2 vs v3

v2

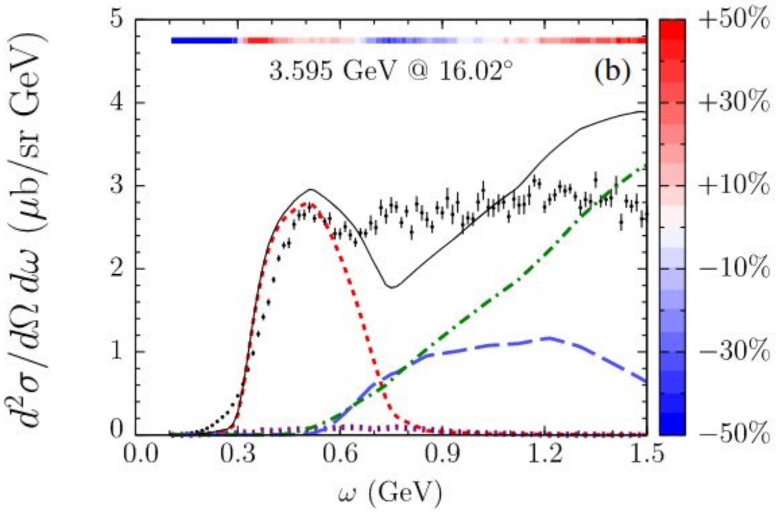

v3

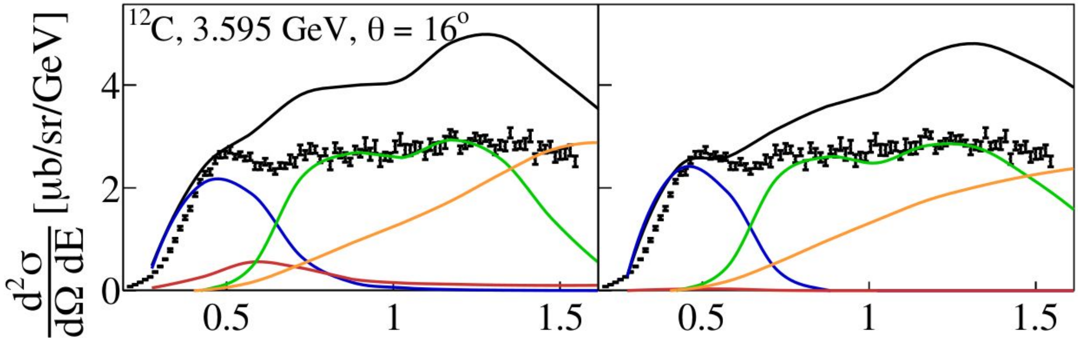

PRD 102, 053001 (2020)

arXiv:2009.07228 [nucl-th]

Mismodelling Impact On Mixing Parameters

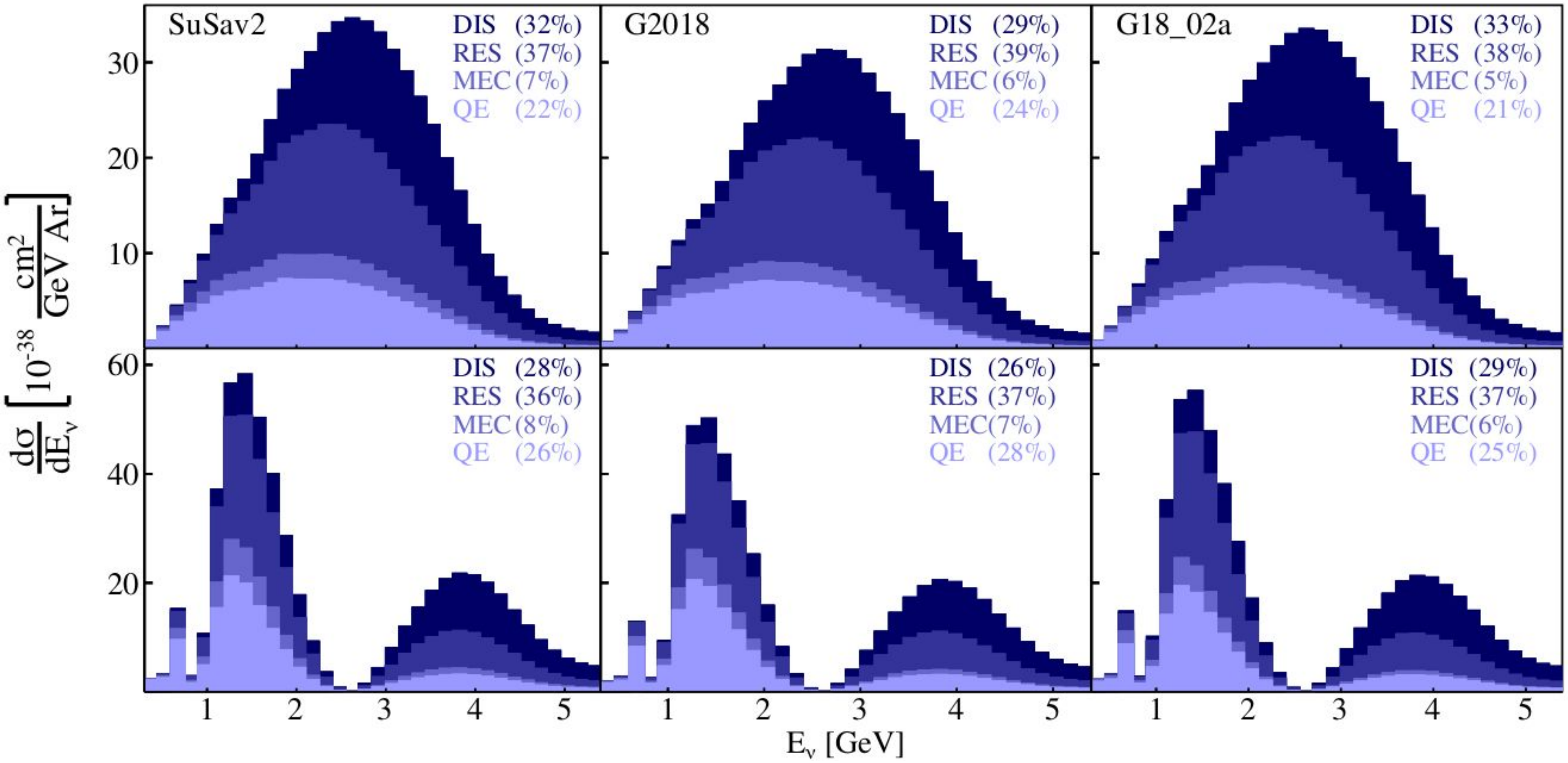

arXiv:2009.07228 [nucl-th]

Mismodelling Impact On Mixing Parameters

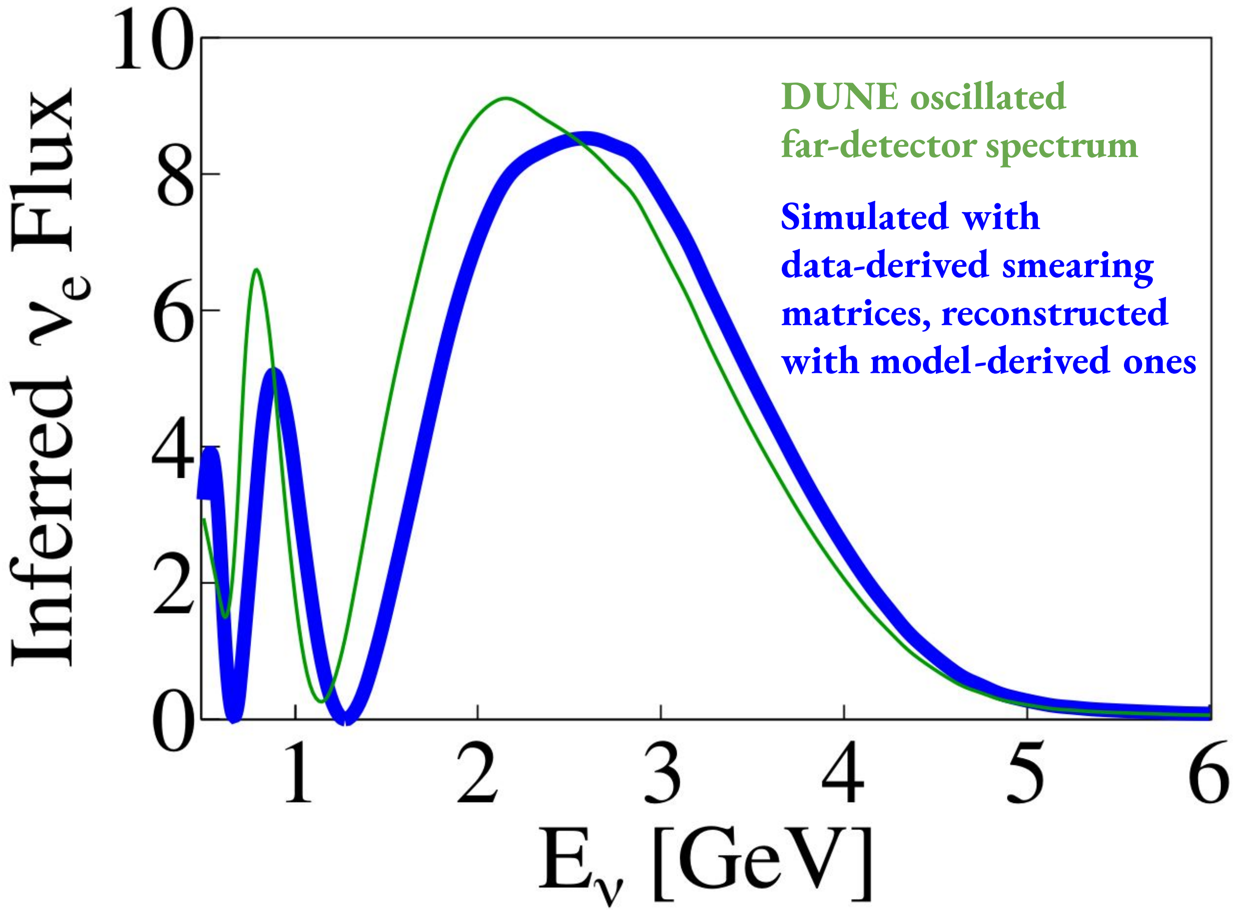

Available Data Sets

- Targets
  ^{4}He, ^{12}C, ^{56}Fe

T2K	H_2O
NOvA	CH
SBN Program, DUNE	Ar

- Energies
  1, 2 & 4 GeV

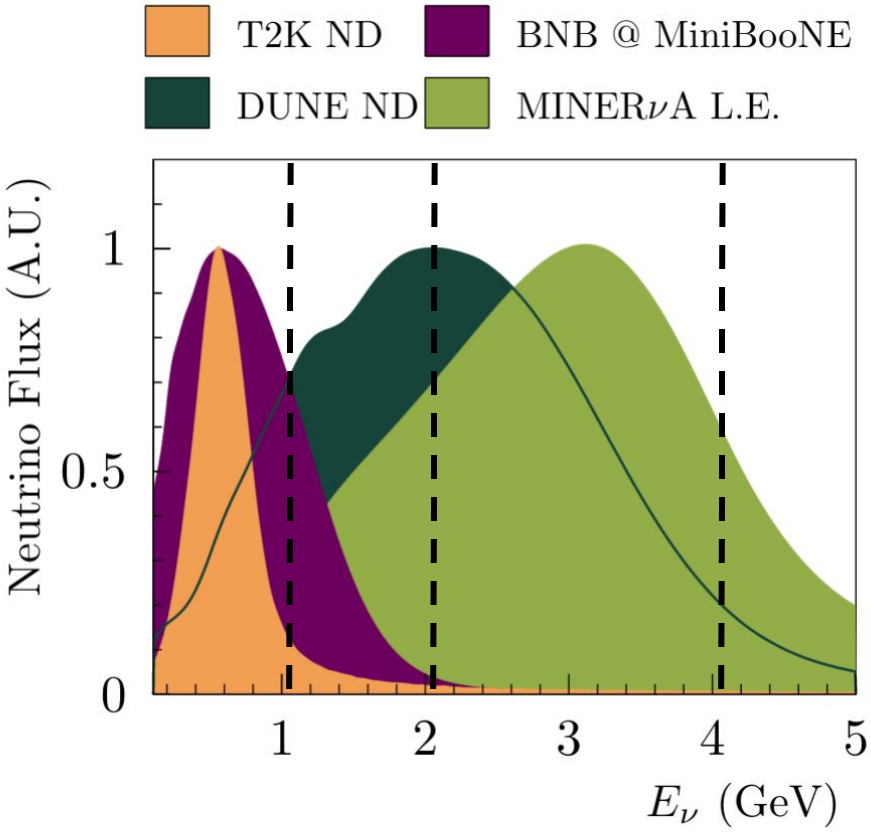

Credit: L. Pickering

Nuclear Model Impact

arXiv:2009.07228 [nucl-th]

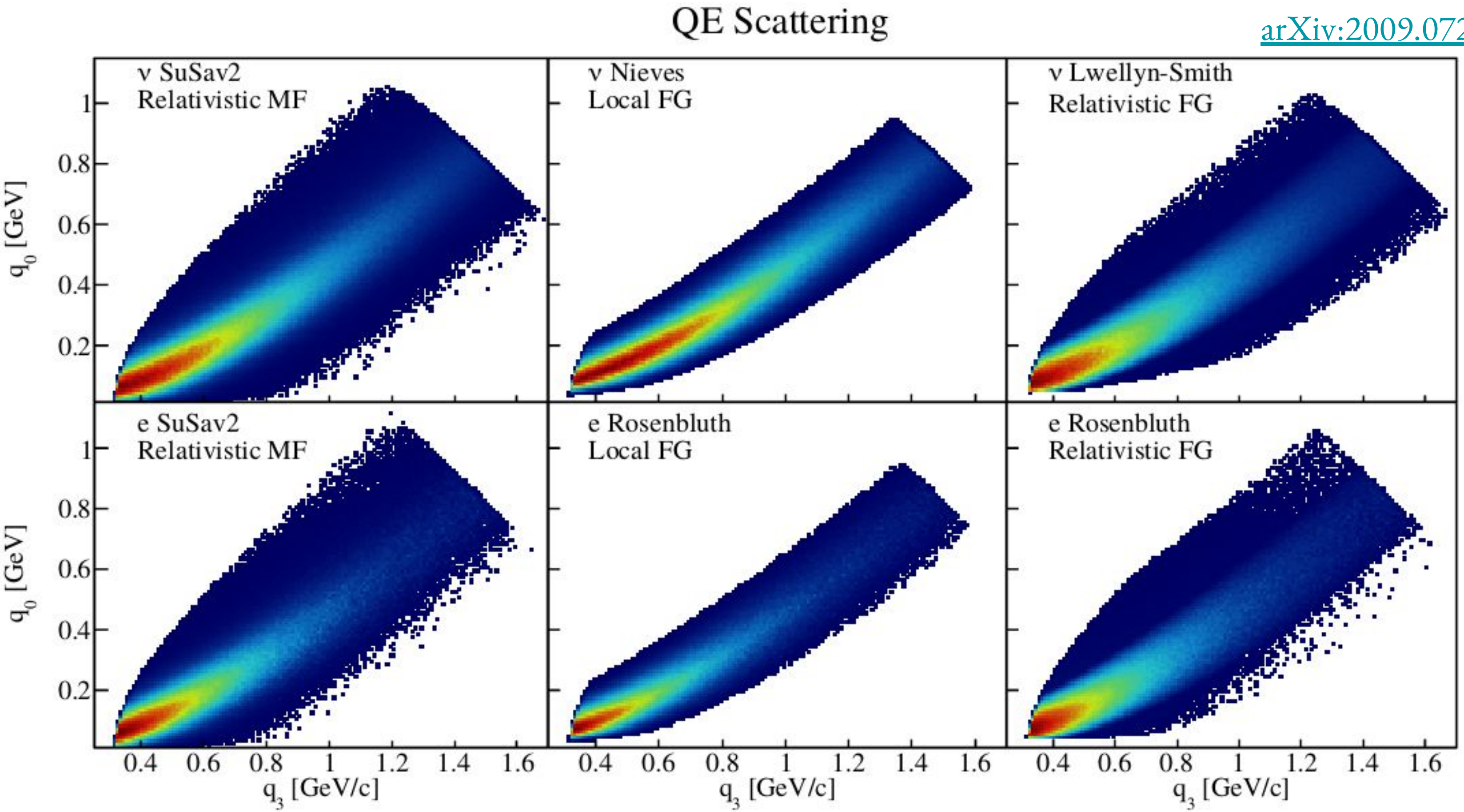

Background Subtraction

Non-(e,e'p) interactions lead to multi-hadron final states
Gaps make them look like (e,e'p) events

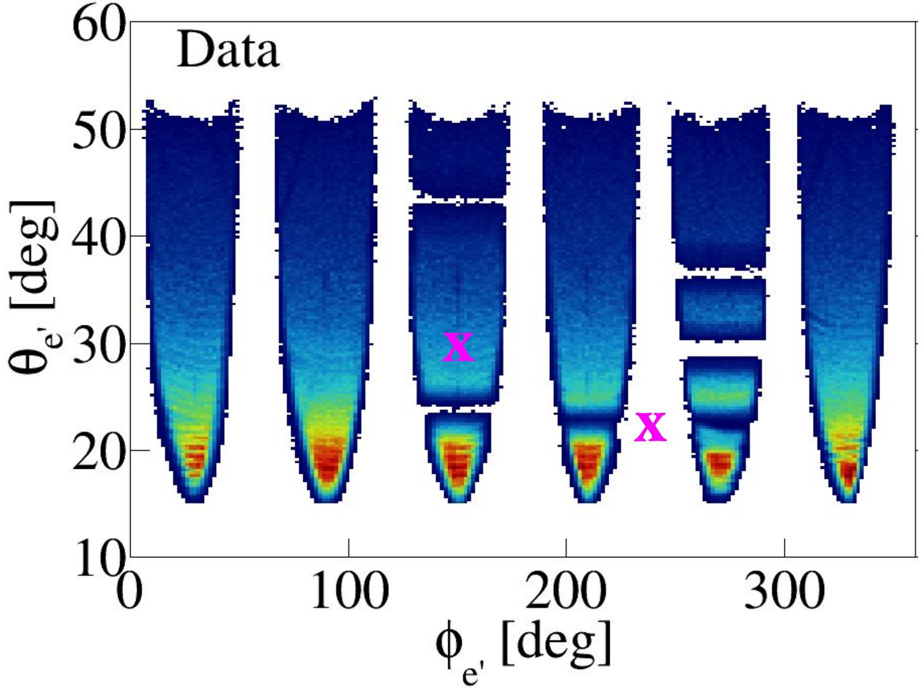

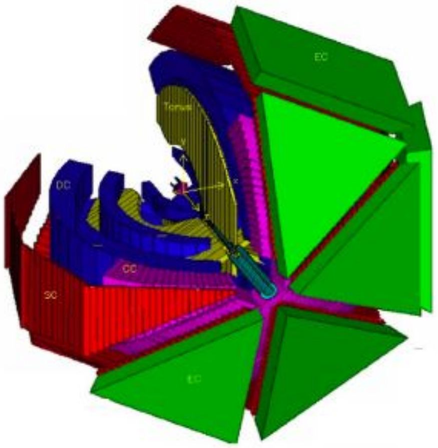

Data Driven Correction

Non-(e,e'p) interactions lead to multi-hadron final states
Gaps make them look like (e,e'p) events

- Use measured (e,e'pπ) events
- Rotate p, π around q to determine π detection efficiency
- Subtract undetected (e,e'pπ)
- Repeat for higher hadron multiplicities

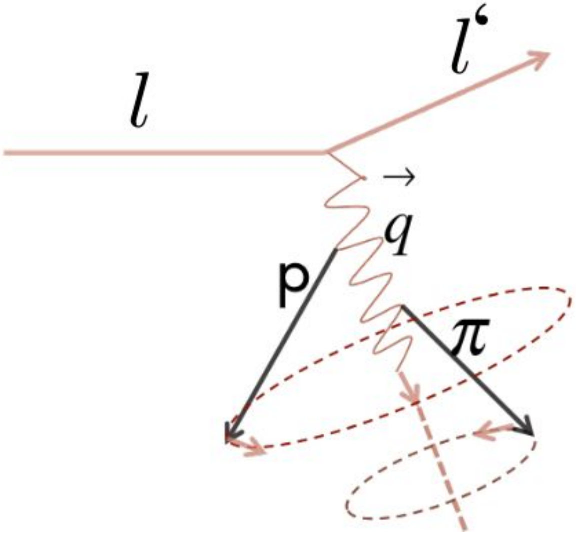

FSI Effects

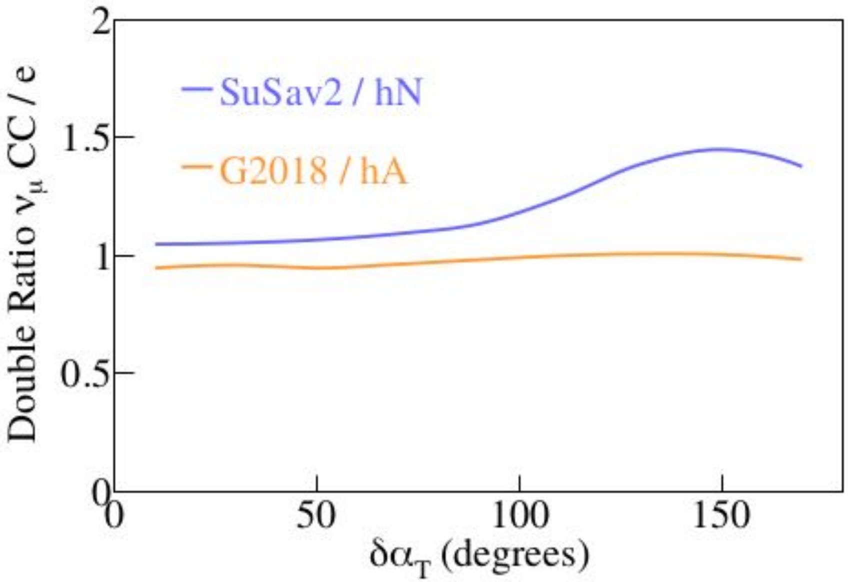

FIG. 13. Illustration the effect of FSI on $\delta\alpha_T$ on ^{12}C at 1.161 GeV for a QE selection with $Q^2 \geq 0.1\,GeV^2/c^2$ requiring exactly one proton with $P_p \geq 300$ MeV/c, no charged pions with $P_\pi \geq 70$ MeV/c and no neutral pions or photons of any momenta. The electron events have been scaled by Q^4.

Migration Matrices: Data vs SuSav2

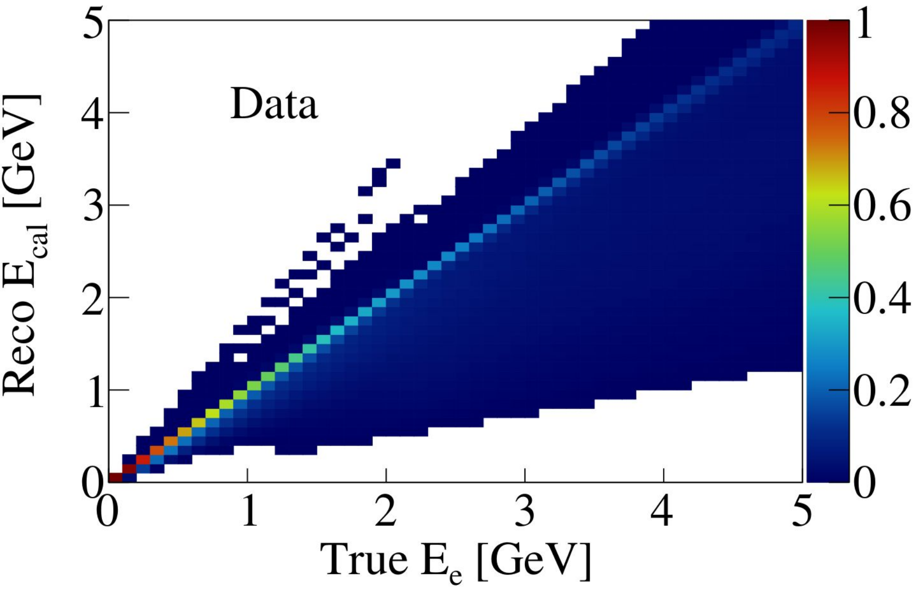

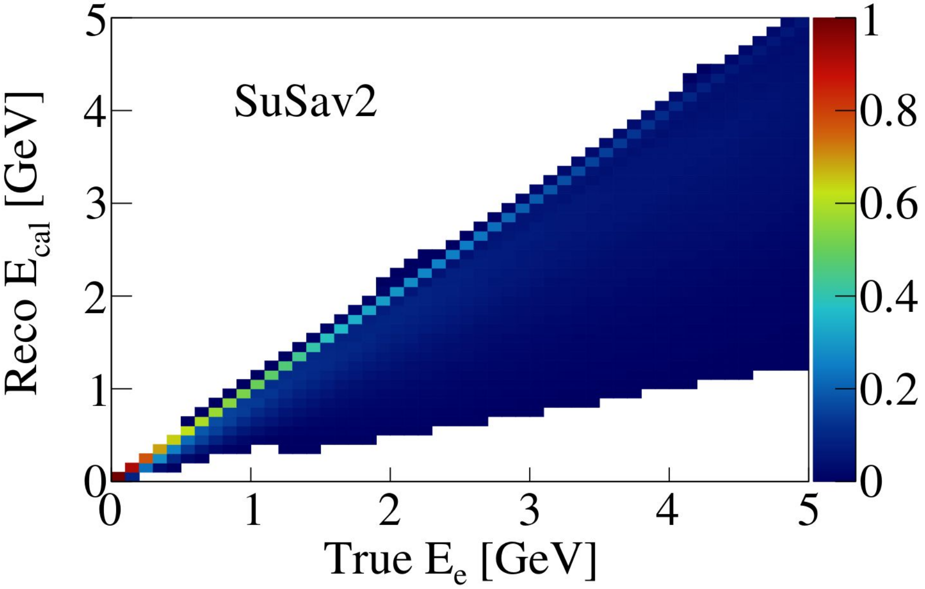

Migration Matrices: Data vs G2018

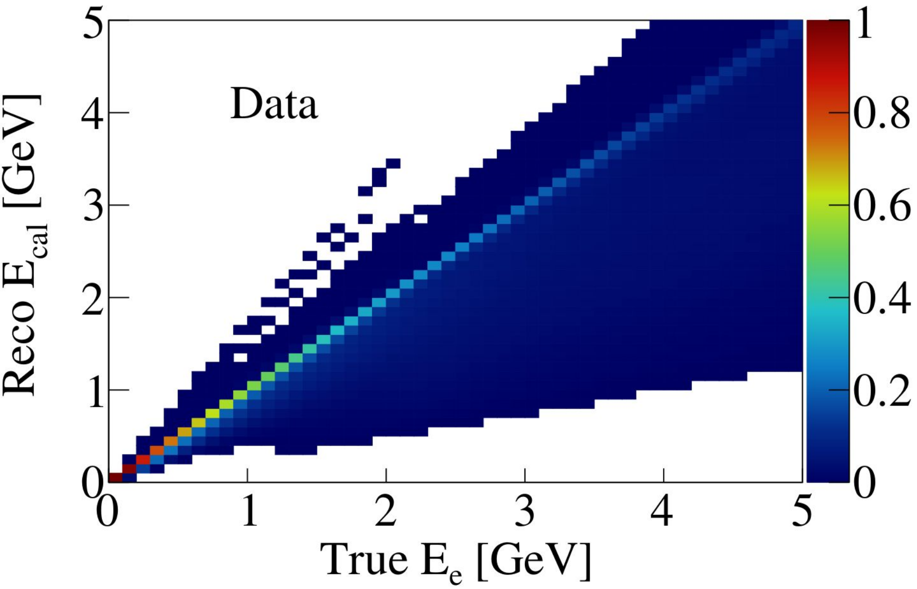

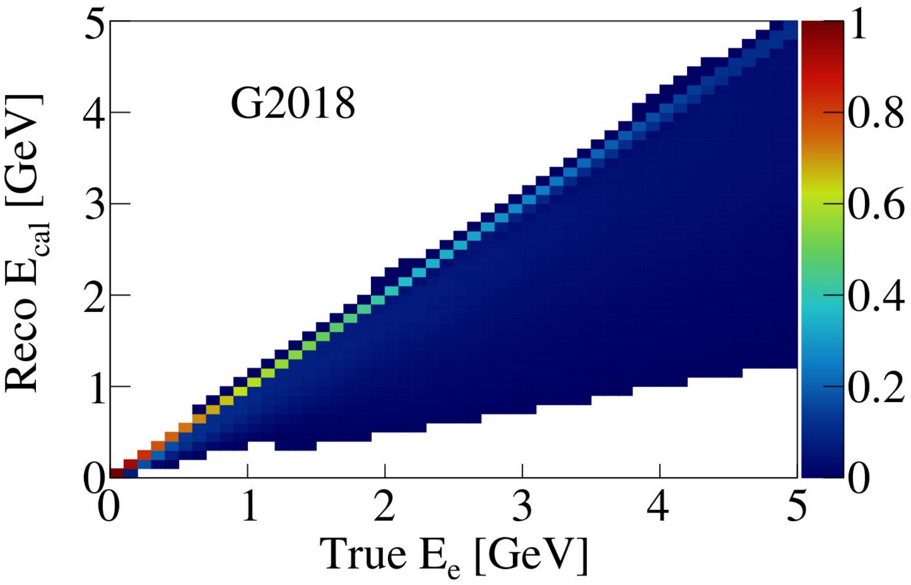

Electrons vs Neutrinos

Where are the remaining differences coming from ?

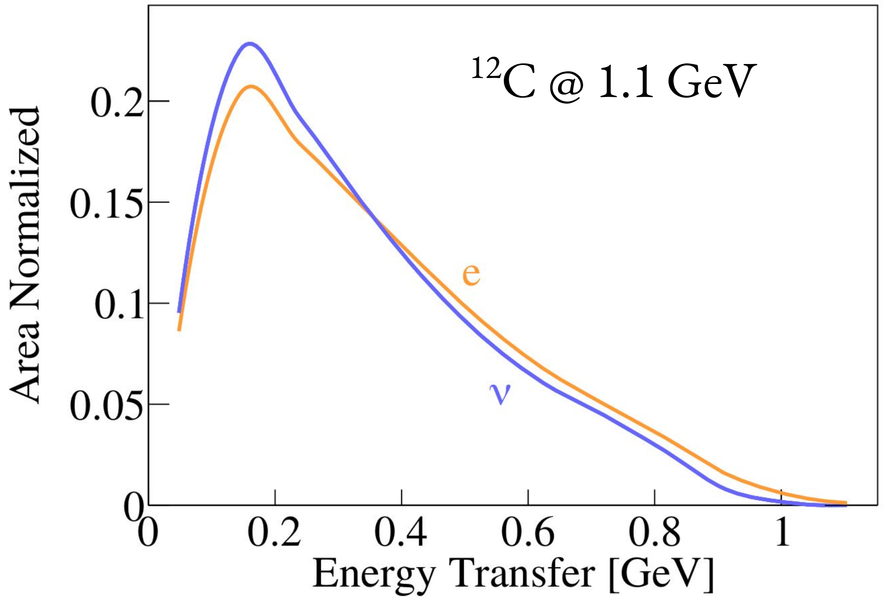

Using SuSav2 / GTEST19_10b_00_000

$$\frac{d^2\sigma^e}{dx dQ^2} = \frac{4\pi\alpha^2}{Q^4}\left[\frac{1-y}{x}F_2^e(x,Q^2) + y^2 F_1^e(x,Q^2)\right] . (1)$$

Here F_1^e and F_2^e are the standard electromagnetic vector structure functions, $Q^2 = \mathbf{q}^2 - \omega^2$ is the squared momentum transfer and $\mathbf{q}$ and ω are the three-momentum and energy transfers, $x = Q^2/(2m\omega)$ is the Bjorken scaling variable, m is the nucleon mass, $y = \omega/E_e$ is the electron fractional energy loss, and α is the fine structure constant. This formula is valid for $Q^2 \gg m^2$ where the electron-nucleon cross section is simplest. Cross sections at lower Q^2 have more complicated factors multiplying each of the two structure functions.

The corresponding inclusive charged current (CC) $(\nu, l^\pm)$ neutrino-nucleon cross section (where $l^\pm$ is the outgoing charged lepton) has a similar form with the addition of third, axial, structure function:

$$\frac{d^2\sigma^\nu}{dx dQ^2} = \frac{G_F^2}{2\pi}\left[\frac{1-y}{x}F_2^\nu(x,Q^2) + y^2 F_1^\nu(x,Q^2) - y(1-y/2)F_3^\nu(x,Q^2)\right] . \quad (2)$$

Here F_1^ν and F_2^ν are the neutrino-nucleus vector structure functions, F_3^ν is the axial structure function, and G_F is the Fermi constant. The parity-conserving structure functions, F_1^ν and F_2^ν, both include a vector-vector term identical to F_1^e and F_2^e, and an additional axial-axial term. See Refs. [4, 6, 7] for more detail.

SuSav2 Configuration / GTEST19_10b_00_000

	Electrons	**Neutrinos**
QE	SuSav2	SuSav2
MEC	SuSav2	SuSav2
RES	Berger-Sehgal	Berger-Sehgal
DIS	AGKY	AGKY
FSI	hN2018	hN2018
Nuclear Model	Relativistic Mean Field	Relativistic Mean Field

G2018 Configuration / G18_10a_02_11a

	Electrons	Neutrinos
QE	Rosenbluth	Nieves
MEC	Empirical	Nieves
RES	Berger-Sehgal	Berger-Sehgal
DIS	AGKY	AGKY
FSI	hA2018	hA2018
Nuclear Model	Local Fermi Gas	Local Fermi Gas

Closure Test

- Use GENIE files
- Filter specific topologies (e.g. 1p0πp + 1p1π)
- Subtracted & True 1p0π are in good agreement

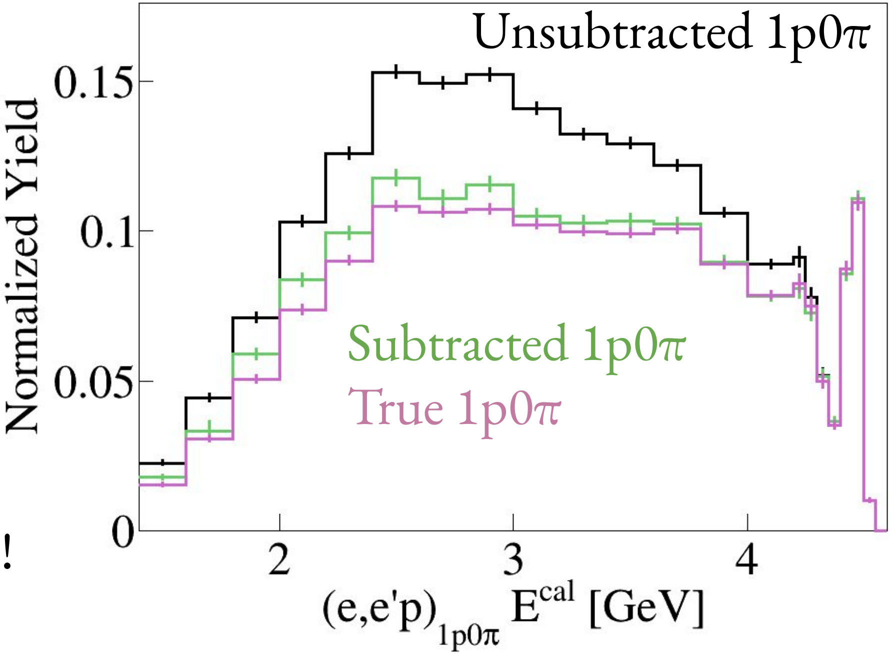

Ready to look at Data/MC comparisons!

Single Transverse Variables (STV)

https://arxiv.org/pdf/1605.00179.pdf

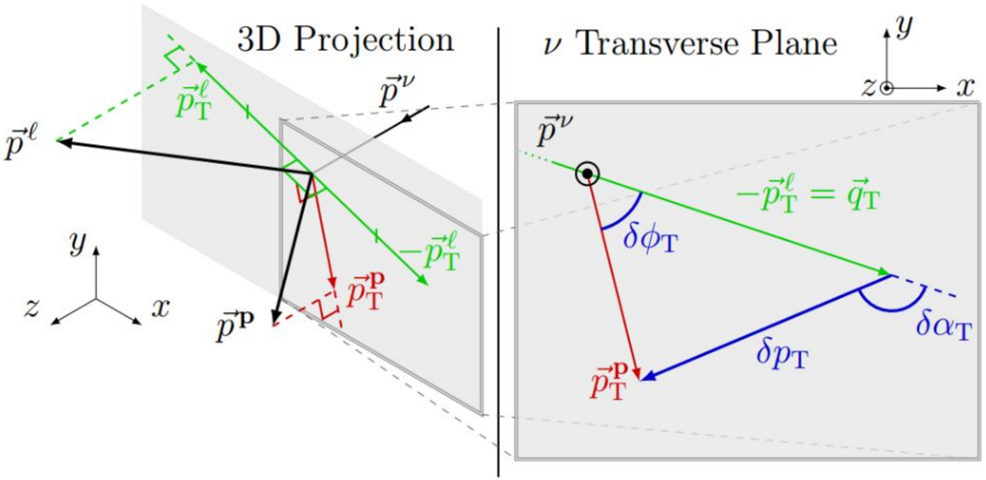

$$\delta\vec{p}_T = \vec{p}_T^{\ell} + \vec{p}_T^{p},$$

$$\delta\phi_T = \arccos\frac{-\vec{p}_T^{\ell}\cdot\vec{p}_T^{N}}{p_T^{\ell}p_T^{N}}, \text{ and}$$

$$\delta\alpha_T = \arccos\frac{-\vec{p}_T^{\ell}\cdot\delta\vec{p}_T}{p_T^{\ell}\delta p_T}.$$

Well defined signal definition: Min θ_e Cut

@ 1.1 GeV: $\theta = 17 + 7 / P$

@ 2.2 GeV: $\theta = 16 + 10.5 / P$

@ 4.4 GeV: $\theta = 13.5 + 15 / P$

See backup for p / $\pi^{+/-}$ definitions

- We do not acceptance correct below min θ

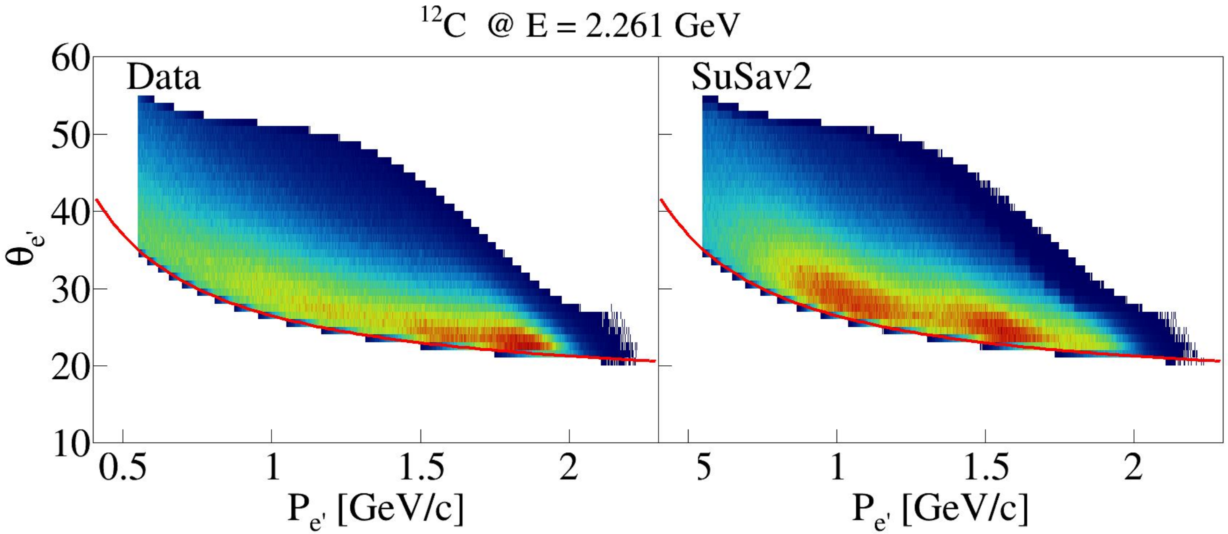

Well defined signal definition: Min θ_e Cut

@ 1.1 GeV: $\theta = 17 + 7 / P$

@ 2.2 GeV: $\theta = 16 + 10.5 / P$

@ 4.4 GeV: $\theta = 13.5 + 15 / P$

See backup for p / $\pi^{+/-}$ definitions

- We do not acceptance correct below min θ

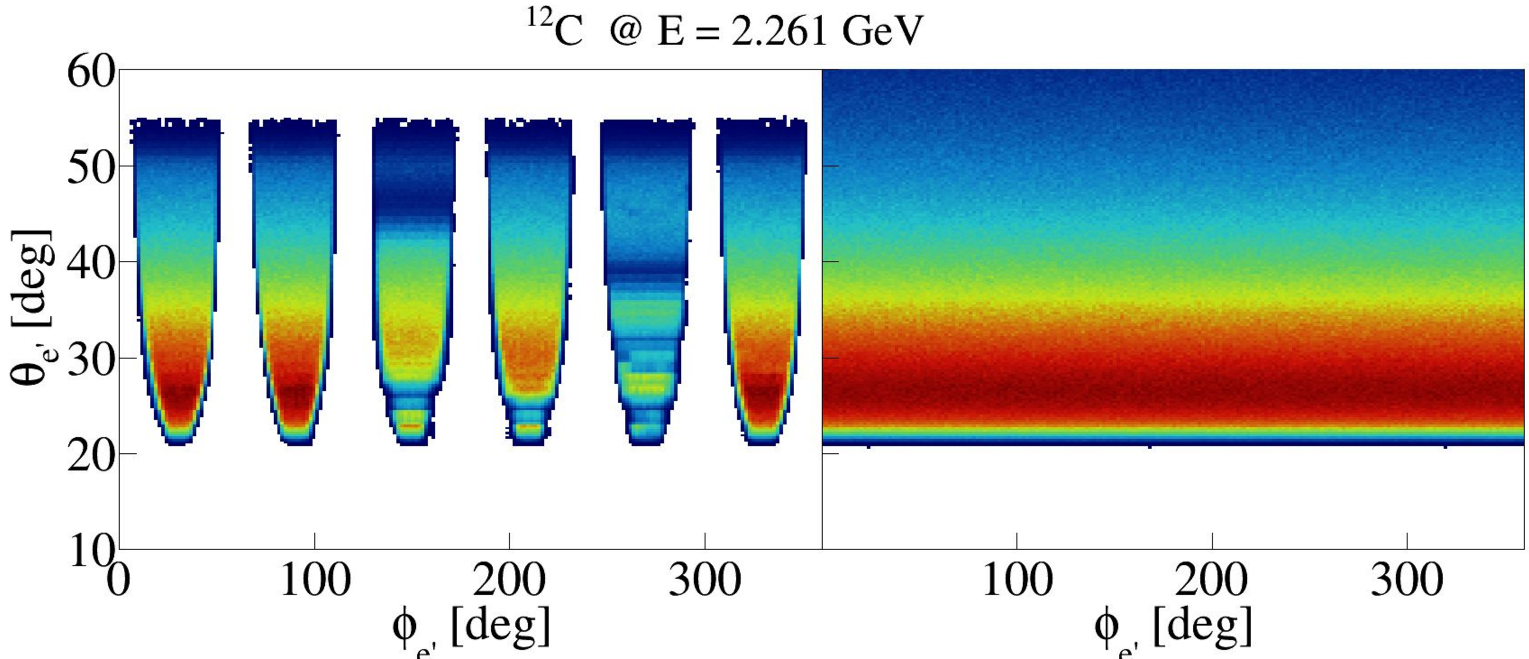

Min θ_p Cut = 12 deg

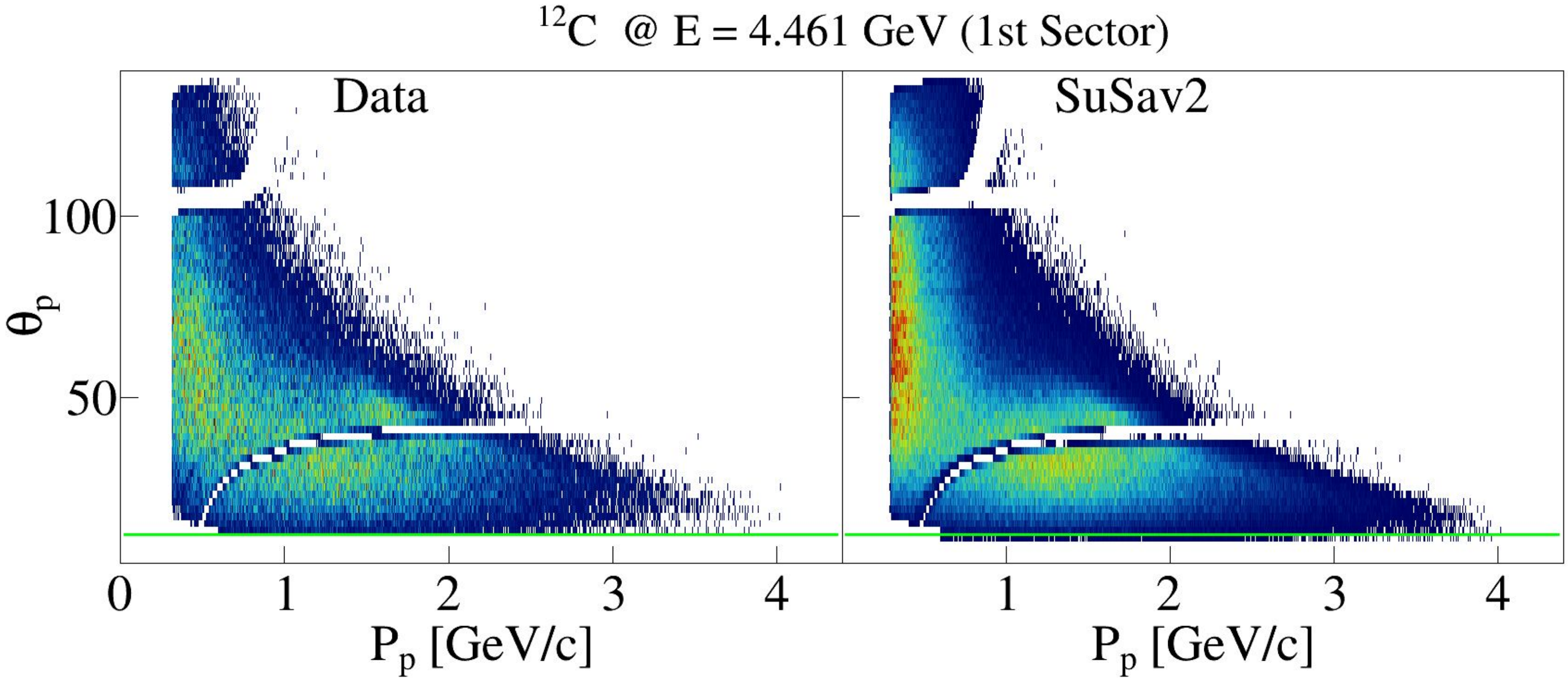

Min $\theta_{\pi+}$ Cut = 12 deg

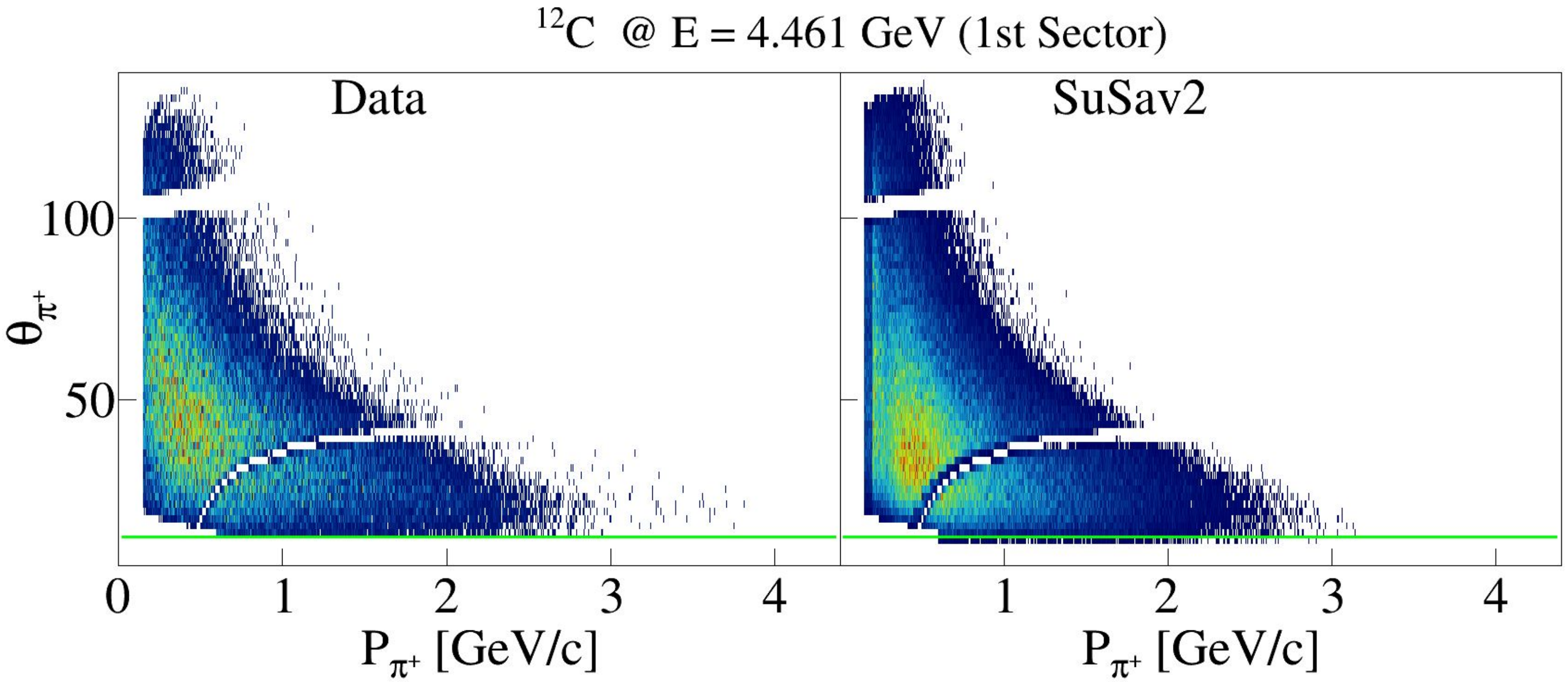

Min θ_{π^-} Cut

@ 1.1 GeV: $\theta = 17 + 4 / P$

@ 2.2 GeV: $\theta = (P<0.35)*(25+7/P) + (P>0.35)*(16+10/P)$

@ 4.4 GeV: $\theta = (P<0.35)*(25+7/P) + (P>0.35)*(16+10/P)$

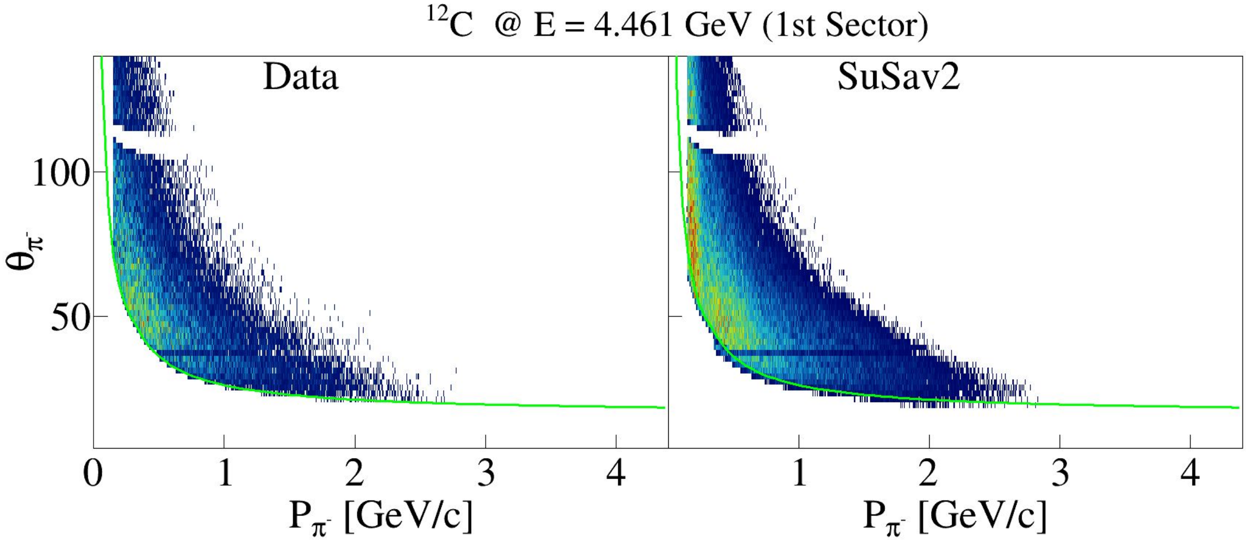

Systematics: Number of rotations

5.1 Statistical uncertainty due to the number of rotations

The statistical uncertainty due to the number of rotations contributes to the uncertainty of the obtained weights used for subtraction for undetected hadrons. This can be described by the uncertainty of probability in binomial distribution given by

$$\sigma = \frac{n}{N}\sqrt{\frac{1}{n} - \frac{1}{N}} \tag{36}$$

$$\lim_{n \to 0} \sigma = \frac{\sqrt{n}}{N} \tag{37}$$

$$\lim_{n \to N} \sigma = \frac{\sqrt{N - n}}{N} \tag{38}$$

where N is the total number of trials and n is the number of successes, and is kept small with sufficient number of rotation (is not included in uncertainty calculation).

Systematics: pion electro-production angular cross section dependence

$$\frac{d\sigma}{d\Omega_\pi^*}(W, Q^2, \theta_\pi, \phi_\pi) = A + B\cos\phi_\pi + C\cos 2\phi_\pi \tag{43}$$

$$A = (\sigma_{\rm T} + \epsilon\sigma_{\rm L})\frac{p_\pi^*}{k_\gamma^*} \tag{44}$$

$$B = \sigma_{\rm LT}\frac{p_\pi^*}{k_\gamma^*}\sin\theta_\pi\sqrt{2\epsilon(\epsilon+1)} \tag{45}$$

$$C = \sigma_{\rm TT}\frac{p_\pi^*}{k_\gamma^*}\sin^2\theta_\pi\epsilon \tag{46}$$

where p_π^*, θ_π and ϕ_π are the absolute value of the three momentum, polar and azimuthal angles of the π^0 in the CM-frame, and $k_\gamma^* = k_\gamma M/W$. ϕ_π is shown in Fig. 181 and is the azimuthal angle between the hadronic and leptonic planes and θ_π is the angle between the direction of the pion and the virtual photon. These expressions are taken from $\pi^0 p$ electroproduction studies in [23], but they can also be used for charged pion production studies, like in our case.

When subtracting for undetected one pion events in inclusive analysis we have assumed that the second and third terms on the right side of the Eq. 43 are negligible compared to the first term, and so the dependence of the cross section on ϕ_π can be neglected. To check if this assumptions is valid or not we have estimated the number of undetected 1 charged pion events with and without taking into account the ϕ_π dependence of the cross section, and have found that both lead to similar results.

For this study we have used the values of exclusive structure functions $\sigma_{\rm T} + \epsilon\sigma_{\rm L}$, $\sigma_{\rm TT}$ and $\sigma_{\rm LT}$ from [23] shown for $\cos\theta_\pi = 0.1$ and $0.4 \leq Q^2 \leq 1$ GeV^2. We have used the biggest provided absolute values $\sigma_{\rm T} + \epsilon\sigma_{\rm L} = 30$ μb, $\sigma_{\rm TT} = -10$ μb and $\sigma_{\rm LT} = -2$ μb corresponding to $Q^2 = 0.45$ GeV^2.

Systematics: pion electro-production angular cross section dependence

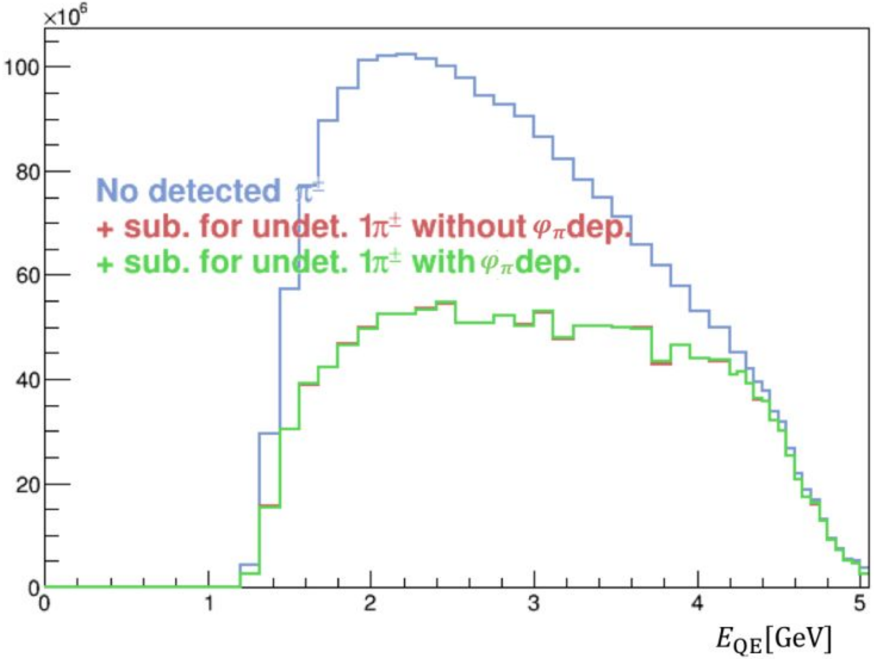

Figure 182: E_{QE} 0 pi spectrum for $A(e, e')$ subtracted for undetected 1 charged pion events with (green) and without (red) accounting for ϕ_π dependence of the cross section at 4.4 GeV for ^{56}Fe target.

Systematics: Photon Identification Cut

5.3 Systematic uncertainty due to photon identification cut

In order to separate photons from neutrons, we cut on the neutral particle velocity. The velocity distribution of neutral particles has a peak at $\beta = 1$ corresponding to photons and

155

another at lower velocity corresponding to neutrons. To select photons we cut 2σ to the left of the photon peak and select the region above it. At 1.161 GeV we cut 3σ away from the photon peak as the neutron and photon peaks are well separated at this energy. The photon selection cuts for all the targets and beam energies are listed in Table.8.

In addition to the β cut, we require the energy of the photons to be greater than 0.3 GeV. This additional PID cut applied on photon reduces the estimated photon contamination. Therefore we add a 3% systematic uncertainty to the photon subtraction.

Systematics: Photon Identification Cut

Beam energy	Target	Cuts on β_{EC}	Δt_{EC}^{offset} for different sectors 1	2	3	4	5	6
1.1 GeV	^{3}He	0.89	−0.73	−0.81	−0.91	−0.94	−0.92	−0.81
	^{12}C	0.89	−0.71	−0.77	−0.87	−0.91	−0.89	−0.79
2.2 GeV	^{3}He	0.93	−1.37	−1.42	−1.55	−1.53	−1.49	−1.44
	^{4}He	0.92	0.72	0.27	0.16	0.21	0.22	0.21
	^{12}C	0.92	0.50	0.39	0.29	0.29	0.32	0.33
	^{56}Fe	0.90	0.75	0.49	0.37	0.39	0.43	0.44
4.4 GeV	^{3}He	0.92	−0.15	−0.26	−0.41	−0.29	−0.25	−0.23
	^{4}He	0.91	−0.01	−0.11	−0.23	−0.26	−0.21	−0.09
	^{12}C	0.92	−0.01	−0.11	−0.23	−0.27	−0.21	−0.08
	^{56}Fe	0.91	−0.49	−0.14	−0.32	−0.25	−0.17	−0.35

Table 8: The EC timing offsets for different sectors and the cuts applied on the velocity of neutral particles to select photons for all targets at 2.2 and 4.4 GeV.

Systematics: Fiducial cuts on undetected particle subtraction

5.4 Effect of fiducial cuts on undetected particle subtraction

If we were able to obtain the ideal fiducial cuts that describe perfectly the geometrical acceptance with flat detection efficiency for different particles, our energy reconstruction results would be independent of how tight or wide the geometrical acceptance is. This is however hard to achieve in real analysis. We have estimated the sensitivity of energy reconstruction results to the change in geometrical acceptance. We have obtained the reconstructed energy spectra after changing the original fiducial cuts for charged pions and photons in different CLAS sectors. We have moved the left and right sides of θ vs ϕ distribution outline inwards in ϕ by 3^o. This results in the geometrical acceptance in each sector becoming narrower by 6^o in ϕ. We have applied this change to the geometrical acceptances of charged pions and photons. We have then compared the reconstructed energy spectra obtained with original fiducial cuts to the ones obtained with modified tighter fiducial cuts. The plots for E_{calor} energy reconstruction

Systematics: Fiducial cuts on undetected particle subtraction

The systematic uncertainty due to the change in geometrical acceptance is the RMS of these two results obtained using the original and modified geometrical acceptances. The systematic uncertainty for each bin in reconstructed energy spectrum is calculated the same way as in the previous section and is given by the following formula:

$$x^i_{\mathrm{RMS}} = \sqrt{\frac{(x^i_1 - x^i_{\mathrm{mean}})^2 + (x^i_2 - x^i_{\mathrm{mean}})^2}{2}} \tag{50}$$

where x^i_{mean} is the mean bin content for bin i and is equal to $x^i_{\mathrm{mean}} = (x^i_1 + x^i_2)/2$, where x^i_1 and x^i_2 are the contents of the ith bin of the 1st and 2nd results.

The ratio of $\sigma_{E_{\mathrm{cal}}}$ systematic uncertainty distributions over the E_{cal} reconstructed energy spectra are shown on the right side of Figure 186. This uncertainty is the biggest at 4.4 GeV analysis and is below 4%. At 2.2 GeV analysis it is less than 1.2% and at 1.1 GeV it is less than 0.8%.

Systematics: Sector Dependence

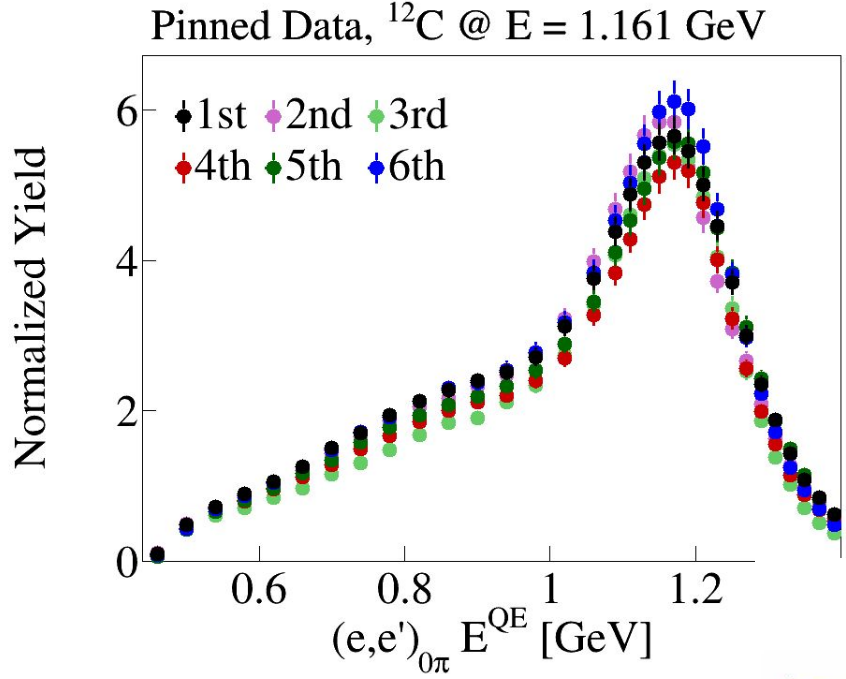

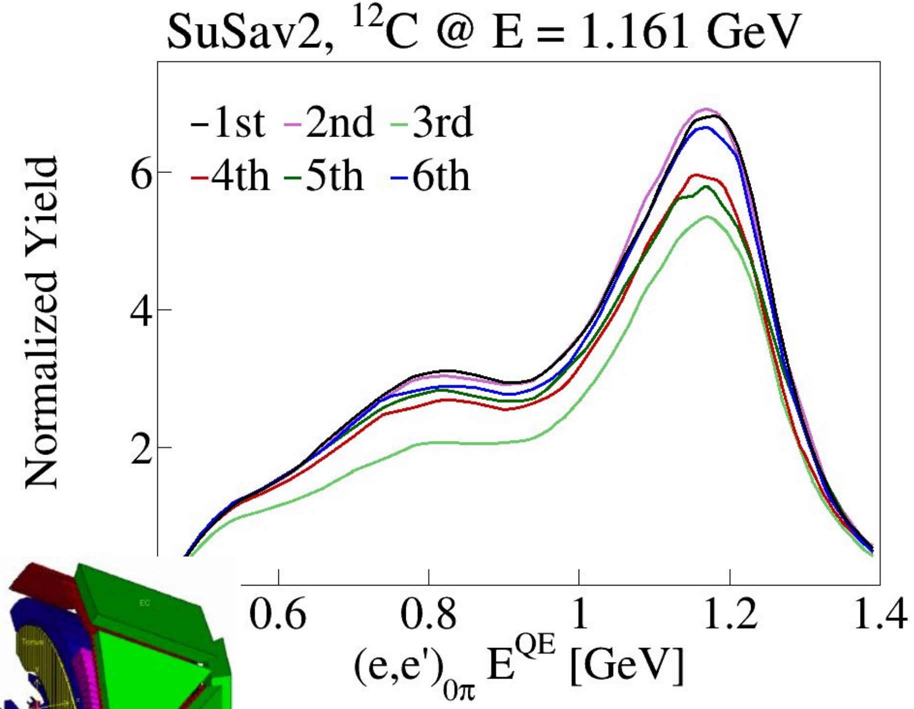

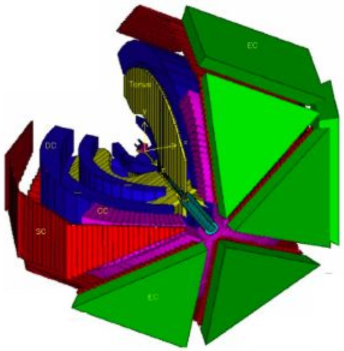

Systematics: Sector Dependence

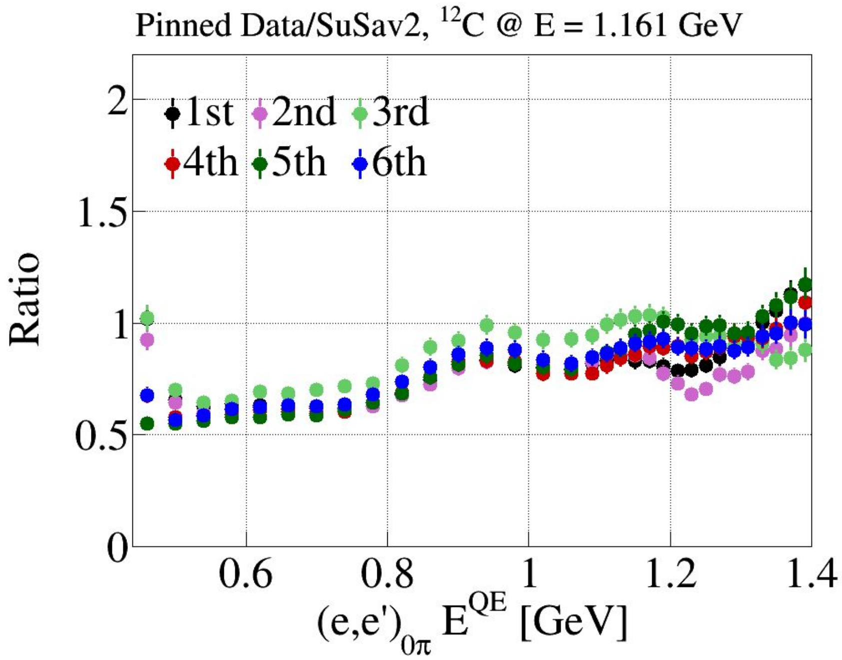

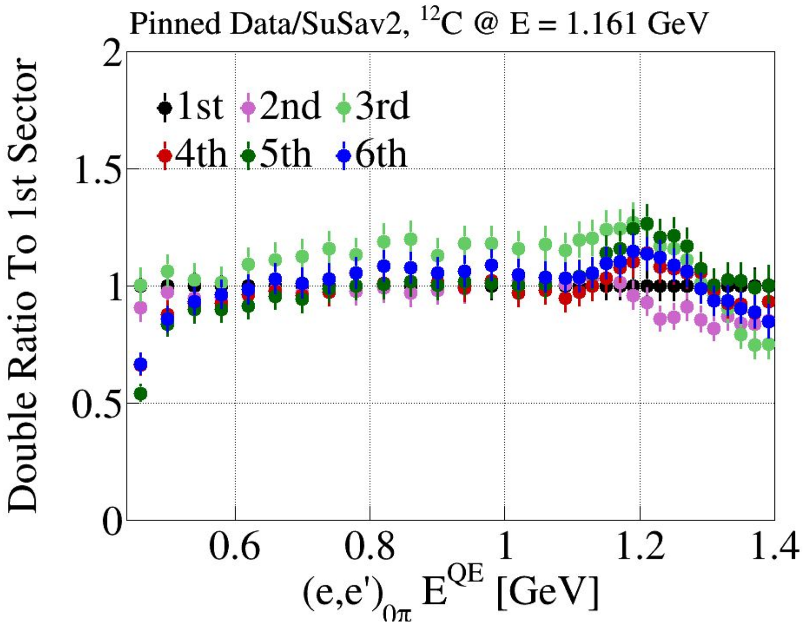

Systematics: Sector Dependence

Quantifying uncertainty by using
unweighted variance & by subtracting variance from statistical uncertainty

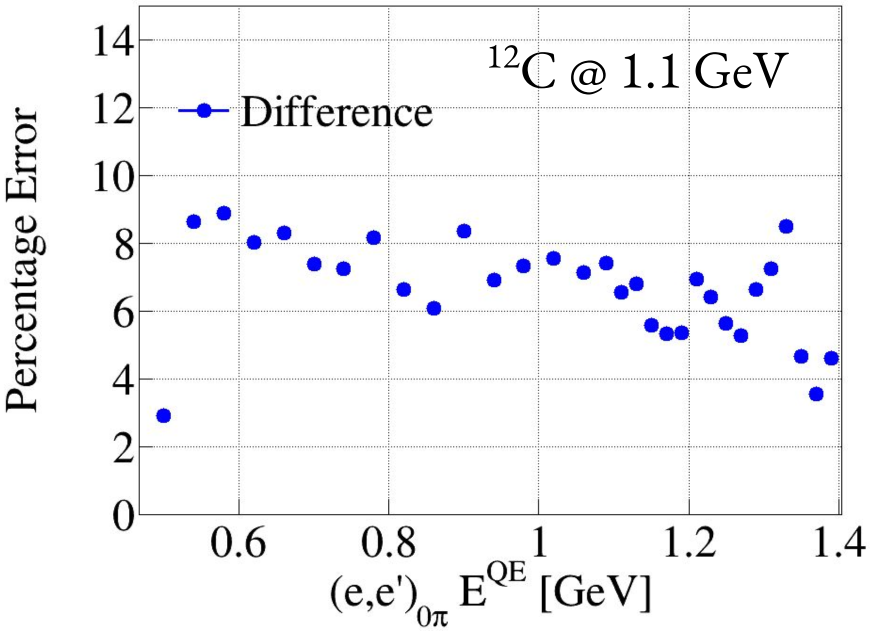

- Playing this game across all nuclei & energies
- Division by $\sqrt{N_{sectors}}$
- Flat uncertainty of 6%

Full analysis

Systematics: Normalization Uncertainties

PHYSICAL REVIEW C **73**, 025204 (2006)

Single π^+ electroproduction on the proton in the first and second resonance regions at $0.25\ \mathrm{GeV}^2 < Q^2 < 0.65\ \mathrm{GeV}^2$

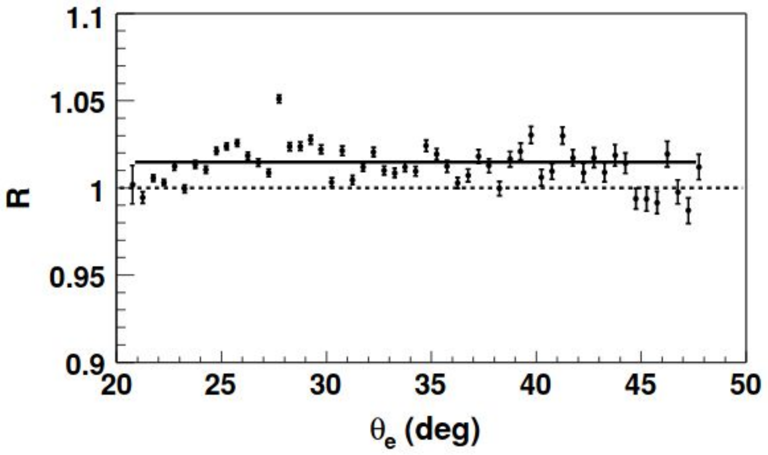

FIG. 12. The ratio of the measured elastic cross section to the parametrization of the world data [28]. The error bars represent the statistical uncertainty only. The solid line is from the fit of the data points to a constant.

1st e4ν Submission

Calorimetric energy reconstruction using the 1p0π channel

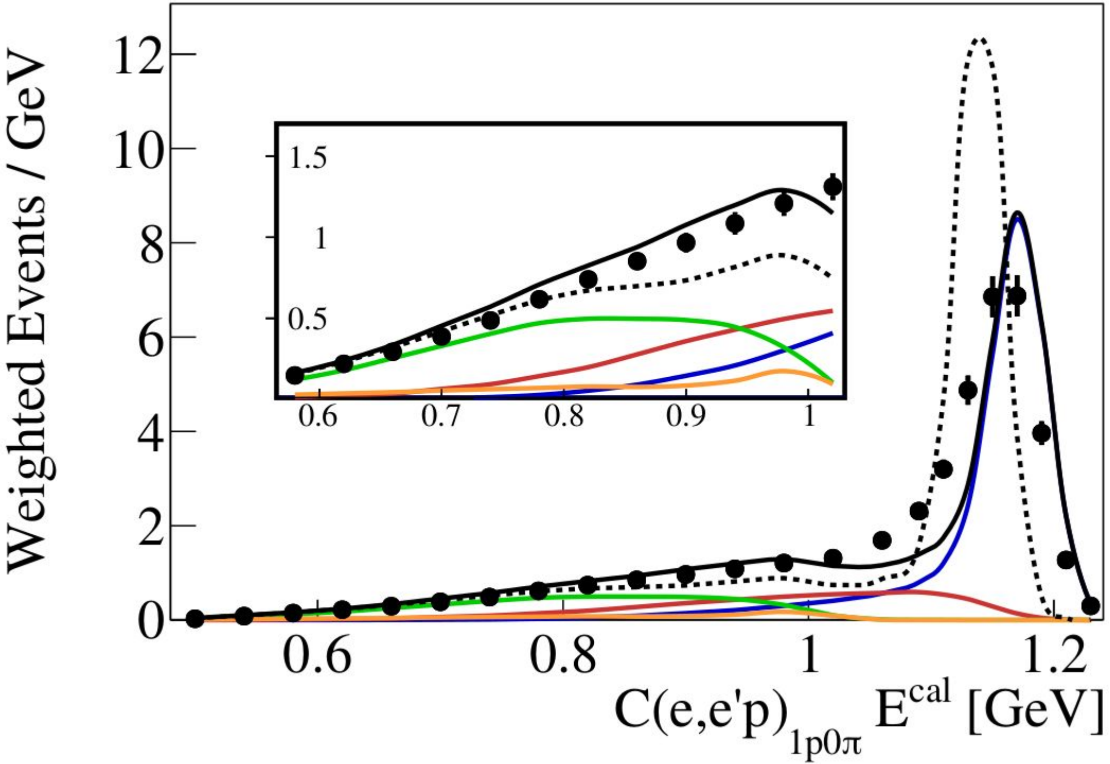

- Area normalized results
- No information with respect to absolute scale
- G2018 offset potentially due to binding energy issue

Data
SuSav2 (Total)
–QE –MEC
–RES –DIS
- - G2018

Step #2: Normalized Yield

Data

- Divide # events by integrated charge & target thickness to get xsec in μb
- Divide by bin width to get μb/GeV

Simulation

- Get GENIE total cross section for E_e / target A & Q2 > $Q2_{min}$
- xsec = (Selected detected events / all generated events) * total xsec / bin width

No corrections for CLAS acceptance or for bremsstrahlung radiation

Step #2: Normalized Yield

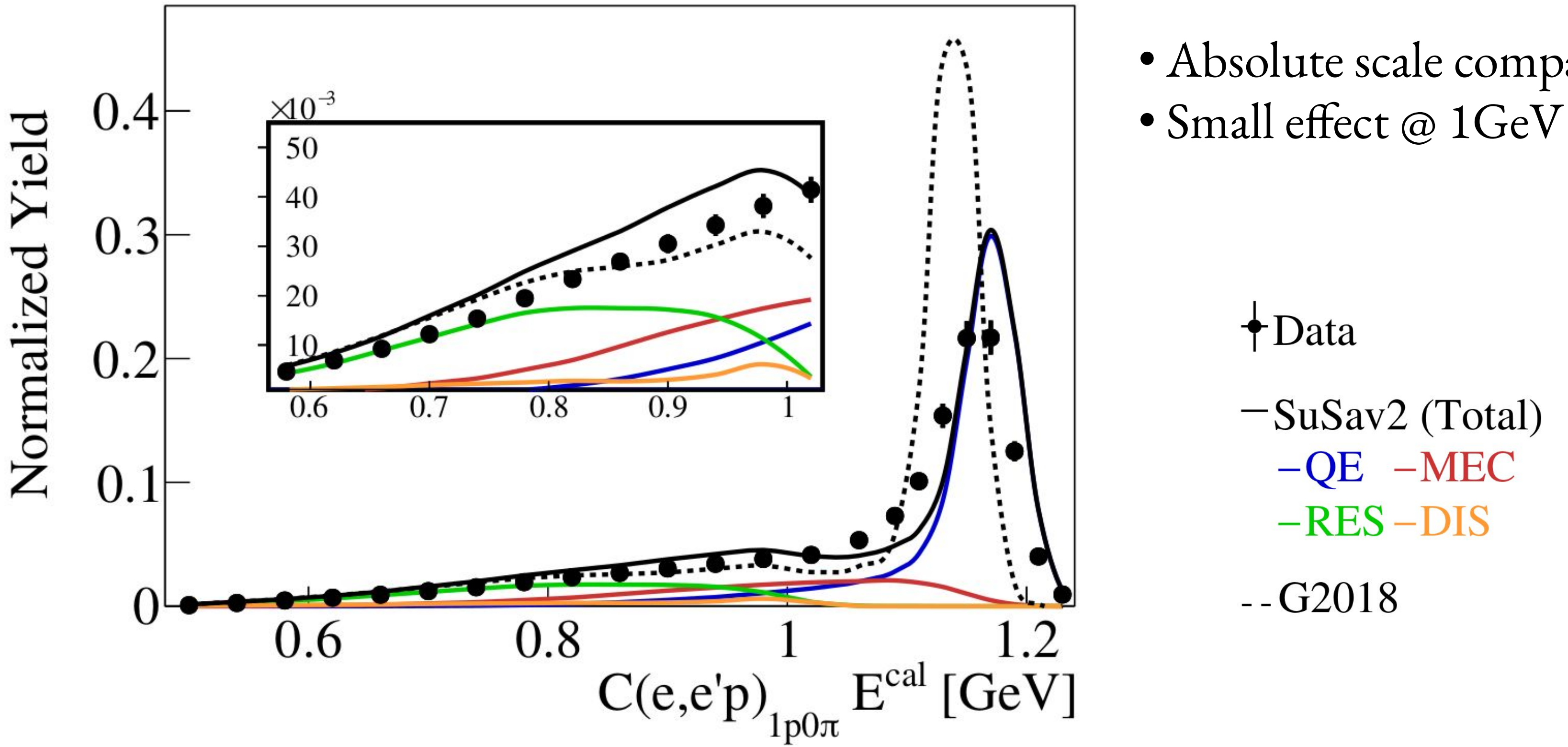

- Absolute scale comparison
- Small effect @ 1GeV

Step #3a: Acceptance Correction

- Start from reco / true ratio w/o radiation to obtain acceptance correction
- Average on a bin-by-bin basis x = |SuSav2 + G2018| / 2
- Due to offset, G2018 Ecal predictions have been shifted by 10/25/36 MeV for 4He/12C/56Fe respectively

Step #3a: Example 12C @ 1.1 GeV

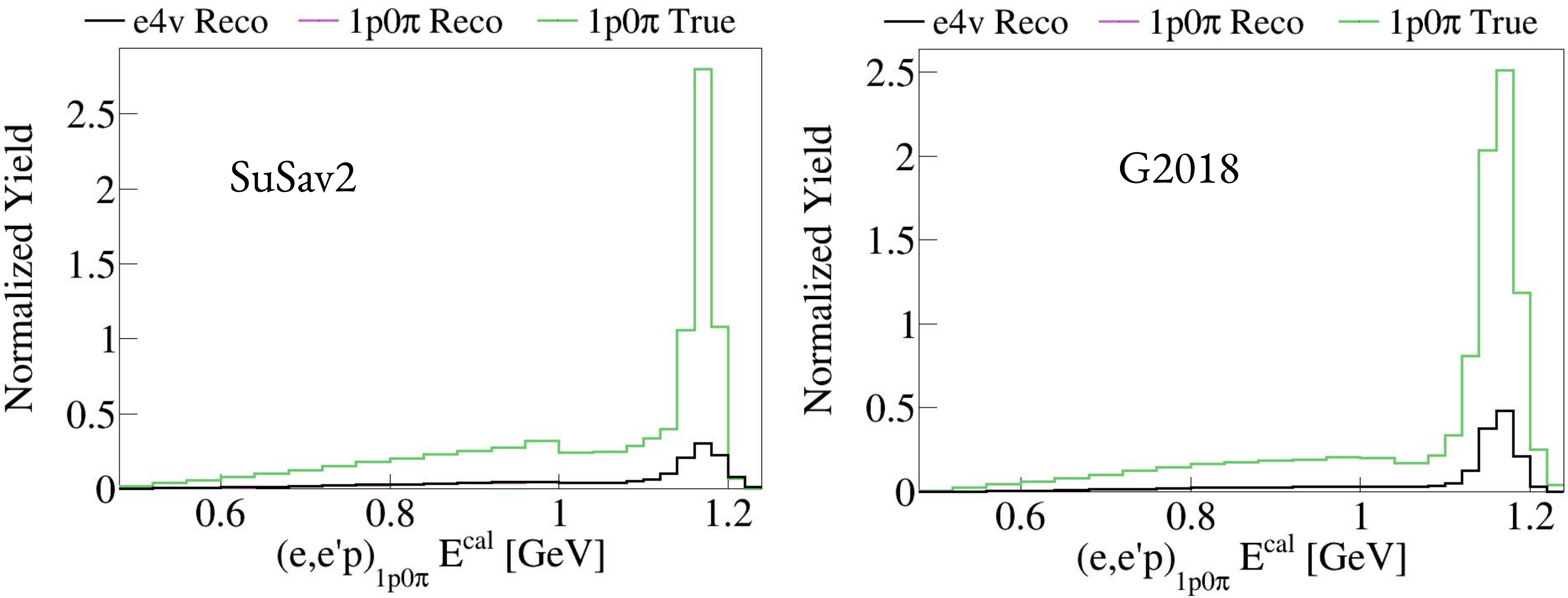

Use reco / true ratio to obtain acceptance correction

Step #3a: Acceptance Correction

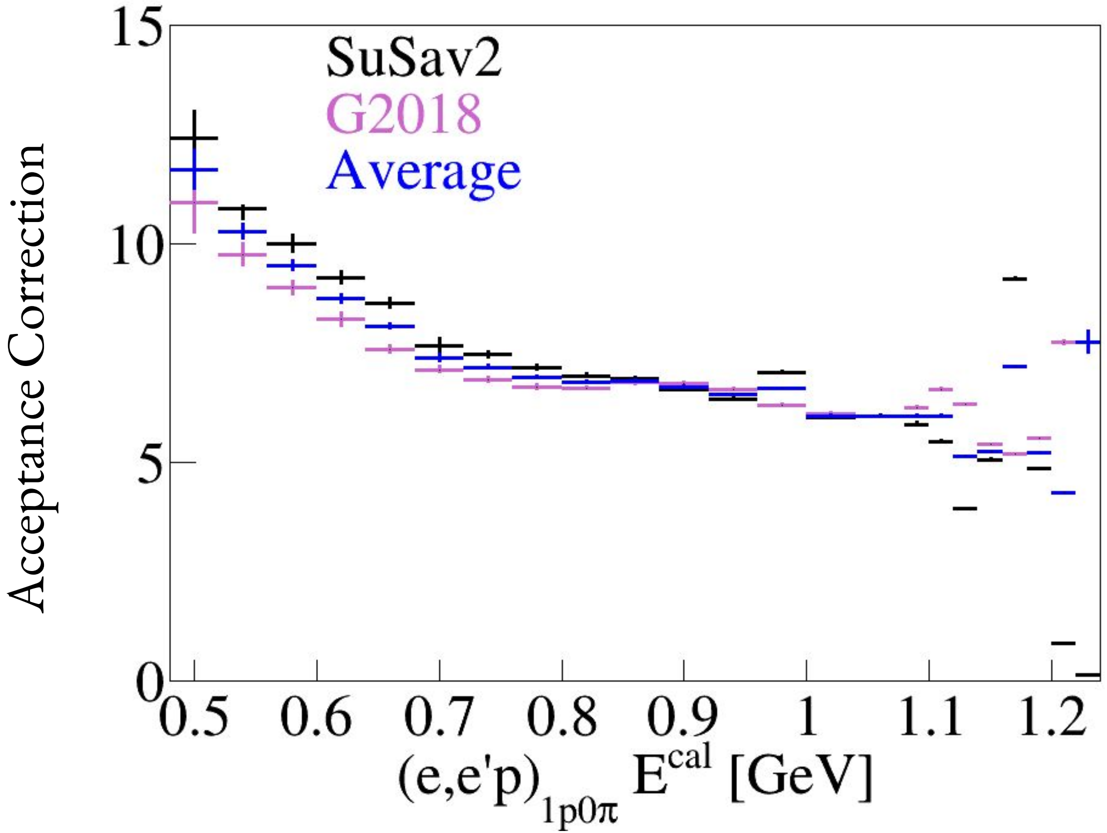

Use average to apply acceptance correction

Step #3b: Radiation Correction

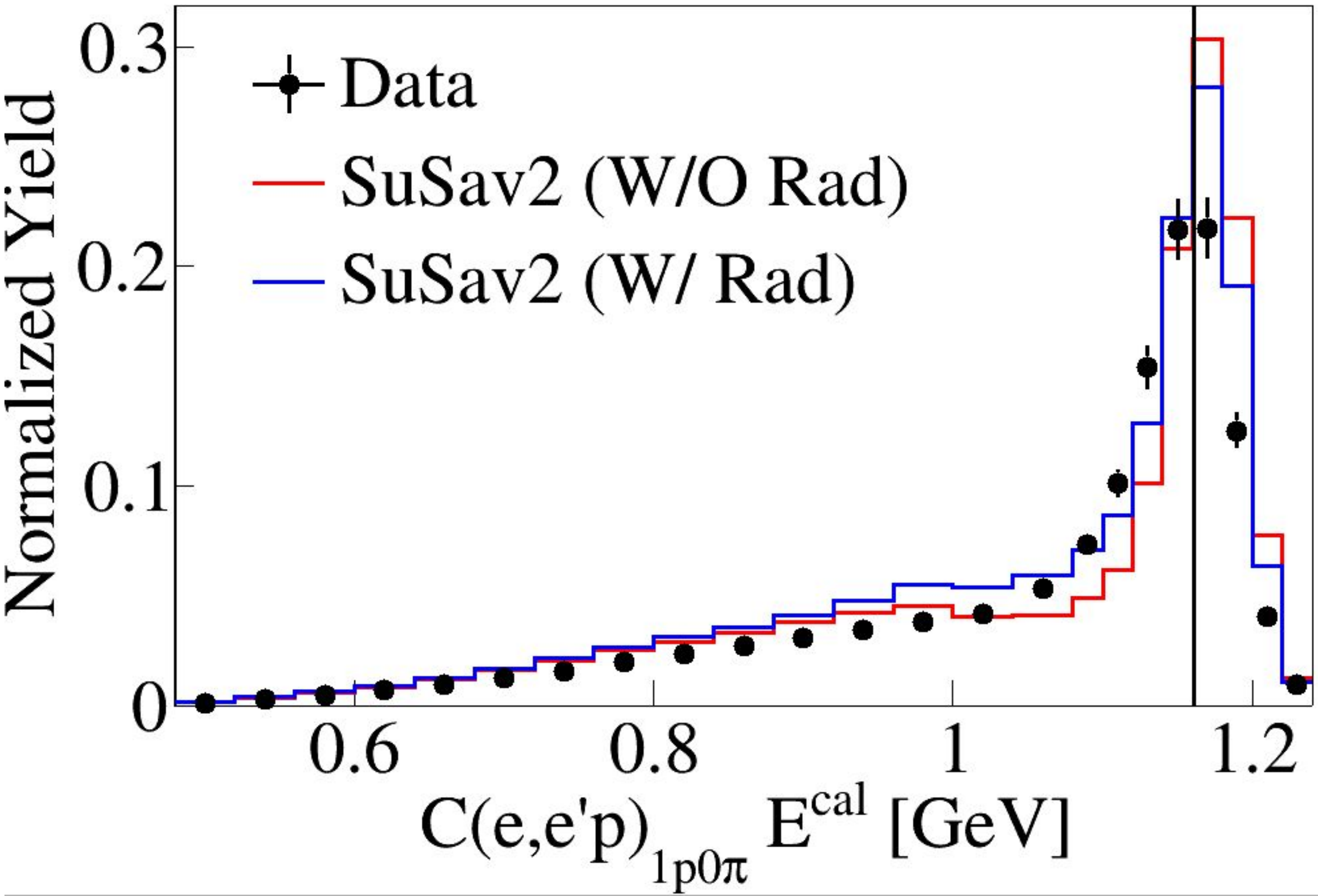

Use ratio of red / blue to correct for radiation

Acceptance Correction Factors

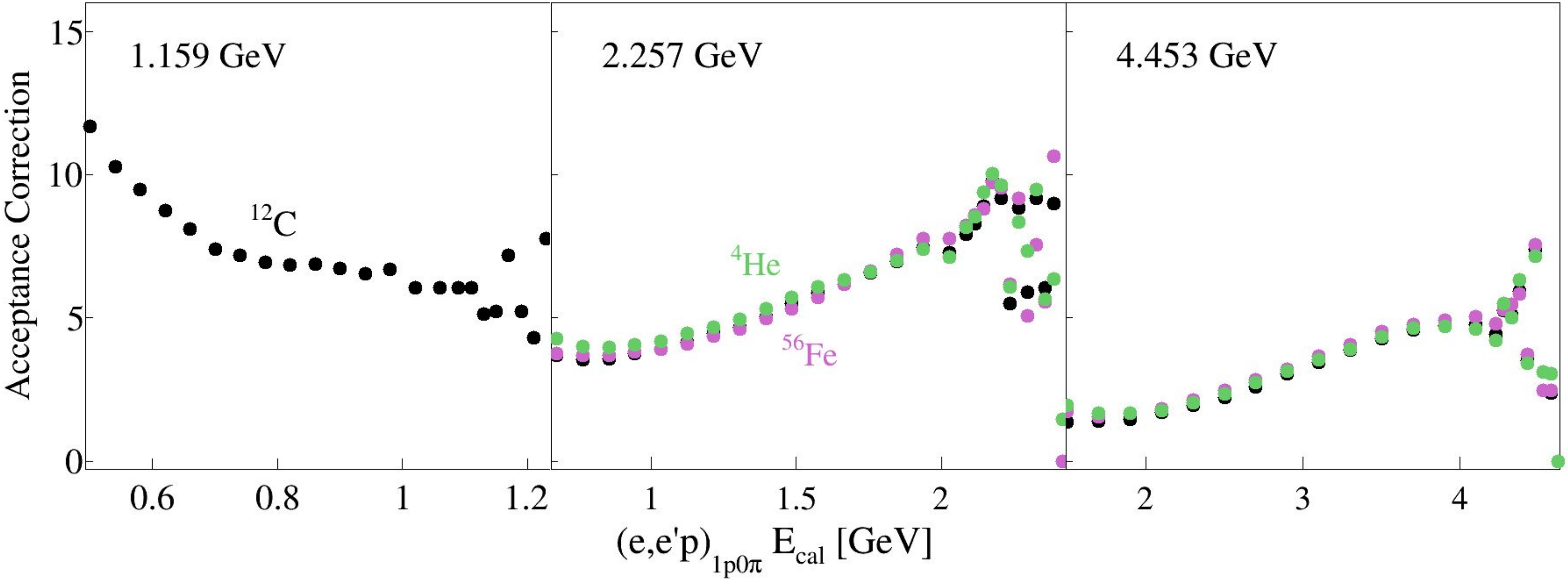

Step #4: Absolute Cross Sections

After both acceptance & radiation corrections, without systematics yet

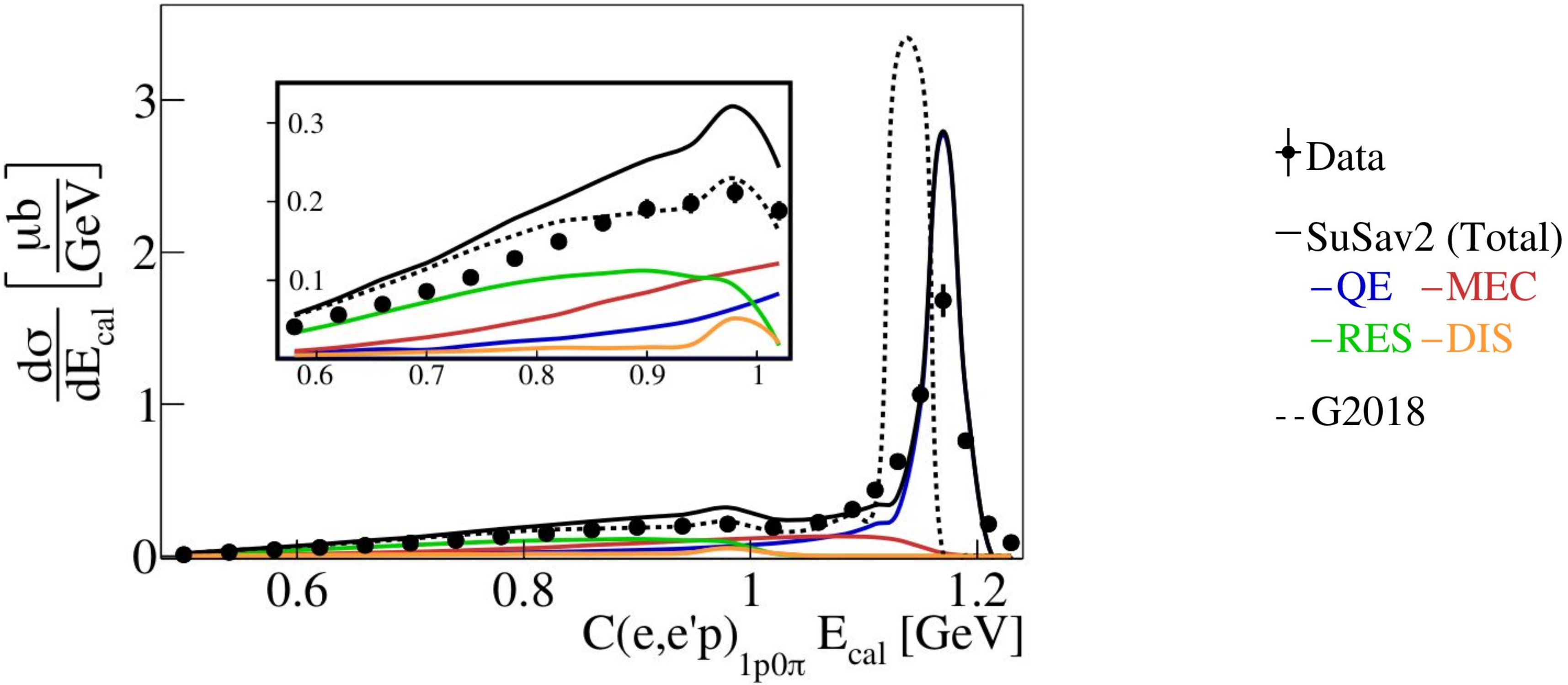

Energy Reconstruction Accuracy

Peak Fraction (%)		1.161 GeV	2.261 GeV	4.461 GeV
^{4}He	**Data**	-	41	38
	SuSav2	-	45	22
	G2018	-	39	24
^{12}C	**Data**	39	31	32
	SuSav2	44	27	12
	G2018	51	37	23
^{56}Fe	**Data**	-	20	23
	SuSav2	-	21	10
	G2018	-	30	19

Less than 50% of our selected events result in an E_{reco} close to E_{beam}

Averaged Acceptance Correction Uncertainty Over True Beam Energy

On a bin-by-bin basis

x = |SuSav2 - G2018| / Sqrt(12)

Bin Entry = x / Average * 100 %

Same recipe as for acceptance correction but,
to avoid infinities, will use average (1 bin) around the peak and
average(reco) / average(true) for correction factor

Example: Reco & True Spectra for 12C @ 1.1 GeV

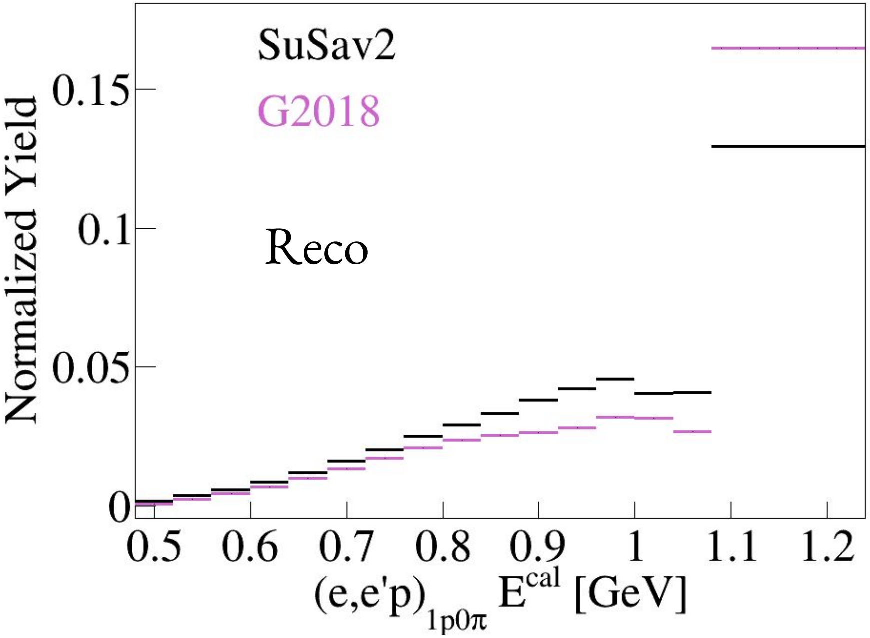

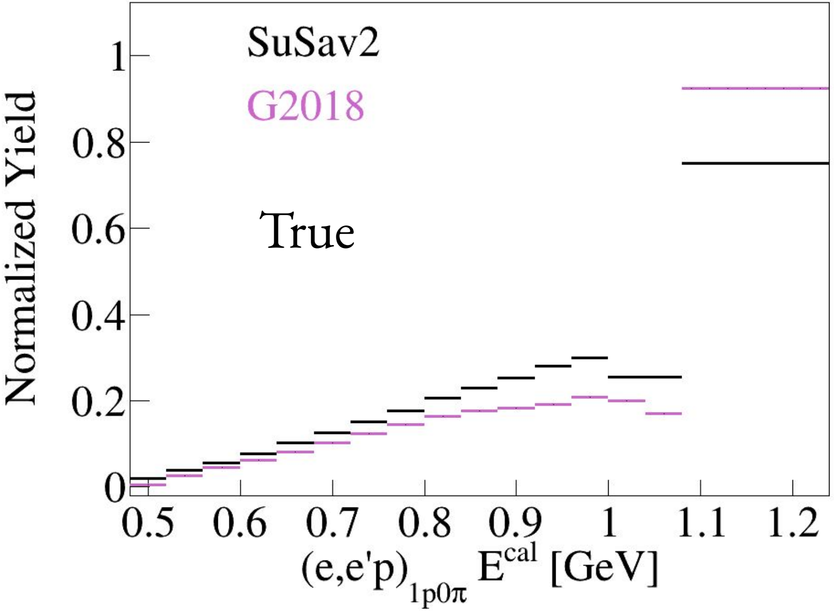

Acceptance correction = True / Reco

Example: Acceptance Correction for 12C @ 1.1 GeV

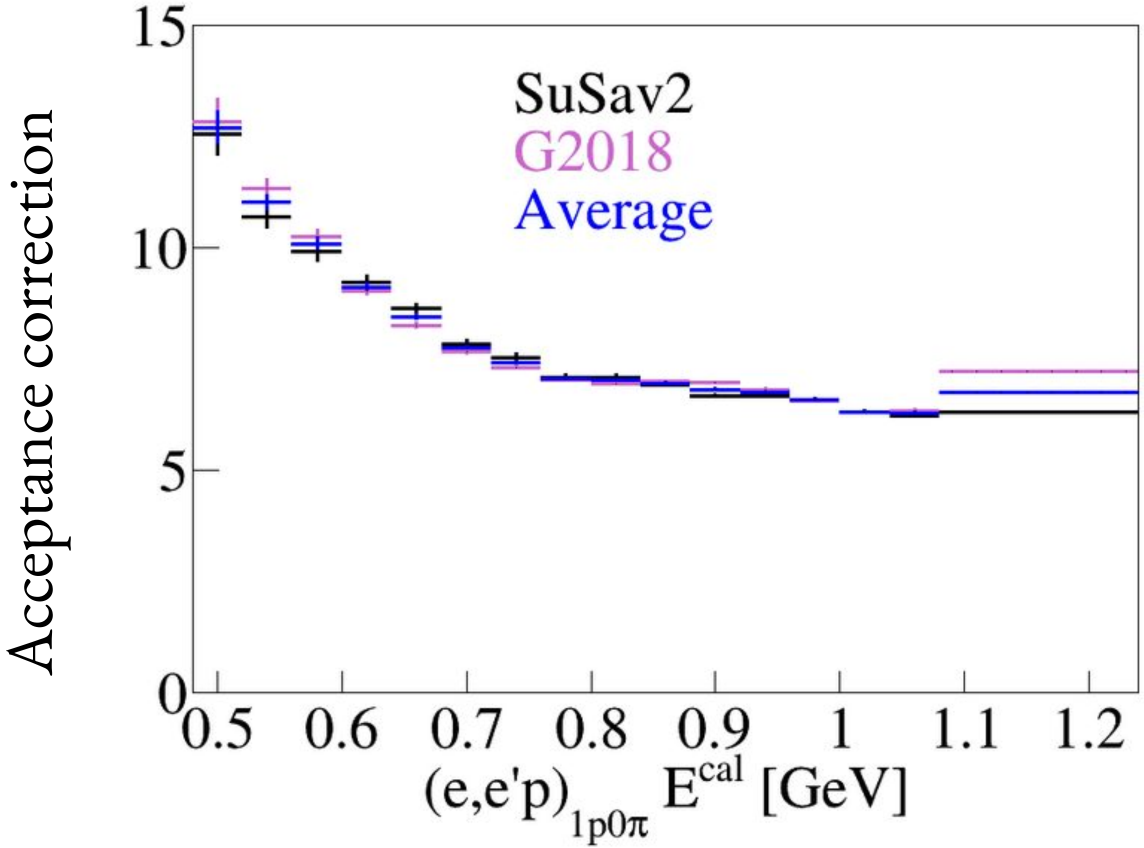

All Nuclei & Energies

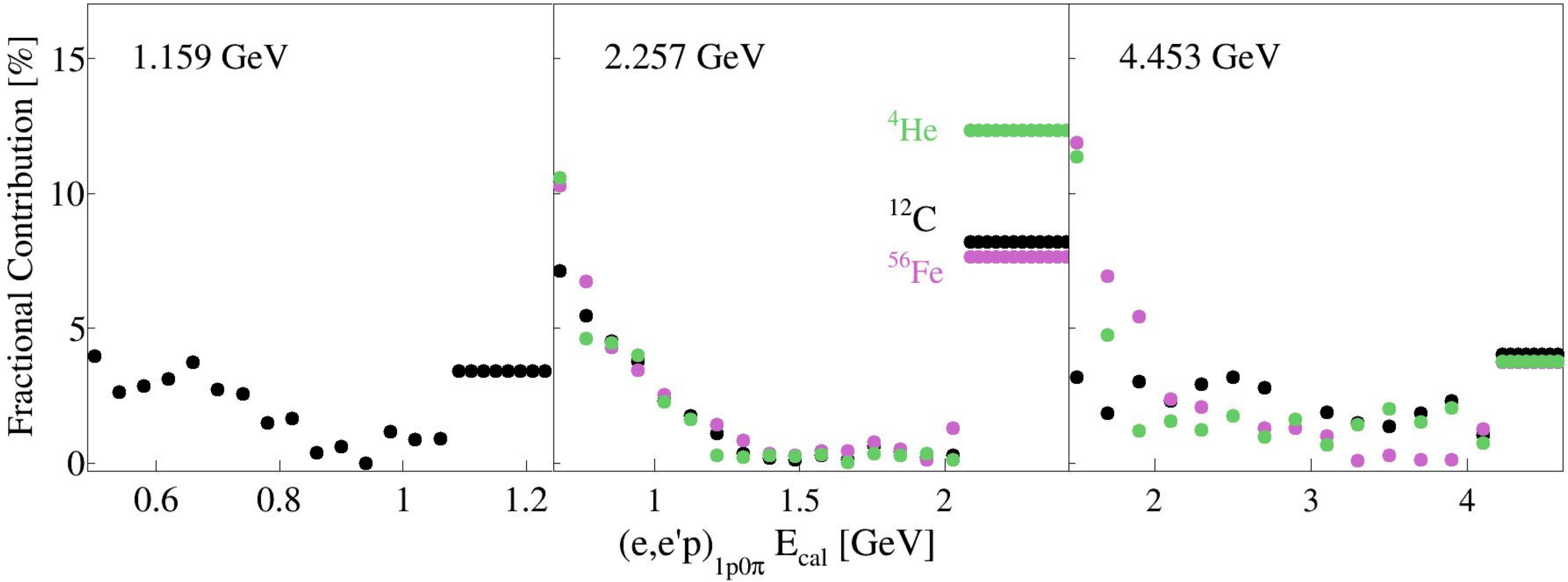

Systematics

- Sector dependence
- Detector acceptance
- Photon identification cuts
- $\varphi_{q\pi}$ cross section dependence
- Number of rotations

Systematics

Source	Uncertainty (%)
Detector acceptance Identification cuts $\varphi_{q\pi}$ cross section dependence Number of rotations	2,2.1,4.7 (@ 1.1,2.2,4.4 GeV)
Sector dependence	6
Acceptance correction	2-15
Overall normalization	3
Electron inefficiency	2

* See backup slides

Q4 Scaling Effect

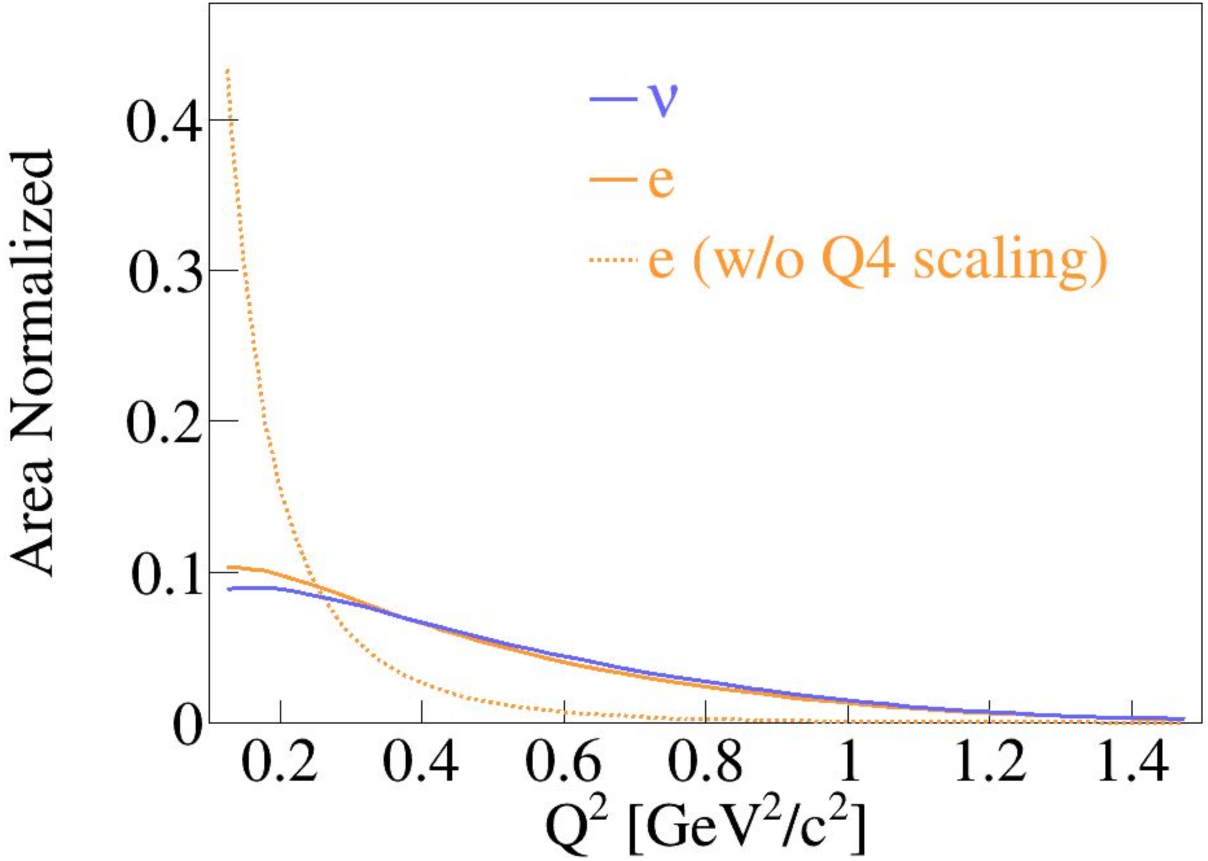

CLAS6 Detector

Hall A NIM

J. Alcorn et al. / Nuclear Instruments and Methods in Physics Research A 522 (2004) 294–346

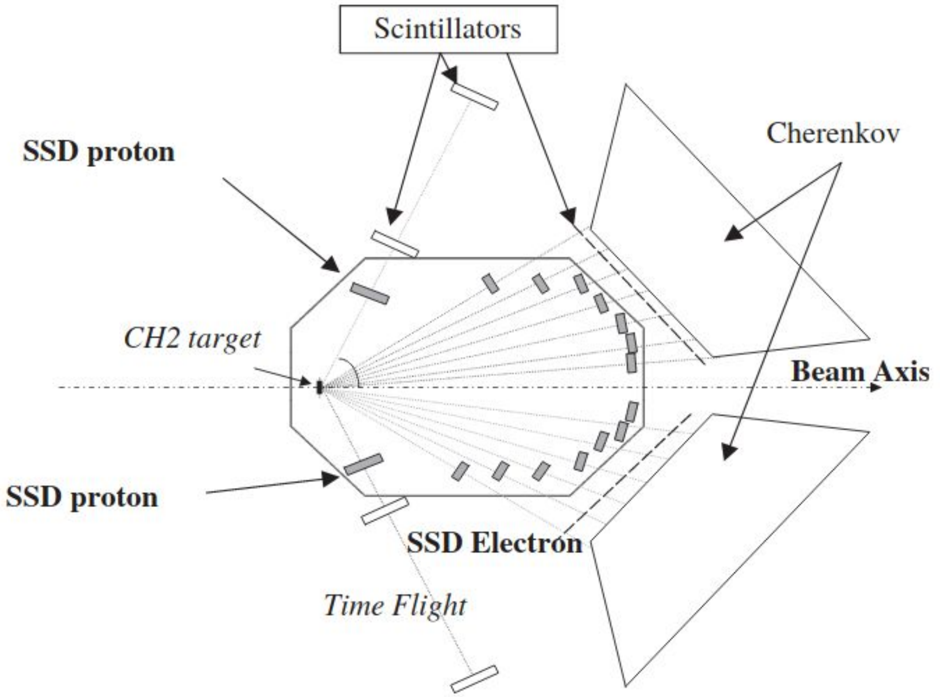

Schematic layout of the eP energy measurement system, showing the arrangement of its components, the polyethylene (CH2) target, the Cherenkov detectors, the silicon-strip detectors (SSD) for protons and electrons and the scintillator detectors, used for time-of-flight measurements.

MAMI Detector

Spectrometer A:

- Data taking

  65 kinematic points

- Angles:

  20 - 80° (7 configurations)

- Momentum:

  200 - 600 MeV/c (11 configurations)

Electron Beam:

- Energy: 600 MeV
- Current: > 20μA

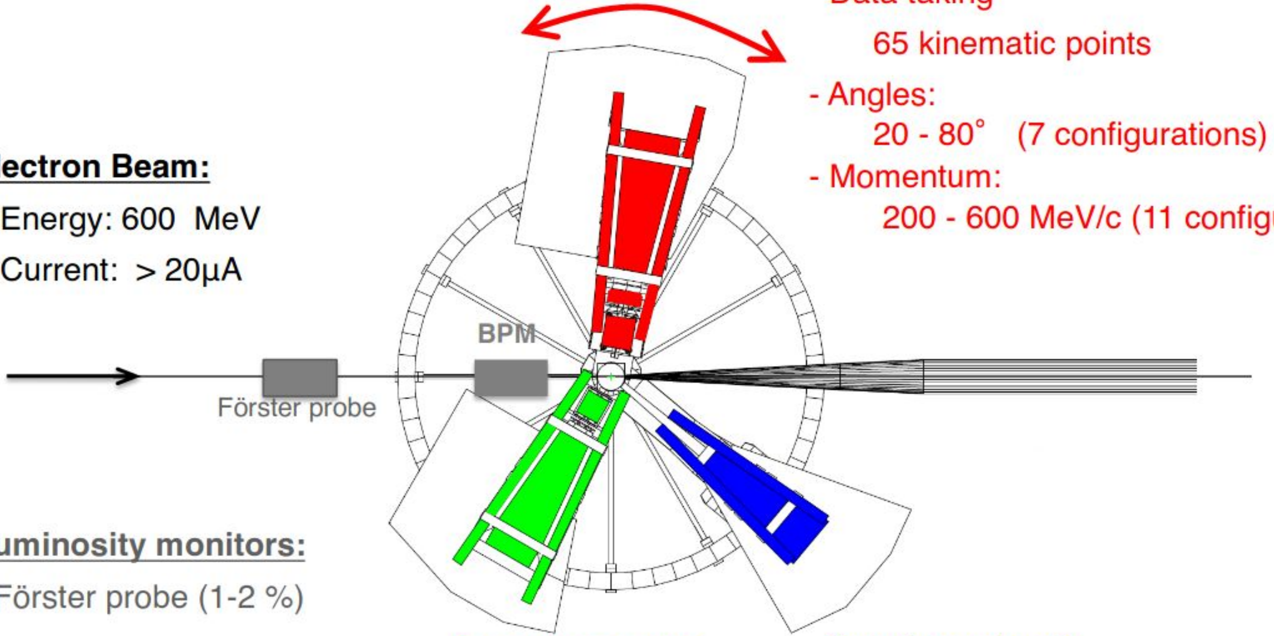

Luminosity monitors:

- Förster probe (1-2 %)

Spectrometer C:

- Not used

Spectrometer B:

- Luminosity monitor (const. setting)
- Momentum: 600
- Angles: 50°